

UNCLASSIFIED

AD 115156

Armed Services Technical Information Agency

Reproduced by

DOCUMENT SERVICE CENTER

KNOTT BUILDING, DAYTON, 2, OHIO

This document is the property of the United States Government. It is furnished for the duration of the contract and shall be returned when no longer required, or upon recall by ASTIA to the following address: Armed Services Technical Information Agency, Document Service Center, Knott Building, Dayton 2, Ohio.

NOTICE: WHEN GOVERNMENT OR OTHER DRAWINGS, SPECIFICATIONS OR OTHER DATA ARE USED FOR ANY PURPOSE OTHER THAN IN CONNECTION WITH A DEFINITELY RELATED GOVERNMENT PROCUREMENT OPERATION, THE U. S. GOVERNMENT THEREBY INCURS NO RESPONSIBILITY, NOR ANY OBLIGATION WHATSOEVER; AND THE FACT THAT THE GOVERNMENT MAY HAVE FORMULATED, FURNISHED, OR IN ANY WAY SUPPLIED THE SAID DRAWINGS, SPECIFICATIONS, OR OTHER DATA IS NOT TO BE REGARDED BY IMPLICATION OR OTHERWISE AS IN ANY MANNER LICENSING THE HOLDER OR ANY OTHER PERSON OR CORPORATION, OR CONVEYING ANY RIGHTS OR PERMISSION TO MANUFACTURE, USE OR SELL ANY PATENTED INVENTION THAT MAY IN ANY WAY BE RELATED THERETO.

UNCLASSIFIED

AD No. 115156

FILE COPY

Sipre Report 30

JULY, 1956

Excavations in Frozen Ground

FC

**Part I. Explosion Tests
in Keweenaw Silt**



**SNOW, ICE AND PERMAFROST
RESEARCH ESTABLISHMENT**

Corps of Engineers, U. S. Army

EXCAVATIONS IN FROZEN GROUND
Part I. Explosion Tests in Keweenaw Silt

by
C. W. Livingston

ABSTRACT

Mining Research Corporation, Inc., under contract with Snow, Ice, and Permafrost Research Establishment, Corps of Engineers, U. S. Army, conducted explosion tests in frozen Keweenaw silt, to determine: (1) the most efficient type of explosive for blasts in frozen ground, (2) the fundamental relation between weight of explosive and depth of charge, (3) the proper position of the charge relative to the frozen-ground interface, (4) the feasibility of fracturing the frozen layer by placing a charge in the underlying unfrozen material, and (5) the effect of the diameter of the borehole and of the shape of the charge upon the results of blasting.

Information obtained from the tests applies to the specific problem of excavating in frozen ground and to fundamental explosives research. Conclusions and recommendations based on this information are presented here concerning the feasibility of using explosives for fox-holes in frozen ground; methods of placing the charge; mechanics of crater formation; the crater equation; future instrumentation; classification of explosives; and correlation of blast data.

CONTENTS

Preface	Page i
Abstract	iii
Chapter I. Introduction to problem	1
1. Previous attempts at blasting frozen ground	1
2. Necessity for fundamental approach	1
3. Terminology	2
4. Description, objectives, and scope of the Keweenaw Tests	4
5. Selection of explosives	5
6. Classification and properties of commercial explosives	6
7. Characteristics of explosives in the Keweenaw Tests	7
8. Comparison of Atlas, Hercules, and Du Pont nitroglycerine-base explosives	9
Chapter II. Test program	10
Section I. Field tests	10
1. General	10
2. Test site	10
3. Field test procedure	10
a. Site preparation	12
b. Instrumentation	13
c. Snow removal	14
d. Determining depth of frozen ground	14
e. Soil sampling and coring	14
f. Layout of the test site	19
g. Spacing of blast holes	19
h. Blast-hole drilling	19
i. Blasting procedure	21
j. Field analysis and crater surveys	21
k. Data-sheet computations	23
l. Photography	24
Section II. Laboratory tests	25
1. Soil handling and storage	25
2. Soil classification tests	25
a. Specimen preparation	25
b. Test procedure	26
c. Test results	26
3. Tests to determine stress-strain relationship	27
a. General	27
b. Specimen preparation for unconfined compression tests	31
c. Test procedure	31
d. Results	33
e. Observations	37
Chapter III. Analysis of blast tests	41
Section I. Mechanics of crater formation in frozen Keweenaw silt	41
1. Introduction	41
2. Shock phenomena	41
3. Expansion of the gas bubble	42
4. Rupture of surface and conversion of pressure head to velocity head	44
Section II. Blast Test A — Relationships of explosive, radius of crater, volume of crater, and depth of crater	45
1. Introduction	45
2. Description	47
3. Results and analysis	49
4. Summary of observations	51

Section III. Blast Test B — Energy utilization in blasting	52
1. Introduction	52
2. Description	53
3. Results and analysis	53
4. Summary of observation	67
Section IV. Blast Test C — The frozen-ground interface	68
1. Introduction	68
2. Relation of frozen-ground interface to scaling laws	68
3. Relation between the ratio of chamber volume to crater volume and the volume-utilization factor	69
4. Increase in volume-utilization factor for charges placed below the frozen layer	73
5. Position of the gas bubble relative to the frozen-ground interface	77
6. Igloo-type foxhole construction	77
Section V. Blast Test D — Foxhole construction	79
1. Introduction	79
2. Application of shaped charges to foxhole construction	79
3. Application of hand-auger drilling to foxhole construction	81
4. Conclusions	81
Section VI. Blast Test E — Temperature effect	82
1. Introduction	82
2. Description	82
3. Results and analysis	83
4. Summary of observations	83
Section VII. Blast Test F — Effect of charge shape	85
1. Introduction	85
2. Description	86
3. Conclusions	86
Chapter IV. Summary of objectives; conclusions and recommendations	87
Section I. Summary of objectives	87
1. Introduction	87
2. Objective 1: Most efficient type of explosive for blasts in frozen ground	87
3. Objective 2: Fundamental relation between weight of explosive and depth of charge	88
4. Objective 3: Proper position of charge relative to the frozen-ground interface	94
5. Objective 4: Feasibility of fracturing the frozen layer by placing a charge in the underlying unfrozen material	94
6. Objective 5: Effect of diameter of the borehole and shape of charge on results of blasting	95
Section II. Conclusions and recommendations	95
1. Feasibility of using explosives for constructing foxholes in frozen ground	95
2. Methods of placing the charge	96
3. Mechanics of crater formation	96
4. The crater equation	96
5. Future instrumentation	97
6. Classification of explosives	97
7. Correlation of blast data	97

Appendix: Data sheets, Experiments 1-13.

ILLUSTRATIONS

	Page
Figure 1. Location of test site -----	11
Figure 2. Grain-size distribution in typical soils from the test site -----	12
Figure 3. View of test site cleared of snow -----	13
Figure 4. View of test site during spring thaw -----	13
Figure 5. SIPRE bare-wire temperature probe -----	15
Figure 6. Temperature variations in the Keweenaw silt during the test period, 1954-----	16
Figure 7. Mining Research Corporation drill rig -----	17
Figure 8. Core barrel and tungsten carbide insert coring bit used in the tests---	17
Figure 9. Modified calyx barrel and core retriever -----	17
Figure 10. Diamond core sample removed from core barrel -----	17
Figure 11. Sampling technique with thin-wall sampler -----	18
Figure 12. Chunks of soil disrupted by explosion -----	18
Figure 13. Typical soil stratification -----	18
Figure 14. Distortion of strata due to explosion pressure -----	18
Figure 15. Drilling with the wagon drill. Used for 2-5 in. holes -----	20
Figure 16. Ka-Mo augers and cutting heads-----	20
Figure 17. Auger drilling with the Mining Research Corporation rig -----	20
Figure 18. Priming technique -----	20
Figure 19. Blowing holes with compressed air to remove loose material -----	22
Figure 20. Tamping the charge -----	22
Figure 21. Recording depth to the top of the charge -----	22
Figure 22. Placing stemming material -----	22
Figure 23. Cross-sectioning a crater -----	22
Figure 24. Ice lens detail -----	29
Figure 25. Original frozen chunk -----	30
Figure 26. Rough cutting process-----	30
Figure 27. Rough trimming process -----	30
Figure 28. Final trimming process -----	30
Figure 29. Cutting ends of specimen -----	30
Figure 30. Weighing specimen -----	30
Figure 31. Measuring specimen -----	32
Figure 32. Strain gage details -----	32
Figure 33. Drilling holes in specimen for gage points -----	32
Figure 34. Placing gage points -----	32
Figure 35. Tempering cabinet -----	32
Figure 36. Compression test assembly showing specimen prior to test -----	32
Figure 37. Gradation curves, compression test samples loaded at 400 psi/min--	34
Figure 38. Gradation curves, compression test samples loaded at 1000 psi/min--	34
Figure 39. Compression test data, Sample 6 -----	34
Figure 40. Compression test data, Sample 9 -----	35
Figure 41. Compression test data, Sample 2 -----	35
Figure 42. Compression test data, Sample 7 -----	36
Figure 43. Compression test data, Sample 10 -----	36
Figure 44. Sample 2 before compression test -----	37
Figure 45. Sample 2 after compression test-----	37
Figure 46. Sample 7 before compression test -----	39
Figure 47. Sample 7 after compression test -----	39
Figure 48. Sample 10 before compression test -----	39
Figure 49. Sample 10 after compression test -----	39
Figure 50. Compressive strength vs. volume of ice/volume of soil -----	40

	Page
Figure 51. Rupture of the frozen-ground interface due to downward expansion of the gas bubble -----	43
Figure 52. Radial (R) cracks in Keweenaw frozen silt associated with near critical-depth blast -----	43
Figure 53. Gas-bubble cavern below the frozen layer before removing the debris that has fallen back from the blast -----	43
Figure 54. After removal of debris -----	43
Figure 55. Surface break-through of the gas bubble at a weight slightly in excess of the critical weight -----	44
Figure 56. Surface break-through of the gas bubble at weight slightly in excess of the optimum weight -----	44
Figure 57. Crater radius vs. charge weight, Keweenaw Blast Test A -----	46
Figure 58. Crater volume vs. charge weight, Keweenaw Blast Test A -----	48
Figure 59. Crater depth vs. charge weight, Keweenaw Blast Test A -----	50
Figure 60. Radius of crater vs. depth of charge. Atlas 80% Gelatin -----	54
Figure 61. Radius of crater vs. depth of charge. Atlas 60% Gelatin -----	55
Figure 62. Radius of crater vs. depth of charge. Gelodyn 1 -----	56
Figure 63. Radius of crater vs. depth of charge. Coalite 7S -----	58
Figure 64. Radius of crater vs. depth of charge, four types of explosives -----	59
Figure 65. Radius utilization factors vs. depth ratio. Blast Test B -----	60
Figure 66. Volume of crater vs. depth of charge, four types of explosives -----	62
Figure 67. Summary curves, Keweenaw explosives -----	63
Figure 68. Volume utilization factor vs. depth ratio. Blast Test B -----	64
Figure 69. Explosive cost at various depth ratios -----	66
Figure 70. Critical weights of explosives for blasts in frozen Keweenaw silt -----	70
Figure 71. Volume utilization factor as related to ratio of chamber volume to crater volume -----	72
Figure 72. Prototype volumes at various depth ratios, Blast Test C -----	74
Figure 73. Effect of frozen ground interface at break-through -----	76
Figure 74. Igloo-type foxhole produced by blast of Atlas 80 Percent Straight Gelatin at critical weight below the frozen layer -----	78
Figure 75. Igloo-type foxhole produced by blast of Atlas 60 Percent Straight Gelatin at critical weight below the frozen layer -----	78
Figure 76. Igloo-type foxhole produced by blast of Coalite 7S at critical weight below the frozen layer -----	78
Figure 77. Hemispherical depression produced by 10-lb shaped charge -----	80
Figure 78. "Plaster shot" of 2.5 lb of Gelodyn 1 before detonation -----	80
Figure 79. Crater produced by first "plaster shot" -----	80
Figure 80. Foxhole produced by second "plaster shot" -----	80
Figure 81. Temperature effect, February 17 -----	84
Figure 82. Blast using critical weight at lower temperatures produced a crater in sandy soil at near-melting point -----	85
Figure 83. Blast using nearly double critical weight at lower temperatures did not produce a crater in silt at near-melting point -----	85
Figure 84. Volume of craters in frozen Keweenaw silt -----	92, 93

PREFACE

The planning and analysis of blasts in frozen Keweenaw silt were preceded and influenced by several years of research at Colorado School of Mines. This research was influenced in turn by the association of C. W. Livingston (then Head of the Department of Mining Engineering at Colorado School of Mines) as consultant to the Protective Construction Branch, Office Chief of Engineers, U. S. Army. It was also influenced by Mr. Livingston's association with Colorado School of Mines Research Foundation as Project Manager for such projects as Series I and II Experiments of the Underground Explosion Test Program, the Castledale Project, and the Bomb Penetration Project. As an outgrowth of this research work, graduate courses were introduced at Colorado School of Mines in such subjects as barodynamics, rock excavation, and photoelasticity. Many graduate students became interested in these studies and conducted research work leading toward the degrees Master of Science and Doctor of Science.

Knowledge of the subject of explosions has been advanced greatly as a result of the Underground Test Program¹; Series I and II Experiments²; the Bomb Penetration Project³; and Cole's report on Underwater Explosions⁴. Though the opinions expressed by the writer do not necessarily represent the opinions of the Corps of Engineers, it is difficult if not impossible to use a fundamental approach to the problem of blasting in frozen ground — and the fundamental approach is most necessary — without drawing upon all information the writer possesses. It would be impractical within the scope of this report to consider all aspects of the subject; also, it would be impossible to repeat all the background research that has influenced the planning and analysis of the Keweenaw Tests.

Although much progress has been made in explosives research, much remains to be done. Satisfactory criteria of rock failure must be evolved if we are to progress beyond the present empirical stage both in utilization of explosives and in control of subsidence. It is impossible, with our present state of knowledge, to correlate the great mass of data available for blasts in soils and rocks. It is also impossible to select — on other than a cut-and-try basis — the proper type of explosive for excavations in various materials.

Frozen ground may be regarded as a rock type. It exhibits properties intermediate between those of rocks and soils. It is an ideal medium for research in blasting because of its freedom from such geologic features as fracturing, folding, jointing, hydrothermal alteration, and weathering. Perhaps frozen-ground studies may provide the means of tying together the subjects of soil mechanics and barodynamics.

The writer has drawn freely from courses which he taught at Colorado School of Mines; from Series I and II Experiments²; from the Bomb Penetration Project³, and from graduate theses directed by him.⁵

1. Engineering Research Associates (1953) Underground Explosion Test Program, Vol. II, Rock, Final Report. April 30, 1953. CONFIDENTIAL
2. Livingston, C. W. (1949) Series I and II Experiments, Underground Explosion Test Program, Report of the Colorado School of Mines, 150 pages. RESTRICTED
3. Livingston, C. W., and Smith, F. L. (1951) Bomb Penetration Project, Colorado School of Mines Research Foundation, Inc., 245 pages. CONFIDENTIAL
4. Cole, R. H. (1948) Underwater Explosions. Princeton, N. J.: Princeton University Press, 424 pages.
5. See, for examples:
Livingston, C. W. (1951a) An introduction to the design of underground openings for defense, Quarterly of the Colorado School of Mines, vol. 32, no. 1.
Livingston, C. W. (1951b) Research at Colorado School of Mines in subjects related to the mechanics of rock failure, Transactions of the American Geophysical Union, vol. 32, no. 2.

McCutchen, W. R. (1949) The behavior of rocks and rock masses in relation to military geology, Quarterly of the Colorado School of Mines, vol. 44, no. 1, and the large number of references on rock failure that each of these publications contains.

CHAPTER I. INTRODUCTION TO PROBLEM

1. Previous attempts at blasting frozen ground

"Previous military experience in frozen ground has shown that failure of troops to be able to entrench themselves properly has resulted in high casualties both from cold weather and from enemy fire. Statistics¹ show that casualties from frostbite were decreased from 800 men to 4 men in a single day as a result of adequate entrenchment. However, it was borne out in this report that large quantities of explosives (approximately 10,000 pounds to form a crater to hold 3 to 5 men) were required to form the excavation and that the noise accompanying the explosion gave the impression of a heavy barrage.

"In Exercise Eager Beaver (combined United States - Canadian Engineer USER Trial 1951-1952) various methods of digging fox-holes with explosives were tried. These trials showed that a minimum 30-pound shaped charge was required to make a borehole and at least 20 pounds of explosive was needed to disturb sufficient earth to permit the digging of a regulation foxhole. The report stated that the amount of any type of explosive at present in use cannot be carried by the infantry man, the process is not safe in untrained hands, the noise resulting from the method is considerable and attempts at concealment of a position would be hampered."²

Conferences with representatives of manufacturers of commercial explosives, whose experience resulted from blasting frozen ground in open-cut stripping operations for coal and iron ore, have made it clear that considerable difference of opinion exists regarding the type of explosive to use. Some preferred high-velocity explosives; others preferred low-velocity explosives. Manufacturers' representatives were unable to offer specific data on the quantity of explosive required and on the size, burden, or spacing of blast holes.

2. Necessity for fundamental approach

Blasting results depend upon physical, elastic, and plastic properties of the material blasted and upon physical and chemical properties of the explosive. Numerous failure criteria have been proposed by investigators who approached the problem from the basis of statics. Theories also have been proposed by those who have approached the problem from the bases of dynamics and wave propagation. Yet, none of these theories has advanced to the state where accurate predictions of damage can be made based upon the properties of the material and upon the properties of the explosive. Much experimental work has been done on cratering in soils and in various types of rocks. Penetration of projectiles into soils, reinforced concrete, and rocks has been studied. Yet, it is impossible to correlate all the data available, because of lack of knowledge of fundamentals.

As a starting point it does not seem unreasonable to assume that frozen ground behaves much like a rock. Because ice is the cementing material which converts the soil mass into a solid, it seemed reasonable to assume in planning the experiments that the elastic properties of frozen ground are related in some manner to the elastic properties of ice. Reported values³ of Poisson's ratio for ice, as determined both by static methods and by dynamic methods without lateral confinement, range from 0.36 to 0.38. Judging from this range of values, frozen ground may behave partly as an elastic and partly as a plastic medium. It is possible that frozen ground may exhibit properties intermediate between those of soils and of rocks. It is conceivable, therefore, that data available for blasts in both soils and rocks can be correlated with data obtained by blasts in frozen ground if the research is directed towards determining the fundamental properties of the material blasted and of the explosive used.

1. Department of the Army (1951) Military Improvisation During the Russian Campaign, D. A. Pamphlet 20-201, Historical Study, p. 23.

2. Boyd, W. K. (1953) Minutes, Consultant's Conference, SIPRE Project on Excavations in Frozen Ground, 10 November 1953.

3. Snow Ice and Permafrost Research Establishment (1951) Review of Properties of Snow and Ice, (Report 4) Corps of Engineers, U. S. Army, p. 4-8.

3. Terminology

Various terms peculiar to explosives research are used in this report. Terms relating to the planning of field experiments and the analysis of data are defined below. Other terms relating to classification of explosives or to field procedure are introduced and discussed in the appropriate section. Certain terms, such as optimum weight and maximum effective weight, were evolved as a result of this project. They are defined here and discussed further in their appropriate places.

Borehole pressure is the peak pressure developed by the gas within the borehole at the instant of rock failure. Borehole pressure is dependent both upon the material blasted and upon the explosive. Explosion pressure is dependent only upon the explosive.

Burden is usually measured in a nearly horizontal direction. It is the shortest distance between the center of gravity of an explosive charge and the nearest vertical free-face.

Cartridge strength refers to the bulk strength or volume strength of an explosive. Manufacturers have not agreed on a standard, but it is generally accepted that cartridge strength should be referred to cartridges $1\frac{1}{4}$ in. in diameter by 8 in. in length and weighing 50 lb per 100 cartridges. If the number of cartridges per 50-lb case is more than 100, the cartridge strength is less than the weight strength.

Critical burden is that burden sufficient to retain the energy of the explosion without damage to a vertical free-face. An increase in weight of explosive or a decrease in burden would cause the vertical face to be destroyed.

Critical depth is the minimum depth (measured vertically from the surface to the center of gravity of the explosive charge) at which the energy of the explosion is dissipated into the mass of earth or rock without visibly damaging the surface above the charge.

Critical weight is that weight of a particular explosive which satisfies the critical-depth requirement for a particular medium and for a given depth.

Depth ratio is the ratio of the charge depth to the critical depth. Shallow charges produce excessive noise and excessive air-blast. As the depth of the charge increases, the proportion of the energy of an explosion that is lost into the atmosphere decreases. At a depth ratio of 1.0 (critical depth) all of the energy of the explosion is transmitted to the medium without surface rupture. (See Energy Utilization - Blast Test B)

Energy utilization number: The constant K of the model-law equation (see Chapter III, Section IV, 2):

$$b = K \sqrt[3]{w}$$

is considered by Livingston to equal the product of three numbers, called the ABC product.

$$K = A B C$$

where A is the energy-utilization number, B is a rock factor, and C is a stress-distribution factor. The energy-utilization number depends upon the type of explosive and the depth ratio, and is a measure of the "effect-of-depth" or "coupling effect." Blasts in which the same proportion of the total energy of the explosive is utilized by the medium have the same energy-utilization number.

Explosion pressure is the maximum pressure that can be produced with any given explosive at constant volume. It is estimated theoretically, using the chemical formula for the reaction, Abel's Gas Law, and correcting for the co-volume of the molecules of gaseous products.

Explosion temperature is the temperature at which the explosion pressure is measured. It is estimated theoretically from the composition, the heat of formation, the specific heat of explosion products, the gas law obeyed by the gaseous products

of explosion, and the heat losses.

Flyrock travel-distance is the horizontal distance from the borehole (measured on a horizontal plane through the collar of the borehole) that flyrock is thrown by a blast. Both flyrock travel-distance and flyrock travel-height are a function of the depth ratio. For blasts in frozen Keweenaw silt, both are considered to be related to the velocity of expansion and the energy of the gas bubble at breakthrough.

Flyrock travel-height is the vertical distance above the ground surface that particles from a blast are thrown. Flyrock travel-height is a function of the depth ratio and of the type of explosive. As flyrock travel-height increases, the proportion of the total explosion energy that is utilized by the medium decreases.

A free-face is the interface or surface towards which material broken by a blast is thrown. The free-face may be horizontal, vertical, or inclined. It may be bounded by gas, liquid, or solid. It may be curved or regular. One or more free-faces may be affected by a blast.

The gas bubble is the gas-filled explosion cavity caused by detonation of the explosive and expansion of the products of combustion. (See Mechanics of Crater Formation, Chapter II, Section I, Items 1-4.)

The interface ratio, as applied to this project, is the ratio of the depth of the center of gravity of the explosive charge to the thickness of the frozen ground. The contact between frozen and unfrozen ground is considered to be an interface.

The length-scale ratio is the ratio of any dimension of a blast to the same dimension of a prototype blast hole. A prototype hole in the Keweenaw Tests is one 18 in. deep and $2\frac{1}{2}$ in. in diameter. The scale of such a blast is 1.0 regardless of the weight or type of explosive, and regardless of the shape of the resulting crater.

Maximum effective weight (see Blast Test A) is that weight of explosive which produces the maximum volume of crater with a given type of explosive detonated at a given depth of center of gravity of charge below the surface.

Oxygen balance has been defined as "the percentage of oxygen required for complete conversion of the carbon and hydrogen present in explosives to carbon dioxide and water. An explosive in which the ingredients are so balanced that all the oxygen is converted to carbon dioxide and water has a zero oxygen balance, one lacking sufficient oxygen has a negative balance, and one containing excess oxygen has a positive balance."¹

Optimum depth is the depth at which a given weight of explosive produces the greatest volume of excavation per unit weight of explosive (see Volume-Utilization Factor). The optimum depth of the Keweenaw Test explosives in frozen Keweenaw silt ranges from a depth ratio of 0.9 to 1.0. At a depth ratio of 1.0 the optimum depth equals the critical depth.

Optimum weight (see Blast Test A) is that weight of a particular explosive at which the quantity of material loosed by a blast at a given depth or burden is maximum per unit weight of explosive.

Prototype volume: A blast using the critical weight of explosive at 1.0-ft depth of center of gravity is a prototype blast at depth ratio 1.0. At depth ratios less than 1.0, craters are produced using the same weight of explosive. The volumes of the craters are referred to in this report as "prototype volumes." The prototype volumes decrease as the depth ratio decreases. The dimensions of an unknown crater at the same depth ratio using the same explosive are a function of the length ratio of the two blasts. The volume of an unknown crater is a function of the ratio of the cubes of the critical weights or of the ratio of the cubes of the critical depths. Inasmuch as

1. W. C. Lathrop and G. R. Handrick (1949), The relation between performance and constitution of pure organic explosive compounds, Chemical Reviews, vol. 44, no. 2.

the critical depth for the prototype blast is 1.0 ft, the volume of crater in frozen Keweenaw silt for a blast at any depth of charge equals the prototype volume at the corresponding depth ratio multiplied by the cube of the critical depth for charge x . (See Examples 1 and 2, Chapter III, Section IV, 4.)

The r/d ratio is the calculated crater radius (see Data Sheet Computations, Chapter II, Section I, 3k) divided by the depth to the center of gravity of the explosive charge. It is a measure of the shape of a crater.

Radius-utilization factor: The radius of a crater in feet divided by the weight of explosive in pounds (the number of feet of crater radius per pound of explosive).

Rock factor: Failure of a mass of earth, rock, or other structural material depends upon two factors: (1) the properties of the material and (2) the nature of the deforming stress. The first of these factors, the property of the material, determines the resistance of the material to the deforming stress. Livingston has shown that the penetration of projectiles into rocks depends upon elastic (and plastic) properties and has derived a mathematical expression called the "rock factor," (B of ABC product) which expresses as a ratio the depth of penetration in a specific rock relative to the penetration in a prototype rock. The rock factor may apply also to blasting in most materials, including blasts in frozen ground.

The **similitude ratio** provides a means of comparing craters of different sizes but similar shapes. It is the distance from the center of gravity of the explosive charge to the bottom of the resulting crater divided by the shortest distance from the center of gravity of the explosive charge to the ground surface above the explosive. A critical-depth blast results in a similitude ratio of 1.0.

Springing, chambering, or squibbing refers to a method of enlarging a borehole using light charges of explosive. Enlargement may be due to crushing or to plastic flow, depending upon the nature of the material blasted.

Stemming is the material used to fill the borehole above the explosive charge to confine the gases resulting from an explosion.

Stick count is the number of $1\frac{1}{4}$ -in. by 8-in. cartridges per 50-lb case.

The **stress-distribution factor** is the term C in the ABC product (see **Energy Utilization Number**, **Rock Factor**; also Chapter III, Section VII). The stress-distribution factor expresses the influence of more than one free-face upon the results of blasting. The effect of the frozen-ground interface upon the results of blasting in frozen Keweenaw silt appears to be related in a complex manner both to the interface ratio and to the depth ratio: As the number of free-faces increases interface ratios and depth ratios must be determined for each face.

Tamping is the act of placing stemming in a borehole or of compacting an explosive or other substance.

The **volume-utilization factor** is the number of cubic feet of excavation or of material broken per pound of explosive.

Weight strength: Manufacturers of explosives rate explosives both on weight strength and on cartridge strength. These terms relate to weight and to volume respectively. The strength of an explosive is relative, but refers to the power or force developed and to the work the explosive is capable of doing. Straight dynamites are rated according to the percentage of nitroglycerine present. Other types of dynamites have the same weight strength if they develop the same strength, weight for weight, or produce the same deflection of a ballistic pendulum.

4. Description, objectives, and scope of the Keweenaw Tests

The Keweenaw Tests were designed to obtain fundamental data needed to produce excavations in frozen ground both for entrenching troops and for structures. They consisted of a series of 16 field experiments together with laboratory tests of specimens of frozen Keweenaw dredge-fill silt. Three hundred and thirty-one crater

blasts were fired in ground frozen to depths ranging from 15 to 24 in. Charge holes ranged from 1 to $8\frac{3}{4}$ in. in diameter and from 4 to 63 in. in depth.

The field experiments were directed towards determining (1) the most efficient type of explosive for producing craters in frozen ground; (2) the fundamental relation between weight of explosive and depth of charge for blasts in frozen ground at various scales; (3) the effects of the diameter of the borehole and the shape of the explosive charge upon the results of blasting; (4) the proper position of the explosive charge relative to the interface between the frozen and the unfrozen soil, and (5) the feasibility of fracturing a layer of frozen ground of finite thickness by placing an explosive charge in the underlying unfrozen material.

The laboratory work was directed towards measuring the physical and elastic properties of the frozen ground to provide, if possible, an index of its elastic or plastic behavior in various stress ranges and obtain data necessary to develop a "rock factor" for use in a crater formula for blasting in frozen ground.

The field and the laboratory work were supplemented by field instrumentation to provide a record of temperature and moisture at various depths within and below the frozen layer, and a record of wind direction, wind velocity, ambient temperature, and maximum and minimum daily air temperature.

5. Selection of explosives

High-velocity explosives are said to have a "shattering action," and low-velocity explosives are said to have a "heaving action." The term hard rock is associated with brittle rocks such as igneous and metamorphic rocks, and the term soft rock is associated with sedimentary rocks and nonmetallic minerals such as salt, gypsum, coal, and potash. Usually, high-velocity explosives are used in blasting hard rocks and low-velocity explosives are used for soft rocks. Thus, according to the popular concept, it might seem logical to assume that low-velocity explosives would be better adapted to blasting frozen ground.

Fundamentally, the terms heaving action, hard rock, and soft rock are relative. Studies of the elastic and plastic behavior of rocks have shown that "soft rocks" may be stronger under lateral confinement in high stress ranges than "hard rocks." It has been shown also that the elastic and plastic properties of a rock are more indicative of its behavior under stress than is the strength of the rock in compression, tension, or bending. It is probable that the "shattering action" produced by high explosives and the "heaving action" by low explosives are due to the properties of the rock as much as to the velocity of the explosion.

The problem of selecting an explosive for blasting in frozen ground resolves itself into three parts: (1) a study of the properties of explosives, (2) a study of the action of various types of explosives in Keweenaw silt, and (3) a study of the physical, elastic, and plastic properties of frozen Keweenaw silt relative to the physical, elastic, and plastic properties of other types of frozen ground or of other types of rocks (if it can be shown that frozen ground behaves as a rock).

Obviously, it would have been impossible to test all types of explosives during the 3 months of field work. Accordingly, four representative types were selected — three commercial explosives and one military explosive.

When detonated unconfined and in the open, nitroglycerine, the principal ingredient of most commercial explosives, has a velocity of 20,000 ft/sec. When other ingredients are added to produce various types of dynamite, the velocity is reduced. The velocity of most military explosives exceeds 20,000 ft/sec. Demolition Block M3 (Composition C-2), the military explosive requested for the tests, has a velocity of 25,100 ft/sec. Unfortunately, we were unable to obtain military explosives, and it was necessary to substitute a high-velocity commercial explosive.

It was desirable to choose explosives with widely differing characteristics so that an appreciable difference in action, attributable solely to the composition of the explosive, might be observed. Because of the conditions of the test, it was necessary also that the

explosives chosen have high resistance to moisture and cold. It may be necessary in certain military applications to select an explosive with good fume characteristics, particularly if the excavation must be occupied immediately after the blast.

Blasting action does not depend solely upon the velocity of an explosive, but also upon the explosion pressure, the energy of the explosion, and the physical and elastic properties of the material blasted. Physical and elastic properties of the frozen ground may be appraised without regard to the composition of the explosive. The energy of the explosion is related to the weight of explosive and thus is within the control of the blaster. Explosion pressure and velocity of detonation both depend upon composition. Explosion pressure and velocity decrease in nitroglycerine-base dynamites as the percentage of nitroglycerine or blasting gelatin decreases. It is not to be inferred that nitroglycerine is the only energy-producing ingredient of high explosives or that velocity is dependent solely upon the nitroglycerine content. The fact that velocity and explosion pressure are dependent upon composition was helpful in choosing the types of explosives for the Keweenaw Tests.

Coalite 7S, Gelodyn 1, and Atlas 60 Percent Straight Gelatin were selected because they represent a complete range in velocity of commercial explosives; their velocity ranges do not overlap; and their water resistance, cold resistance, and fume characteristics meet the requirements of blasting in frozen ground. Coalite 7S is an Ammonia-Base Permissible explosive such as is used in coal mining. The "heaving effect" characteristic of low-velocity explosives such as black powder is characteristic of Coalite when used in blasting coal. Gelodyn 1 is a semi-gelatin generally recommended for cratering in rock. Gelodyn 1 has a higher velocity than Coalite 7S but lower than Atlas 60 Percent Straight Gelatin.

When it became evident that Demolition Block M3 (Composition C-2) could not be obtained for the Keweenaw Tests, Atlas 80 Percent Straight Gelatin was substituted. Its velocity is equal to that of either blasting gelatin or nitroglycerine, the highest obtainable with commercial explosives, but only 1000 ft/sec more than that of Atlas 60 Percent Straight Gelatin when detonated under confinement using a strong primer.

6. Classification and properties of commercial explosives

Each of the major manufacturers of commercial explosives, for all practical purposes, produces equivalent types of explosives (see Table I). Commercial explosives containing nitroglycerine may be divided into three types: nitroglycerine dynamites, gelatin dynamites, and permissible explosives. Nitroglycerine is the base for nitroglycerine dynamites. The base for gelatin dynamites is blasting gelatin, which consists of nitroglycerine and guncotton.

Properties of various types of dynamite are related to the properties of nitroglycerine and blasting gelatin. Nitroglycerine is a liquid, is insoluble in water, explodes when heated to 392°F, is sensitive to shock, is difficult to transport, and detonates unconfined in the open at a velocity of 20,000 ft/sec. Blasting gelatin contains 90-93 parts of nitroglycerine to 7-10 parts of guncotton. It is a tough, elastic, jelly-like mass, with a texture like that of Para rubber. It is highly water-resistant, is less sensitive to shock and friction than nitroglycerine, is safe to handle except when frozen, and detonates at the same velocity as nitroglycerine.

Permissible explosives were developed for use in coal mines where there is danger of explosions of mine gas and coal dust due to flame issuing from blast holes. By reducing the temperature and duration of the flame, the coal-mine explosion hazard is minimized. Both nitroglycerine and blasting gelatin have high explosion temperatures. Gelatinous Permissibles are made by adding large quantities of ammonium chloride or sodium chloride to gelatin dynamites. Ammonia-Base Permissibles are made by adding large quantities of ammonium nitrate or cellulose to nitroglycerine dynamite, thus minimizing the percentage of the high-flame-temperature ingredient.

The essential ingredients of the three principal types of explosives are presented in chart form in Table I. Straight Dynamite is a nitroglycerine dynamite made by adding sodium nitrate and cellulose or other combustible to nitroglycerine. Straight Gelatin

differs from Straight Dynamite only in that the ingredients are added to blasting gelatin as an explosive base rather than to nitroglycerine. Extra Dynamites are made by adding ammonium nitrate to Straight Dynamite, or by replacing sodium nitrate with ammonium nitrate. Extra Dynamites are sometimes known as Ammonia Dynamites. Gelatin Extra is equivalent in the gelatin dynamite series to Extra Dynamite in the nitroglycerine dynamite series.

When nitroglycerine explodes, all the products of combustion are gases. These combustion products are carbon dioxide, water vapor, nitrogen, and oxygen. Incomplete combustion, a deficiency of oxygen, or an excess of oxygen produces toxic fumes such as carbon monoxide, oxides of nitrogen, or hydrogen sulfide. In general, the higher the nitroglycerine content of a dynamite, the greater is the volume of the resulting gas and the greater the likelihood that poisonous fume will be present. Thus, as indicated by the arrows in Table I, fume decreases as the nitroglycerine content of the various types of dynamite decreases.

Dynamites that absorb water have their efficiency impaired. Nitroglycerine is insoluble in water. Sodium nitrate and ammonium nitrate absorb water and are deteriorated. As shown in Table I, water resistance decreases as the nitroglycerine content decreases or as sodium nitrate or ammonium nitrate is substituted for nitroglycerine. Increasing the thickness of the paraffin coating on an explosive cartridge increases the water resistance of the wrapper, but the paraffin is converted to smoke (solid particles) upon detonation. Moreover, a paraffin-dipped cartridge is little protection if the wrapper is broken by tamping the charge to fill a wet borehole. Tamping to fill a borehole increases the charging density and in turn the borehole pressure and is generally considered to be good blasting practice in underground metal mining.

The velocity of an explosive is its rate of detonation or the rate at which the detonation wave passes through the explosive, converting it from a solid to a gas. Reducing nitroglycerine content of a commercial explosive by adding other ingredients decreases the velocity, because the velocity of other ingredients is less than that of nitroglycerine or blasting gelatin. Velocity of detonation is influenced also by confinement and by cartridge size. Nitroglycerine dynamites detonate at a higher velocity when confined. Large cartridges detonate at a somewhat higher rate than small cartridges. Although blasting gelatin contains from 90-93% nitroglycerine, straight gelatins, which contain blasting gelatin as the explosive base, have the peculiar property of detonating at a much lower rate when unconfined than when confined. In the Keweenaw Tests, all charges were detonated with Primacord, which acts as a "booster" or strong primer; all were confined in a borehole in frozen ground; and all were tamped with sand stemming.

Nitroglycerine does not have high resistance to freezing, but manufacturers can regulate the cold resistance of nitroglycerine-base dynamites by adding antifreeze. If it is necessary to use commercial explosives at extremely low temperatures, the manufacturer should be notified so that he may add the proper quantity of antifreeze when mixing the explosive ingredients. Apparently, a standard test has not been developed to measure cold resistance. The cold resistance of various types of explosives seems to be based upon the experience of the manufacturer in the handling and the storage of explosives in cold climate.

7. Characteristics of explosives in the Keweenaw Tests

Characteristics of explosives used in the Keweenaw Tests are summarized in Table II. Fume and resistance to water and cold are rated from 1 (best condition) to 4 (poorest condition). The stick count is the number of 1 $\frac{1}{4}$ -in. by 8-in. cartridges in a 50-lb case. Cartridge strength and weight strength are defined above (Ch. I, 3).

Comparison of explosives of different weight strengths must be made on an "absolute weight strength" basis, which credits each of the energy-producing constituents for the proportion of the total energy it contributes (Table III).

EXCAVATIONS IN FROZEN GROUND

Table I. Classification of explosives

TYPE	ESSENTIAL INGREDIENTS	REMARKS	ATLAS	HERCULES	DU PONT
COMMERCIAL EXPLOSIVES CONTAINING NITROGLYCERINE	NITROGLYCERINE	$C_3H_5(NO_3)_3$	ATLAS NITROGLYCERINE	HERCULES NITROGLYCERINE	DU PONT NITROGLYCERINE
	STRAIGHT DYNAMITE	$C_3H_5(NO_3)_3 + NaNO_3 + C_{12}H_{22}O_{11}$	GIANT NITROGLYCERINE DYNAMITE	HERCULES NITROGLYCERINE DYNAMITE	DU PONT STRAIGHT DYNAMITE
	EXTRA DYNAMITE	$C_3H_5(NO_3)_3 + NaNO_3 + C_{12}H_{22}O_{11} + NH_4NO_3$	ATLAS NITROGLYCERINE DYNAMITE	HERCULES DITCHING DYNAMITE	RED CROSS EXTRA RED CROSS BLASTING FN DU PONT EXTRA
	BLASTING GELATIN	STRAIGHT DYNAMITE + AMMONIUM NITRATE	GIANT EXTRA, ATLAS EXTRA APEX, FLO-DYN AMODYN, APCODYN	HERCULES EXTRA HERCULITE HERCOMITE	DU PONT BLASTING GELATIN
	STRAIGHT GELATIN	$C_3H_5(NO_3)_3 + C_{12}H_{22}O_{11} + NaNO_3 + C_6H_6O_6$	ATLAS BLASTING GELATIN	HERCULES BLASTING GELATIN	DU PONT GELATIN
	BLASTING GELATIN	BLASTING GELATIN + SODIUM NITRATE + CELLULOSE	ATLAS STRAIGHT GELATIN	HERCULES GELATIN	HI VELOCITY GELATIN
	STRAIGHT GELATIN	$C_3H_5(NO_3)_3 + C_{12}H_{22}O_{11} + NaNO_3 + C_6H_6O_6 + NH_4NO_3$	GIANT GELATIN	HIGH PRESSURE GELATIN	DU PONT SPECIAL GELATIN
	EXTRA GELATIN	STRAIGHT GELATIN + AMMONIUM NITRATE	SELODYN	HERCULES GELATIN EXTRA GELAMITE	SELEX
	PERMISSIBLES	$C_3H_5(NO_3)_3 + C_6H_6 + NaNO_3 + C_6H_6O_6 + NH_4NO_3 + NH_4Cl + NaCl$	SELCOALITE	HERCOGEL	SELABEL
	PERMISSIBLES	STRAIGHT GELATIN + AMMONIUM CHLORIDE + SALT or GELATIN EXTRA + AMMONIUM CHLORIDE + SALT			
PERMISSIBLE EXPLOSIVES	PERMISSIBLES	$C_3H_5(NO_3)_3 + NH_4NO_3 + C_6H_6O_6$			
	PERMISSIBLES	LOW PERCENTAGES OF NITROGLYCERINE AND HIGH PERCENTAGES OF AMMONIUM NITRATE AND CELLULOSE	COALITE	HERCULES RED H HERCULES COLLIER C HERCULES BITUMINITE-D	DUOBEL MONOBEL LUMP COAL C

Table II. Characteristics of explosives used in the Keweenaw tests.

Explosive	Velocity (ft/sec)		Resistance		Fume	Stick Count	Strength	
	Confined	Open	Water	Cold			Cartridge %	Weight %
Atlas 80% Straight Gelatin	21,000	20,000	1	2	3	100	80	72.6
Atlas 60% Straight Gelatin	20,000	16,000	1	2	1	97	60	52.3
Gelodyn 1	14,000	10,000	2	2	1	110	55	64.6
Coalite 7S	10,000	8,000	2	2	1	120	44	61.9

Table III. Absolute weight strength of commercial explosives used in the Keweenaw tests.

Explosive	Weight Strength	Velocity (ft/sec)	Absolute Weight Strength
Atlas 80% Straight Gelatin	72.6	21,000	83.1
Atlas 60% Straight Gelatin	52.3	20,000	70.6
Gelodyn 1	64.6	14,000	78.2
Coalite 7S	61.9	10,000	76.6

Table IV. Absolute cartridge strength of commercial explosives used in the Keweenaw tests.

Explosive	Weight Strength	Velocity (ft/sec)	Absolute Cartridge Strength
Atlas 80% Straight Gelatin	80	21,000	87.7
Atlas 60% Straight Gelatin	60	20,000	75.4
Gelodyn 1	55	14,000	72.3
Coalite 7S	44	10,000	65.7

When all commercial explosives had a standard count of one hundred $1\frac{1}{4}$ x 8-in. cartridges per 50-lb case, the weight strength and the cartridge strength were the same. As the industry progressed, explosives were marketed in various diameters of cartridges and in various densities. Although all manufacturers have not adopted the same standard, it is generally recognized that cartridge strengths should be compared on a basis of one hundred $1\frac{1}{4}$ -in. by 8-in. cartridges per 50-lb case.

The cartridge strength of a $1\frac{1}{4}$ x 8-in. stick of any type of explosive is the same as the weight strength of a 0.50-lb cartridge of straight dynamite $1\frac{1}{4}$ in. in diameter by 8 in. in length if they produce the same deflection of the ballistic pendulum.

To compare explosives on a cartridge-strength basis, "absolute cartridge-strength" should be used (Table IV).

8. Comparison of Atlas, Hercules, and Du Pont nitroglycerine-base explosives

Although Atlas explosives were used for the Keweenaw Tests, the results obtained should be indicative of those obtainable using comparable explosives of other manufacturers. The close relation between chemical composition and explosive characteristics has been pointed out. It follows that if the composition of the explosives produced by different manufacturers is the same, the blasting characteristics of the two explosives also will be the same.

Accordingly, if the various grades of explosives produced by different manufacturers are classified as Nitroglycerine Dynamite, Gelatin Dynamite, or Permissible Explosive and arranged in order of decreasing weight strength as in Table I, explosives having similar chemical composition and therefore similar blasting characteristics may be compared. For example, Gelcoalite, Hercogel, and Gelobel are Atlas, Hercules, and Du Pont trade names for Gelatinous Permissibles.

Each of the different types of explosives is manufactured in several weight strengths and cartridge strengths. For example, it is possible to select a type of Du Pont Duobel or a type of Hercules Red H that is equivalent to Atlas Coalite 7S. It is also possible to select a type of Du Pont Gelex or a type of Hercules Gelamite that is equivalent to Atlas Gelodyn I.

CHAPTER II. TEST PROGRAM

Section I. Field Tests

1. General

As far as possible, the field experiments were planned and carried out so that a reasonable scale relation was maintained between the depth of explosive charge and the depth of frozen ground. Exploratory drilling of the test site showed that the depth of frozen ground was not uniform but varied with the thickness of snow cover, the proportions of sand and silt, and the thickness and distribution of layers of carbonaceous material deposited with the dredge fill.

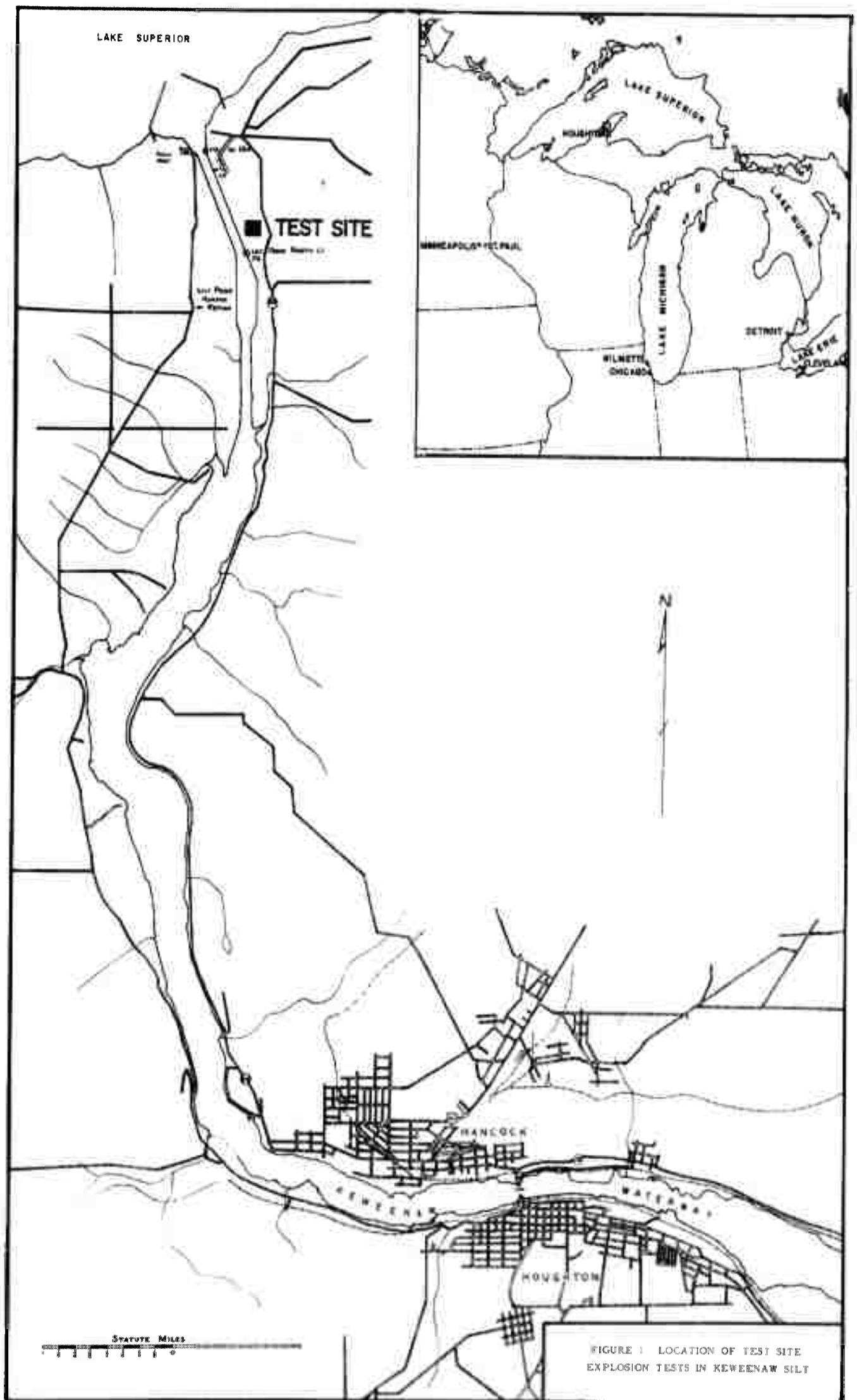
The tests were planned to investigate one variable at a time. In the first experiments, the interface ratio was held practically constant. In deciding what interface ratio to use, the frozen layer was considered analogous to a reinforced concrete slab used in tests of penetration of artillery projectiles. It was reasoned that scabbing of the rear face of the concrete slab due to penetration of a projectile must bear some relation to critical depth. The rear face of the slab would be equivalent to the interface between the frozen and unfrozen ground. Thus, if the nose of a projectile entering the slab is equidistant from the front face and the rear face, the projectile should have the same effect on both faces. Although the rear face of the slab and the frozen ground interface are not equivalent so far as transmission of energy across the interface is concerned, it is reasonable to assume that energy transmitted equal distances towards the two faces would affect both faces to the same degree. Thus, it was concluded that, if an interface ratio of 0.5 or less could be maintained, a reasonable correlation might be possible between critical-depth blasts in frozen ground and critical-depth blasts in other mediums such as rock and soils.

We have assumed that the frozen-ground interface might greatly influence the manner of failure and the results of blasting in frozen ground. This may not be true, but the possibility was not overlooked in planning the experiments.

2. Test site

The site was selected and prepared for the field tests by SIPRE personnel before the Mining Research Corporation blasting party arrived. The site is on U. S. Government property on the east shore of the Keweenaw Waterway, which was used as a spoil bank for hydraulic disposal of sand and silt dredged from the channel about 15 years ago. The site is located about 9 mi north of Hancock, Michigan, and $\frac{1}{2}$ mi from the Coast Guard Station at the upper entrance to Keweenaw Waterway in Houghton County, Michigan (Fig. 1). Factors considered in choosing this site were:

- (a) Mean winter temperatures as indicated by U. S. Weather Bureau records.
- (b) Accessibility of the area.
- (c) Proximity to a laboratory equipped to make the required tests of frozen ground.
- (d) Freedom of the soil from stone and boulders, and uniform composition over the site.
- (e) Exposure to wind, which would aid in keeping snow removed from the working area.
- (f) Government ownership of the land and the distance from structures damageable by air blast, ground shock, or flyrock.
- (g) Cost of clearing and leveling the site.



A preliminary exploration of the test site was made in October 1953 to determine its suitability from the standpoint of soil type and areal extent. The exploration consisted of drilling approximately 30 test holes throughout the area with hand-operated helical augers. The boreholes were spaced to provide complete coverage of the site. Each test hole was extended through the hydraulic fill into the underlying native soil. The results of this preliminary investigation indicated that an area approximately 500 ft square would be suitable as a site for the field tests. The soil in the test area is predominantly silt containing small amounts of organic matter. In general, the silt is stratified with thin lenses of sand and organic deposits which do not appear to be continuous. The exact classification of the soils in the test area, based on the Corps of Engineers Unified Soil Classification System, depends largely on the degree of stratification. Classifications assigned to the soil types found in the area include silt (ML and MH), silt (OL and OH), sandy silt (OL), and silty sand (SM and OL). The predominant types are silt (OL) and sandy silt (OL). Mechanical analyses were made on many soil samples from the test area during the field program. Based on these tests, representative gradation curves have been selected to indicate the range of grain size distribution in the test area (Fig. 2). Plasticity tests conducted on representative samples from the test area indicate that the silty soils are, in general, either non-plastic or of low plasticity. At the outer limits of the test area, sand strata, varying from 1 to 2 ft thick, were encountered within 3 ft of the ground surface. Because of the lack of homogeneity in the stratification at and beyond the limits of the established test area, it was concluded that future expansion of the area would not be feasible.

The preliminary exploration indicated that the artificially deposited silt in the test area is approximately 7 ft deep and is underlain by a highly organic silt (OH). This native soil was found to have high moisture content at the time of sampling, ranging from approximately 50% to slightly more than 100%. An examination of the organic matter contained in the native soil indicated that the soil has been in a saturated or near-saturated condition for a considerable period of time. Based on these findings and an examination of the adjacent terrain, it is considered likely that the dredged fill, in which the explosion tests would be conducted, had been deposited in swamp land. Water table measurements made during the preliminary exploration showed the free water surface to be approximately 5 ft below the surface of the dredged fill. Figure 3 shows the test site at the height of the winter after snow removal and Figure 4 shows the site in March 1954 during a spring thaw.

The preliminary exploration indicated that the artificially deposited silt in the test area is approximately 7 ft deep and is underlain by a highly organic silt (OH). This native soil was found to have high moisture content at the time of sampling, ranging from approximately 50% to slightly more than 100%. An examination of the organic matter contained in the native soil indicated that the soil has been in a saturated or near-saturated condition for a considerable period of time. Based on these findings and an examination of the adjacent terrain, it is considered likely that the dredged fill, in which the explosion tests would be conducted, had been deposited in swamp land. Water table measurements made during the preliminary exploration showed the free water surface to be approximately 5 ft below the surface of the dredged fill. Figure 3 shows the test site at the height of the winter after snow removal and Figure 4 shows the site in March 1954 during a spring thaw.

3. Field test procedure

a. Site preparation. In the fall of 1953, a bulldozer was used to remove the brush, small trees, and humus and to level the soil on three strips, each about 150 ft wide and

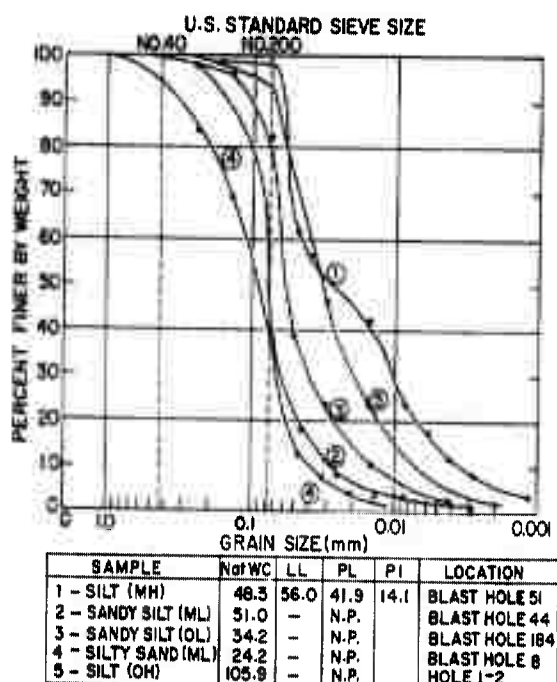


Figure 2. Grain-size distribution in typical soils from the test site.



Figure 3. View of test site cleared of snow.



Figure 4. View of test site during spring thaw.

500 ft long, to the east, southeast, and south from a common corner. After this clearing, the site was laid out in a 50-x 50-ft grid system. Reference stakes were set at irregular intervals at convenient points in each lane. A preliminary examination of the site showed a variation in soil from clean sand to carbonaceous silt. The approximate boundary of the sand areas was marked on a map which served as a guide in laying out the blast holes in the winter.

b. Instrumentation. After the site had been cleared and leveled, but before the weather became cold, four instrumentation holes were drilled at 150-ft intervals along the centerline of the east-west lane of the test site. In these holes, moisture and temperature cells were installed at depth intervals of 6 in. below the surface. The purpose of this instrumentation was to permit accurate determination of the ground temperatures throughout the test area during the explosion tests and to provide an indirect means of observing the fluctuations of the interface between frozen and unfrozen soil. The exact depth of freezing at specific blast holes was measured directly. Two types of soil temperature units were installed, a commercial instrument known as the Colman soil-moisture unit and an experimental unit designed by SIPRE personnel. The latter was designed specifically to provide a minimum of soil disturbance when inserted and a continuous contact with the surrounding soil during subsequent shrinkage and swelling.

The Colman unit consists of a moisture-sensitive element composed of two Monel screen electrodes separated by two thicknesses of glass fiber cloth and wrapped around with three thicknesses of the same material, and a thermally sensitive element composed of a model 7A thermistor manufactured by the Western Electric Company. The thermistor has a resistance of approximately 1000 ohms at 77° F. It has a high temperature coefficient which makes corrections for lead-wire resistance unnecessary and increases the ease with which accurate temperature determinations can be made. The electrical resistance between the screens of the moisture-sensitive element vary in response to changes in moisture content of the soil in which the unit rests. This element is particularly useful for determining whether the soil water is frozen since the resistance rises very abruptly as the soil moisture freezes.*

* For a detailed description of the Colman instrument see: Colman, E. A., and Hendrix, T. M. (1949) The Fiberglass Electrical Soil-Moisture Instrument, Soil Science, vol. 67, no. 6.

The experimental unit designed at SIPRE is composed of two $2\frac{1}{16}$ in. diam stainless steel probes into which thermocouples have been cemented. The probes are $1\frac{1}{2}$ in. long and are set 1 in. apart. The SIPRE bare-wire probe is shown in Figure 5.

The Colman units were installed in four instrumentation holes, I-1, I-2, I-3, and IX-1, at depths of 6, 12, 18, and 24 in. and at the bottom of the hole, which was generally 44 in. below the ground surface. The bare-wire probes were installed in Hole IX-1 at the same depths as the Colman units.

Recording cables were run in trenches from the instrumentation holes to measuring stations along the south side of the lane.

Figure 6 shows the variations in temperature of the Keweenaw silt at 6- and 12-in. depths during the field experiments. At the two gage positions, freezing did not reach the 18-in. depth.

An 8-x12-ft shelter house was built directly over the origin station of the grid system with windows to command a view over the entire site. A kiosk was erected nearby to house a Weather-Bureau-type maximum-minimum thermometer. A recording anemometer was installed on top of the shelter cabin.

After blasting tests had begun, it was found desirable to have information on the depth of the water table. Mining Research Corporation drilled four $2\frac{1}{2}$ -in. holes 12 ft deep and installed casing. The depth of the water table was found to range from 5 to 6 ft below the surface, depending upon the elevation of the ground surface.

c. Snow removal. To permit deep penetration of frost, it was necessary to keep snow cleared from the site. However, because manufacturers failed to deliver the snowplows as promised, a foot or more of snow was left on the site during several weeks of freezing weather. Finally, agreements were made to have the Houghton County Highway Department do the necessary plowing with a Sno-Go rotary plow shortly before the arrival of the Mining Research Corporation party. SIPRE snow-removal equipment was put into operation toward the end of the field work. Snowfall was considerably less than normal, lightening the removal job. However, frequent strong winds made troublesome drifts that, over parts of the site, kept the ground from freezing more than a foot deep. In addition, temperatures were much above normal during the winter, and frost penetration everywhere was far less than anticipated.

d. Determining depth of frozen ground. In view of the above-mentioned conditions, it was realized that the depth of freezing would be limited and must be considered in planning the tests. The first step, then, was to determine the actual depth of frozen ground at various locations on the site. On January 21, 1954, 16 holes were drilled through the frozen ground in lines near the north end, the middle, and the south end of the site. In places protected by deep snow the ground had not frozen. The maximum depth of frozen ground was found to be $18\frac{1}{2}$ in. Obviously, some parts of the site had not then frozen sufficiently deep for the blasting tests. At this time, the depth of freezing was greater in the sandy silts than in the clayey silts. Blasting tests were begun in areas where frozen ground was deepest. The depth of freezing also determined the scale ratio at which tests were begun. The depth of frozen ground at specific locations (see data sheets) was determined before each blasting test by wagon drilling, jackhammer drilling, auger drilling, or diamond drilling.

e. Soil sampling and coring. Soil samples were obtained during the progress of the explosion tests to provide positive identification of soil type and to provide specimens for detailed laboratory tests. The identification samples were obtained principally from the cuttings obtained from the blast hole drilling and from the holes drilled to determine the depth of frozen ground.

Undisturbed samples of frozen ground were obtained (1) with a diamond drill using an NX core barrel, but using compressed air rather than water as a circulating medium; (2) with thin-wall open-drive samplers of 2-in. diam; and (3) from chunk samples of the material broken by the explosion. These samples, which were used for detailed testing, were obtained at the blast hole sites both before and after the explosion test. The diamond core samples taken prior to the explosion tests were used for a series of

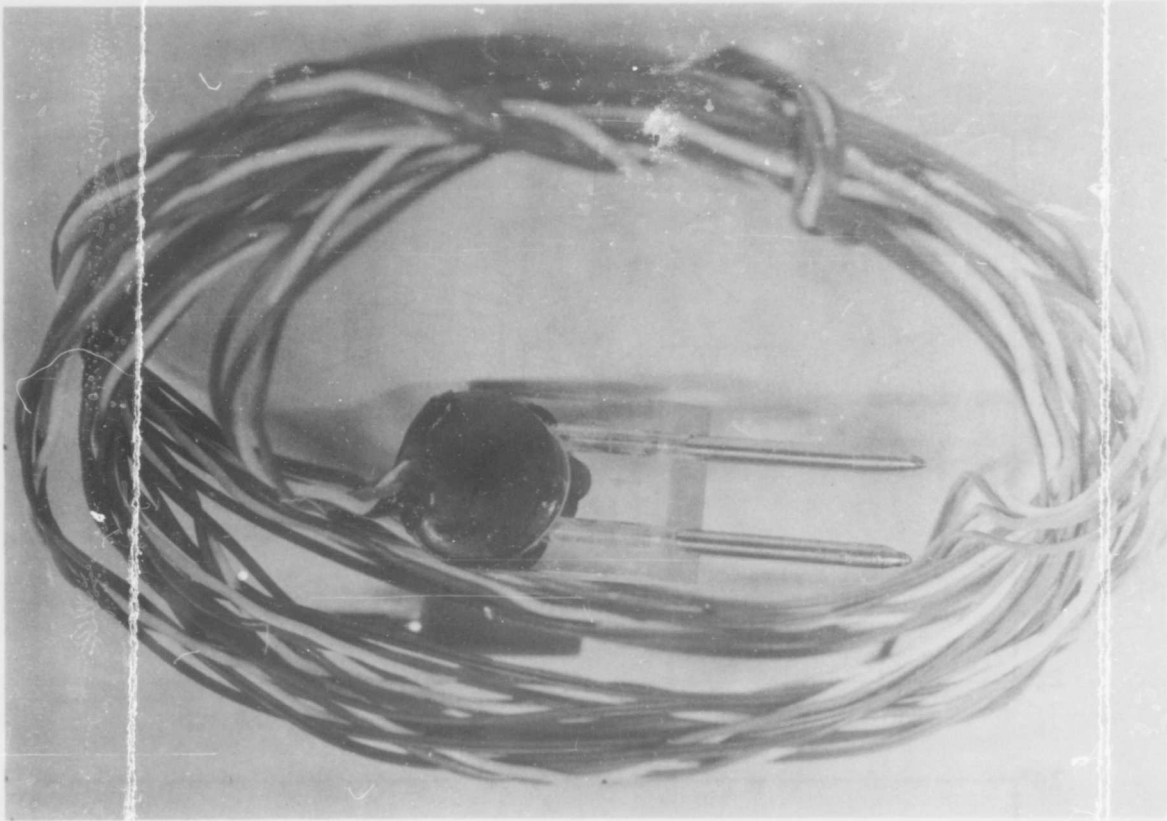


Figure 5. SIPRE bare-wire temperature probe.

unconfined compression tests, which are described in Section II of this chapter. The undisturbed samples taken after the explosion tests were used principally for study of the blast effects on the soil structure. In the sampling operation after the explosion, special attention was focused on the craters produced by the large-scale blasts. Samples with the thin-wall open-drive sampler were taken of the individual layers of disrupted material at the crater rims; of the frozen material which extended beyond the zone of disturbance; and of the unfrozen material both in the disturbed and undisturbed zones.

Figure 7 shows the Mining Research Corporation drill rig. The photograph shows the NX core barrel attached to EX rods and the air line from the compressor to the "air swivel" attached to the EX rods.

Two types of coring bits were tested. One type was set with industrial diamonds, the other with tungsten carbide inserts. The core barrel and the tungsten carbide insert coring bit are shown in Figure 8. Core recovery with the diamond bit was superior to that with the tungsten carbide bit, but it is probable that both the design of the tungsten carbide bit and the technique of coring in frozen ground can be improved.

A variation of the core-drilling technique was employed to recover 10-in. diam cores of frozen ground, using a modified calyx-type barrel equipped with diamond inserts (Fig. 9). Air was used as the circulating fluid. The rate of rotation was reduced to 100 rpm for the large holes. A split-barrel type of core retriever (Fig. 9) was used to break off and lift the core from the drill hole. Figure 10 shows a typical core sample after extrusion from the diamond core barrel.

EXCAVATIONS IN FROZEN GROUND

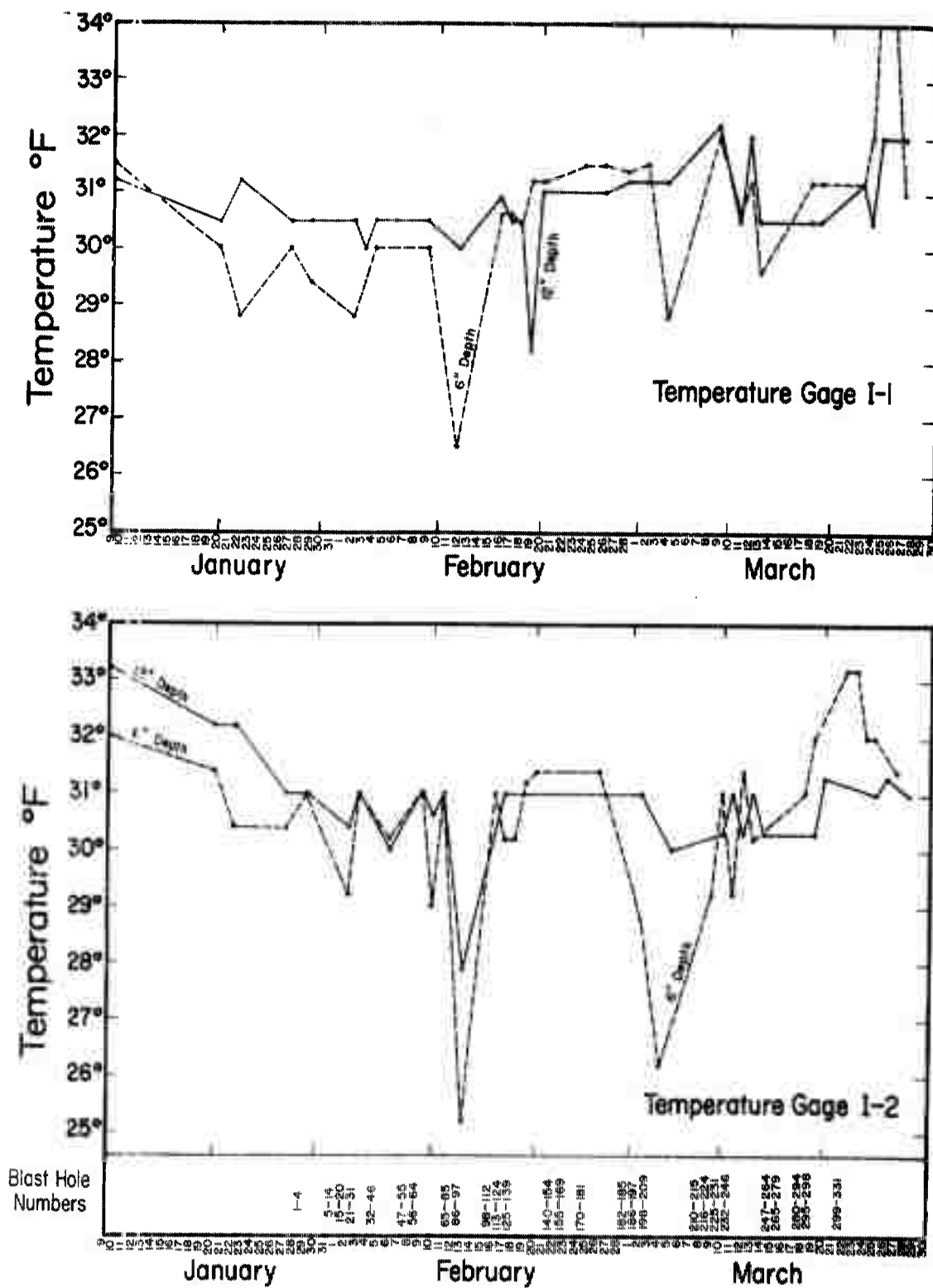


Figure 6. Temperature variations in the Keweenaw silt during the test period, 1954

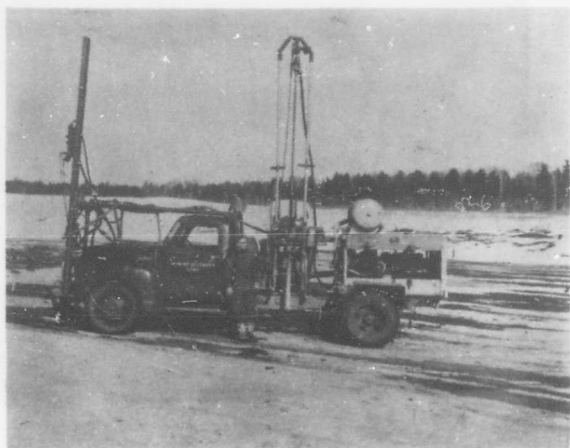


Figure 7. Mining Research Corporation drill rig. Wagon drill mounted at front, diamond drill in center, and air compressor at rear.

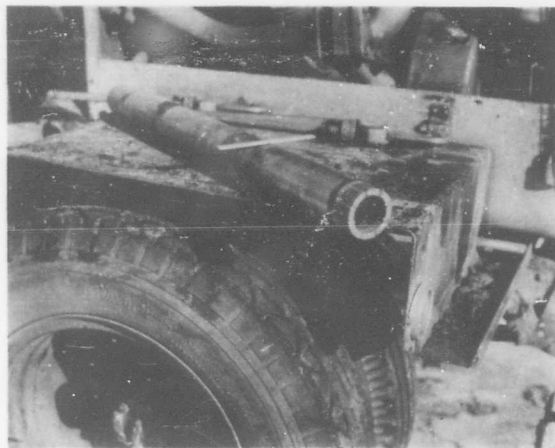


Figure 8. Core barrel and tungsten carbide insert coring bit used in the tests.

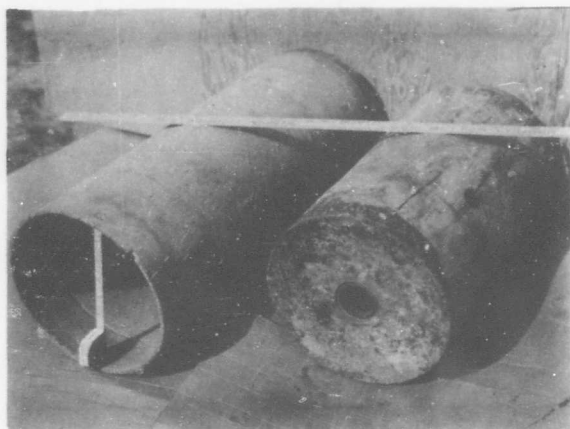


Figure 9. Modified calyx barrel and core retriever. Shows cutting edge of barrel set with diamonds and top of core lifter threaded to fit on EX drill rods.

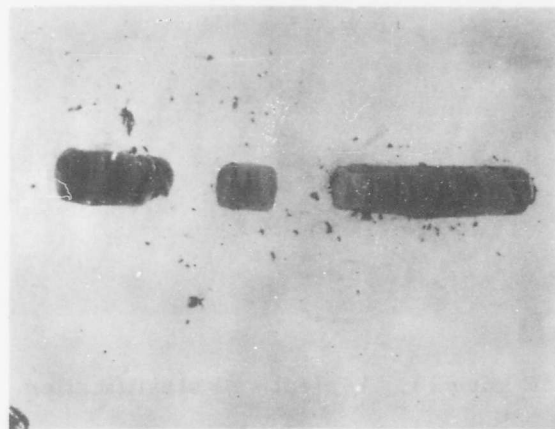


Figure 10. Diamond core sample removed from core barrel.

Figure 11 shows the techniques used in obtaining samples with the thin-wall open drive sampler. The sampler is forced into the frozen or unfrozen soil by either driving or under a steady pressure. The soil adjacent to the sampler tube is then excavated and the tube removed.

Figure 12 shows the type of frozen ground samples which can be obtained from chunks of the material broken by each blast. The effectiveness of this method depends upon the degree of fragmentation of the broken materials. It is impossible to obtain satisfactory samples of the ground immediately adjacent to the explosive charge because of crushing and flowage. In certain blasts when the weight of charge was light relative to the depth of charge, the ground was broken in large slabs that were found to be ideal for preparing test cylinders.

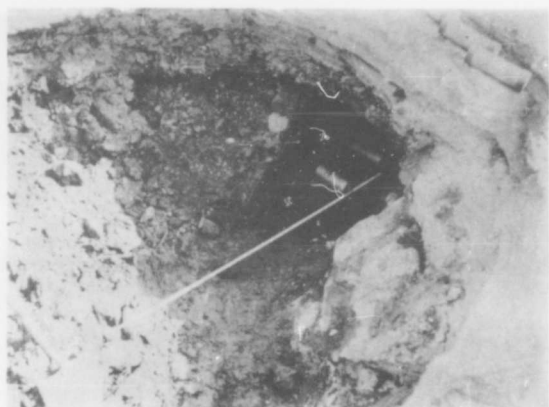


Figure 11. Sampling technique with thin-wall sampler.



Figure 12. Chunks of soil disrupted by explosion.



Figure 13. Typical soil stratification



Figure 14. Distortion of strata due to explosion pressure.

Many photographs were taken of the blast holes, particularly of the walls of the large craters after they were trimmed and polished to an inclined plane surface. Thus, much detail relating to the stratification of the soil and the layered systems resulting from the blast has been preserved for future study. Figure 13 shows the stratification and layered systems in one of the crater walls. In Figure 14, the effect of the explosion pressure on the soil stratification can be clearly seen by examining the small chunk of frozen material near the center of the figure. The stratification has been severely bent and folded by the explosion.

Unsuccessful attempts were made to lift a profile of one of the crater walls by spraying the surface with plastic. However, it was possible to remove a single layer of soil which clearly indicated grain size distribution and lens detail. The plastic coating did not prove to be sufficiently durable for the technique to be of value.

The following observations can be made as a result of visual inspection of many of the craters and a study of the drilling data.

- (1) The zone of disturbance resulting from the explosion extends a considerable

distance laterally from the crater walls, in many cases as much as 20 ft.

(2) There does not appear to be a marked decrease in the intensity of the disturbance with increased lateral distance from the crater walls. This would indicate that the explosion pressure produced a mass movement of the soil rather than a local distortion.

(3) The blast effect on the unfrozen soil appears to lessen abruptly at a certain depth below the base of the crater, at which point little disturbance of the soil is distinguishable.

(4) There does not appear to be a definite relationship between the position of the water table and the cratering action in the soil. It is believed that instruments which will measure the acceleration of the shock waves in the ground water may be proper tools for future study of this kind.

f. Layout of the test site. The layout was controlled by two factors: (1) the depth of frost in different parts of the site and (2) the need to avoid interference with the operation of the snow plows (a snow plow cannot operate over blasted ground). Accordingly, the blast holes were drilled, and blasting was begun, at the far end of each cleared strip in rows at right angles to the centerline of the strip. Drilling and blasting retreated in rows as the tests progressed. This basic plan was varied later, when thawing made some spots inaccessible to the drill truck. At that time, snow removal was not an important factor, and the later holes were located to avoid puddles of water.

g. Spacing of blast holes. The spacing between blast holes depends upon the scale of the blast and upon the r/d ratio of the largest crater that might be produced. The r/d ratio of a crater in any type of ground depends upon the relation between the weight of explosive charge and the depth of the charge. The r/d ratio is greater in brittle rocks than in plastic rocks. This feature is a fundamental characteristic influencing the results of blasting.

The r/d ratio for craters in frozen ground was unknown prior to blasting. Frozen ground, because of its high Poisson's ratio, perhaps behaves plastically and produces craters smaller than those in granite. The r/d ratio for craters in granite approaches 3.0 for moderately heavy blasts which produce conical-shaped craters. This ratio, probably greater than the r/d ratio for frozen ground, was used in planning the spacing of blast holes in the blasting test. The holes were spaced a distance apart equal to 4 times the crater radius, thus providing for a rib of undisturbed ground of width equal to $2r$ (or one crater diameter) between adjacent craters. Using an r/d ratio of 3.0 and a height of charge equal to two-thirds the depth of hole is equivalent to providing a space between holes of 7.64 times the depth of center of gravity of the charge. In planning the layout of the blast holes, a spacing of 8 times the depth of hole was used. The correctness of these assumptions was demonstrated by the first few blasts.

h. Blast-hole drilling. Blast holes ranged from 1 to $8\frac{3}{4}$ in. diam and from 4 to 63 in. in depth. Several different drilling methods were used, depending upon the diameter and depth of hole to be drilled.

The 1-in. holes were bored by hand, using an ordinary ship auger equipped with a ratchet handle, although a regular brace would have been better.

Holes from $1\frac{1}{2}$ to 2 in. diam were drilled with a hand-held 56-lb pneumatic rock-drill (jackhammer). A few holes larger than 2 in. diam were drilled with the hand-held rock-drill because of its portability, but the wagon drill was preferred.

The wagon drill is a larger rock-drill than the hand-held 56-lb machine. The machine used by Mining Research Corporation was a standard Gardner-Denver D73 drill with a 10-ft chain feed, mounted on the front of the drill truck (Fig. 15). Sectional 1-in. hexagonal drill rods, bit adapters, and chuck stubs were used. Except for the larger range of bit sizes used (from 2 to 5 in. diam) the wagon-drilling equipment used for the Keweenaw Tests is standard equipment for deep-hole drilling in sandstone. All drills were equipped with two line lubricators: one for light rock-drill oil, and the other



Figure 15. Drilling with the wagon drill. Used for 2-5 in. holes. Because of the 30°F ground temperature, the cuttings were removed like rock cuttings.

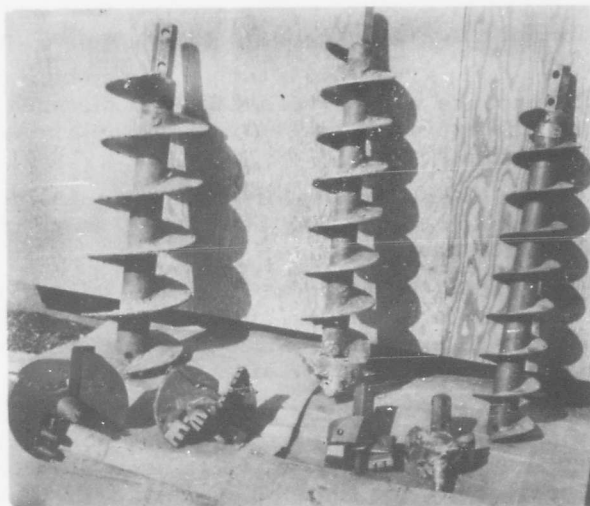


Figure 16. Ka-Mo augers and cutting heads. The long center-screw heads, shown at extreme right and left of photo, did not penetrate the soil as well as the pilot-screw heads, shown in center.



Figure 17. Auger drilling with the Mining Research Corporation rig.

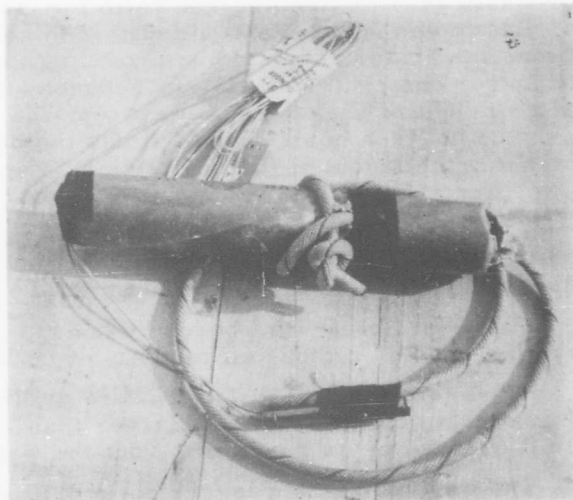


Figure 18. Priming technique. Charges were primed by a piece of Primacord threaded through the charge. A No. 6 blasting cap was taped to one end of the Primacord.

for alcohol to prevent freezing of the machine and drill lines. On cold days when ground temperatures were below 30°F, the rock-drills worked faster and removed the cuttings with compressed air better. Below 30°F, frozen ground drills like a rock, and the cuttings are removed like rock cuttings. As the ground temperature rises, the frozen ground is penetrated more slowly by the drill. Under the friction of impact and rotation, the drill cuttings turn to mud, which plugs the air holes in the bit and may eventually fill up the hollow drill rod. The cuttings are trapped between the rod and the drill hole, ball up, and cannot be removed by compressed air. They must be pulled up as a plug, using the wagon-drill chain feed. The plugged rods must be thawed out over a fire and cleaned, using either compressed air or a stiff wire.

It was found possible to drill holes from 2 to 5 in. diam with the wagon drill. Perhaps the most effective range with the wagon drill is 2 to 3 in. diam. Holes larger than 3 in. require large compressor capacity and perhaps a heavier machine than the D73.

Holes from 5 to 8 in. were drilled with an auger. Two types of "Ka-Mo" cutting heads were tried (Fig. 16). The long center-screw-type heads were found to penetrate frozen Keweenaw silt at a much slower rate than the short, adjustable, pilot-screw-type bits. The action of the augers and the arrangement of equipment on the Mining Research Corporation drill rigs are shown in Figure 17.

i. Blasting procedure. Charges were made up from specifications of charge weight and type of explosive previously computed for each test. A knot was tied in the end of a piece of Primacord and the Primacord threaded through the charge (Fig. 18). The explosive cartridge was taped with electrician's tape to reinforce the cartridge wrapper and prevent loss of powder in transporting the charges to the blast hole. A Number 6 electric blasting cap was taped to the other end of the Primacord to bind the two together securely. A 30-in. length of Primacord was used for all blast holes less than 24 in. deep. It was necessary to increase the length of the Primacord in deep holes so that the electric blasting cap would be out of the drill hole and lie above the ground without any sharp bends. Comparatively few holes deeper than 24 in. were blasted. Charging procedure included the following steps:

1. The depth of the hole was measured and compared with test specifications to make sure that there had been no mistake in drilling, and that no loose material had fallen in.
2. If the hole contained loose material it was blown out with compressed air (Fig. 19).
3. When the hole was found to be of the specified depth and clean, the correctly numbered charge was rammed firmly down into the hole with a wooden tamping stick (Fig. 20).
4. The depth to the top of the charge was measured and recorded (Fig. 21).
5. The hole next was filled to the top with coarse, dry sand "stemming" and tamped with a tamping stick (Fig. 22).
6. After tools and equipment were moved to a safe distance, the leg wires of the blasting caps, previously taped to the Primacord, were connected to the ends of a Number 18 duplex rubber-covered lead wire, which was run out from a blasting reel to the firing point.
7. The lead wires of the blasting reel were connected to a Du Pont CD-24 capacitor-type high-voltage blasting box, and the shot was fired. One or more holes were fired at a time, depending on the size of the charges and the possibility of interference.

j. Field analysis and crater surveys. Field analysis was made by Livingston immediately following each shot. General results and any unusual effects of the blast were observed and recorded. The craters were cleaned out by shoveling and blowing with compressed air. It was difficult to decide just where to stop digging in craters which broke through the frozen-ground interface. However, blackening of the soil by hot gas from the explosion sometimes indicated the limits of the explosion cavity. Because of the difficulty of determining the limits of the crater below the frozen-ground



Figure 19. Blowing holes with compressed air to remove loose material.



Figure 20. Tamping the charge. Charge was rammed into the hole with a wooden tamping stick after hole was clean and of the specified depth.



Figure 21. Recording depth to the top of the charge.



Figure 22. Placing stemming material. Hole was filled with dry sand stemming, and tamped with a tamping stick.



Figure 23. Cross-sectioning a crater.

interface and the considerable labor required, no attempt was made to completely clear out craters produced by large blasts placed below the frozen layer. The rim was cleaned back far enough to expose the limits of heaving or fracturing, and the sides of the crater were uncovered down to the frost interface at least.

Then the cleared craters were surveyed by two men using a plane table, alidade, steel tape, and range pole. The craters were mapped in plan view to a scale of 1 in. equals 1 ft. Crater cross sections were made at the same scale. Two vertical sections of each crater were taken at right angles to each other through the center of the drill hole. The crater-profiling rig (Fig. 23) consisted of a frame of two scantlings spaced 2 in. apart and a sliding block riding between them, with a hole through which a rod of dowel stock could slide up and down. The scantlings were graduated each way from the center point for measurements of horizontal distances, and the dowel was graduated from end to end for vertical measurements. The frame was laid across a crater with its center point over the center of the blast hole, and then leveled by using a small level tube attached to it. The dowel stick then was run down through the vertical hole in the sliding block until it touched the bottom of the crater. The horizontal and vertical coordinates of any point on the wall of a crater could be measured with reference to the center of the hole and the top of the leveled frame. Measurements were taken at changes in slope or at other significant points, such as the frozen-ground interface.

The shape of the chamber produced adjacent to the explosive charge and details of scabbing of the frozen-ground interface below the charge were obtained with a folding rule or other measuring device held horizontally from the dowel stick.

k. Data-sheet computations. The details of each blast and the characteristics of the resulting crater are summarized in the data sheets (see Appendix). The first 13 column headings are self-explanatory or have been discussed. Column headings beginning with "Height of Charge" are explained as follows (left to right):

Height of charge is the height of the explosive charge when tamped in the bore-hole ready to fire. It is obtained by measuring the hole before and after placing the charge.

Height of stemming. The space in the drill hole from the top of the explosive charge to the collar of the drill hole was packed with stemming material before blasting. The height of stemming is therefore the depth from the collar of the hole to the top of the tamped explosive charge.

Surface to center of gravity (C. G.) is the depth from the collar of the hole to the center of the explosive charge, obtained by adding one-half of the "height of charge" to the "height of stemming," assuming the charge to be of uniform density and uniform horizontal cross-sectional area.

Center of gravity to interface, the distance from the center of gravity of the charge to the interface between the frozen and unfrozen ground, is obtained by subtracting the depth of the center of gravity from the depth of frozen ground.

Crater area is the plan area of a crater as measured by planimeter using the plane-table survey, scale 1 in. = 1 ft.

Crater radius is the radius of a circle having an area equal to the crater area.

Crater depth is taken from the crater cross-sections.

Depth of slabbing: For analyzing fully developed craters in which only one zone can be recognized, it was assumed that a plane passing through the center of gravity of the explosive charge and parallel to the surface separates the "slabbing" zone from the "chamber" zone of the crater. Hence, for such craters, the depth of slabbing equals the distance from the surface to the center of gravity of the charge. In some cases, a blast produced both a surface crater and a chamber, separated by a section of unbroken frozen ground. Under such conditions, the depth of slabbing equals the depth of the shallow surface crater above the explosive charge.

EXCAVATIONS IN FROZEN GROUND

Chamber radius is the radius of the hour-glass or bulb-shaped crater produced by plastic flow of the frozen ground as a result of the pressure of the explosion on the walls of the borehole.

The r/d ratio is the calculated crater radius divided by the depth to the center of gravity of the explosive charge. It is a measure of the shape of a crater and of the depth of charge relative to the weight of explosive.

Similitude ratio is the distance from the center of gravity of the explosive charge to the bottom of the resulting crater, divided by the shortest distance from the center of gravity of the explosive charge to the ground surface above the explosive. It provides a means of comparing craters of different sizes but similar shapes. A critical-depth blast results in a similitude ratio of 1.0.

Crater volume is the sum of the slab volume and the chamber volume. To minimize error because of irregularity in shape of crater, the volume is calculated using the average of two areas of revolution obtained from the cross sections and from the area of the crater as determined by the plane-table field measurements. The volume is calculated from the formula,

$$V = \frac{\pi}{3} Ar$$

V is crater volume

A is average area of two crater cross sections at right angles to each other.

r is the radius of a circle of area equal to the crater area.

Slab volume is the portion of the crater volume that is produced by a combination of tension and shear failure associated with surface uplift, rather than by plastic flow. The slab volume is obtained by subtracting the chamber volume from the crater volume.

Chamber volume, strictly speaking, is that portion of the volume of a crater that is produced by plastic flow and "borehole springing." The shape of the chamber is influenced by such factors as weight of charge, depth of charge, and interface ratio. However, because of variations in chamber shape and in the position of the chamber relative to the center of gravity of the explosive charge, it is difficult to define accurately the limits of the chamber. In some instances, the lower half of the chamber is cone shaped; in other instances it is spherical. The reasons for these changes in shape are discussed in this report. As the limits of the chamber cannot be defined for blasts of all types, we have arbitrarily taken the center of gravity of the explosive charge as a point on the plane separating the slab volume and the chamber volume. It is probable, therefore, that the data-sheet figures for chamber volume are only a portion of their true value, but the same procedure has been used consistently.

Values recorded on the data sheet for chamber volume were obtained in the same manner, using the same cross section and the same formula used for slab volume. The value of r in the formula

$$V = \frac{\pi}{3} Ar,$$

was obtained by dividing the sum of the two chamber cone diameters (from the cross sections) by four.

1. Photography. To supplement descriptions of equipment and methods employed in these tests and to show otherwise unrecorded details of the results, a considerable number of photographs were taken. Early work was done with a 35-mm camera, but the film available appeared to be defective and the results were disappointing. Arrangements then were made to use a 4 by 5-in. Speed Graphic camera with film

pack, and excellent results were achieved. The adopted plan was to photograph each blast hole immediately after it was shot. If a crater was produced by the blast, the crater was photographed again after the loose material had been removed. A few pictures were taken from eye level, but most were taken vertically downward from a position on the drill truck about 10 ft above the ground. In some cases the large size of the craters made it impossible to include the entire crater in a vertical photograph, even from the highest available position on the mast of a Corps of Engineers drill truck. Under such circumstances, oblique shots were taken from the best available position. In all photographs, a surveyor's level rod was included as a scale. A title board was used to identify each blast hole and show data regarding the explosive charge used. An aluminum-paint spray was used to outline the crater and add "relief."

Section II. Laboratory Tests

1. Soil handling and storage

The soil samples were transported from the test site to the laboratory at the Keweenaw Field Station for storage. Prior to storage, the core samples were extruded from the core barrels and the chunk samples cut into small specimens for convenience of handling. The samples which were taken with the $2\frac{1}{8}$ in. diam diamond core barrel were found to have a tapered section when removed from the barrel. The area of the upper portion of the sample had been reduced by the longer period of contact with the rotating core barrel. Because of this loss in cross-section, portions of these cores were not sufficiently large to provide specimens for the detailed soil tests. The samples taken with the larger core barrels, ranging to 10 in. diam, were found to be completely usable.

The specimens were stored in a large cold room during the winter months and in either commercial deep freeze units or a refrigerated trailer during the spring and summer. The large cold room was refrigerated by two large cooling units capable of maintaining temperatures below the freezing point during most of the year. During the winter months, the temperature of the cold room was approximately equal to the ambient outdoor temperature. Considerable loss in weight due to surface evaporation was noted when the storage temperature ranged from 32°F to 22°F. To study the effect of the storage temperature on surface evaporation or sublimation, small specimens of the frozen soil, approximately 1-in. cubes with polished surfaces, were prepared and stored at various temperatures. The results indicated that a temperature range from 10° to 14°F effectively reduced the rate of surface evaporation. Various methods were investigated to further reduce sublimation of the samples, since it was recognized that failure to control this factor would result in misleading test results. Surface coatings of synthetic resins, silicone oils, varnishes, natural oils, and other commercially available products were sprayed or painted on the specimens. Vegetable and mineral waxes, used successfully to protect unfrozen soils from loss of moisture, could not be used since they must be heated. Though many of the surface coatings reduced the rate of surface evaporation, none of the coating materials investigated provided complete protection for more than a week. Two fairly successful methods were finally devised: (1) The sample was coated with a synthetic resin and then immersed in kerosine or other non-hygroscopic fluid at sub-freezing temperature as long as protection was required, (2) the sample was wrapped in aluminum foil, known commercially as freezer foil. Samples wrapped tightly in this foil did not lose significant weight when stored at the lower temperature range previously mentioned. This type of protection has an added advantage of eliminating the problem of sample contamination, which is particularly desirable when the soils are to be used for routine classification.

2. Soil classification tests

a. Specimen preparation. Cutting of the cores and chunk samples presented a problem, as the frozen soil exhibited a toughness similar to that of non-ferrous metals. Also, the individual grains, being largely composed of silica, proved to be highly abrasive. The problem of sample cutting was not apparent during the early part of the laboratory program because the chunk samples obtained from the field were generally small. As the scale of the field experiments was increased and the size of the fragmented material from the craters became larger, it became apparent that the

equipment available for cutting, a metal cutting band saw, was ineffective. Although power-driven tools proved adequate for rough cutting of the large fragments, which ranged from 30 to 90 lb in weight and 12 to 30 in. in long dimension, continual maintenance and blade replacement were required. Tests indicated that a metal-cutting band saw blade was completely stripped of teeth in 20 min. of continual operation. No conspicuous difference in blade life was noted between the ferrous, non-ferrous, and wood-cutting blades. A controlled study of this problem should be conducted before drawing any definite conclusions.

b. Test procedure. The basic classification tests which are customarily conducted on unfrozen soil specimens (i.e., mechanical analysis, Atterberg limits, density and water content determination, specific gravity and organic content determination) were conducted on representative specimens from all the blast-hole areas sampled. In addition to these basic tests, hardness tests, using the Shore scleroscope, and unconfined compression tests were conducted to provide additional classification data. In order to study the soil-ice relations, mineral identification, particle shape and the crystal lattice orientation of the ice lenses, polished sections and thin sections were prepared from the frozen soil. To obtain polished sections, the rough-cut section was usually shaped into either a cube or a cylinder. The faces or surfaces of the specimens were prepared by finishing with sandpaper or a scraper to within approximately 2% of the final measured dimensions. A final polish was given the specimen with a hard-backed cloth on at least one surface or face. The polished section provided sufficient detail to permit both the crystal lattice orientation and particles of 0.1 mm size to be easily traced. Color variations of the individual layers in the sedimentary material warranted the use of color photography. Photography also provided an expedient means of illustrating ice forms in the soil. Natural density determinations were made on the cubic or cylindrical specimens. Unconfined compression tests were conducted on 1-in. cube specimens. Cyclic loading was used to evaluate the elastic behavior.

c. Test results. Typical moisture content and gradation data from 10 representative blast holes are presented in Table V. Soil stratification data from Blast Hole 50 are shown in Table VI. To obtain these data the wall of Blast Hole 50 was trimmed, polished for purposes of photography, and sampled to provide data on the stratification. The periodic nature of the gradation percentages with depth is consistent with the mechanics of water-deposited solids. More detailed classification data were obtained at Blast Hole 182 and 184 by sampling of the crater walls (Tables VII, VIII). Samples were taken near the crater of hole 182 so that soil characteristics of the material adjacent to the crater walls can be compared with soil characteristics at some distance from the wall face (Table VIII).

A study of the classification data indicates that the frozen soils with the finest gradation possess the highest moisture content and lowest density, a relationship which has been well established in the field of soil mechanics. The major exception to this relationship is found in the highly organic sandy soil, which exhibits both high density and high moisture. The moisture content of the silts were in many cases found to be in excess of their water-holding capacity, which implies the presence of ice lenses. The study of thin and/or polished sections of frozen ground under the binocular microscope was successfully arranged. Photographs of 15, 30, and 45 power magnification were taken using a photo-flood type of direct lighting. Temperature on the stage must be quite low, approximately +10°F, to prevent melting. Ice lenses in thin sections can be studied by using a conventional focusing light source passed through the ice lens (Fig. 24). The orientation of the ice crystal lattice is clearly defined by using crossed polaroids. Columnar ice with the c-axis very uniformly arranged parallel to the direction of freezing (i.e. normal to the ground surface and soil stratification) was observed in ice lens of 2 mm thickness. The color photography was not too effective because of faulty exposure control. The mechanics involved in a phase change, particularly thawing, were also observed under a binocular microscope. The most valuable information obtained in this manner was a determination of the orientation of the ice crystals in the lens. The interface between the soil and the optically clear ice in lens was found to be very irregular.

Table V. Typical moisture-content and grain-size data.

Blast Hole	Natural Moisture Content (%)	Grain Size Distribution	
		% Finer than 0.074 mm	% Finer than 0.02 mm
8	24.2	32	2
20	31.5	79	13
34	37.2	95	24
35	84.6	72	12
39	51.9	90	35
42	21.1	75	17
44	51.1	52	7
48	50.5	96	29
51	48.3	98	47
56	43.9	94	18

Table VI. Soil stratification data, Blast Hole 50.

Sample No.	Depth (in)	Grain Size Distribution	
		% Finer than 0.074 mm	% Finer than 0.02 mm
15	17	94	44
17	34	75	16
19	51	70	0
21	68	53	2
22	85	74	8
28	102	45	12
29	119	84	29
31	136	94	12
33	153	35	3

3. Tests to determine stress-strain relationship

a. General. A consultant's conference was held in November 1953 to develop a plan of test for the project. At this conference, it was decided that the stress-strain characteristics of the frozen soil to be used for the explosion tests would be studied by use of the unconfined compression test. It was further concluded that these tests would be conducted at varying rates of stress and for a range of temperatures, since the elastic-plastic properties of frozen soil are known to be effectively influenced by changes in these factors. In addition to obtaining the usual axial stress-strain relationship, it was decided to measure the lateral strains during the tests to provide information on Poisson's ratio.

In accordance with the conclusions reached at the conference, one series of tests was conducted at an applied rate of stress of approximately 400 psi/min and another series at a stress rate of approximately 1000 psi/min. Both series of tests were conducted at a temperature of 30°F, which represented the average temperature of the frozen soil during the explosion tests. Tests at other temperatures are to be conducted but were not completed in time for inclusion of this report. To determine the effect of the orientation of the strata on the compressive strength of the soil, test specimens were prepared so that the applied load could be directed parallel to the stratification, normal to the stratification, and inclined to the stratification. The tests at a loading rate of 400 psi/min were run on specimens with the stratification parallel and normal to the direction of loading only; the tests conducted at the higher rate of loading were run on specimens with the stratification parallel, normal, and inclined to the direction of loading.

Table VII. Classification test data from Blast Hole 184.

Sample Depth (in)	Condition	Classification	Liquid Limit	Plasticity Index	Specific Gravity	Unit Dry Weight ¹	Natural Moisture Content (%)	Void Ratio	Saturation ² (%)	Gradation % Finer Than 0.074 mm 0.02 mm
0-5	Frozen	Sandy silt	—	Nonplastic	2.63	78.9	34.1	1.08	83	82
5-9		Sandy silt	—	Nonplastic		87.0	24.2	0.87	72	59
9-12		Silt (OL)	33.0	4.0		41.2	142.9	2.98	100	100
12-18		Silt (OL)	38.0	14.9		50.8	69.0	2.23	81	29
18-21		Silt (ML)	—	Nonplastic		84.7	33.1	0.94	93	57
21-24	Unfrozen	Silt (OH)	61.5	19.7	2.63	56.1	63.6	1.93	87	—
24-48		—	—	—	—	—	—	—	—	—

1. Computed from measured dimensions, weight and water content of frozen specimen after trimming.

2. Based on water content in relation to dry unit weight with all water assumed in frozen state. Values computed to be over 100% are shown as 100%.

Table VIII. Classification test data from Blast Hole 182.

Sample Tube No	Sample Depth (in)	Location Distance from crater (in)	Classification	Liquid Limit	Plasticity Index	Specific Gravity	Unit Dry Weight ¹	Natural Moisture Content (%)	Void Ratio	Saturation ² (%)	Gradation % Finer Than 0.074 mm 0.02 mm
37	24	36	Silt (OH)	100.8	32.6		50.9	79.8	—	—	43
41	36	30	"	75.6	12.6		61.4	72.3	—	—	40
48	42	56	"	63.8	6.4	2.61	59.1	68.5	1.76	100.0	40
49	42	50	"	—	nonplastic		53.8	105.9	—	—	30
52	42	42	"	—	"		68.8	59.6	—	—	35
54	42	46	"	—	"		74.0	51.5	—	—	33
58	42	40	"	57.3	5.7	2.63	53.6	86.8	2.06	100.0	54
68	42	52	"	58.8	0.1		72.6	93.9	—	—	23

1. Computed from measured dimensions, weight and water content of frozen specimen after trimming.

2. Based on water content in relation to dry unit weight with all water assumed in frozen state. Values computed to be over 100% are shown as 100%.



Direct light used
to bring out
soil detail



Top in focus



Bottom in focus

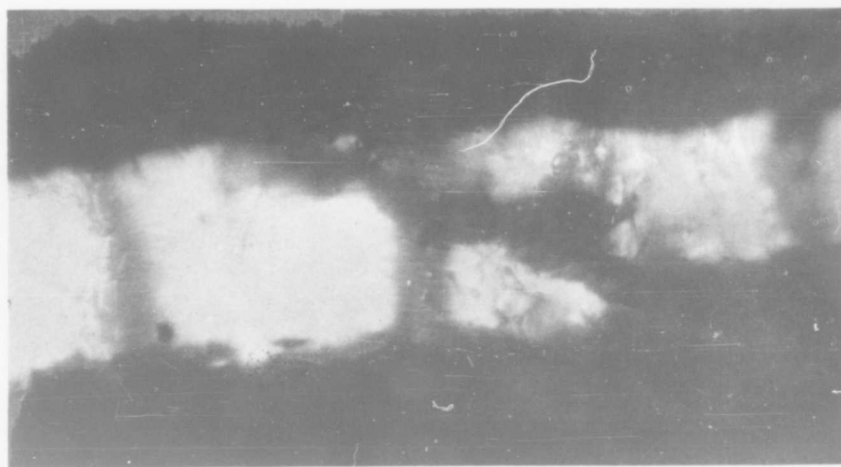


Figure 24. Ice lens detail. Magnification: 30x.

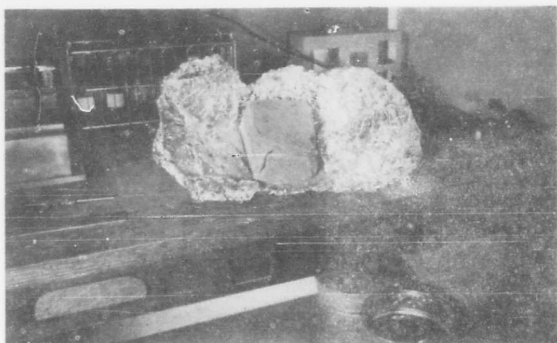


Figure 25. Original frozen chunk just before rough cutting.



Figure 26. Rough cutting process.

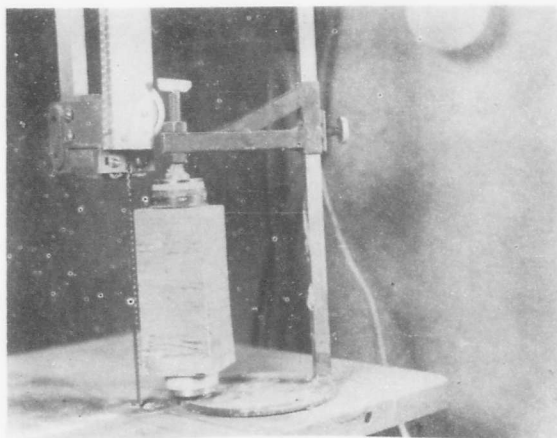


Figure 27. Rough trimming process.

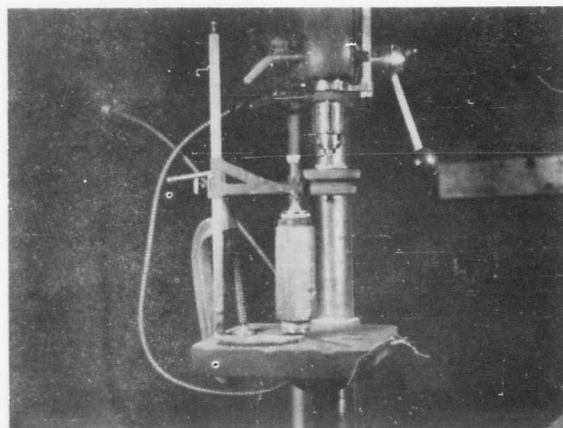


Figure 28. Final trimming process.



Figure 29. Cutting ends of specimen.

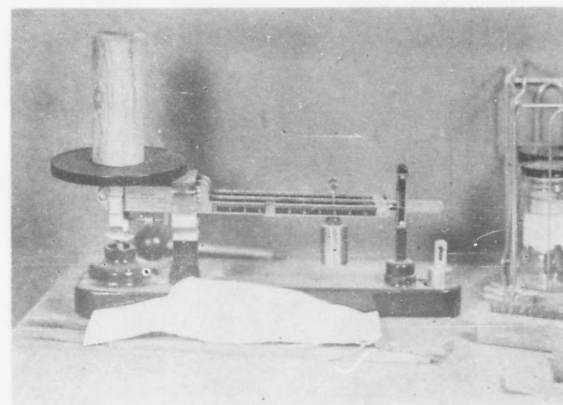


Figure 30. Weighing specimen.

b. Specimen preparation for unconfined compression tests. The test specimens were cylindrical, approximately 2 in. diam and 5 in. long. The height to diameter ratio was maintained at 2.5, within $\pm 0.5\%$, generally by varying the specimen length rather than by changing the diameter of the specimen. Procedures were similar to those used to prepare specimens for classification tests, but some improved techniques were used.

(1) A mass of frozen soil (Fig. 25) was rough cut on the band saw to a shape measuring 2.5 to 3 in. in cross section and approximately 6 in. long (Fig. 26).

(2) The sample was placed in a special jig which permitted the frozen soil mass to rotate about an axis paralleling the 6-in. dimension. The jig and the soil were placed on the band-saw table and the sample was trimmed to the shape of a rough cylinder (Fig. 27).

(3) The jig and soil sample were placed on the drill press table and the jig firmly clamped to the table (Fig. 28). Rotation of the sample was provided by friction contact with a large rubber wheel mounted on the shaft of the drill. If the sample is accurately centered, it will remain in a fixed position while in rotation, so that cutting tools can be used to shape the sample to a precise diameter.

(4) Excess material was trimmed from the sample using an assortment of common tools including knives, rasps, files, steel straight edges, saw blades, and various grades of stiff-cloth-backed abrasive material. The latter tool proved to be the most successful. To prevent clogging with cuttings, the abrasive was applied under a vibrating action which tends to clean the cutting surface. A machinist's square and calipers were used to determine when the desired diameter and plane were reached. The cylinder was polished with a soft cloth to bring out the natural soil structure. The best temperature for the laboratory where the final trimming is done varies somewhat with the type of soil composing the sample. The range of temperatures used was from $+10^{\circ}\text{F}$ to $+25^{\circ}\text{F}$.

(5) After the correct diameter was obtained, the sample was removed from the jig and placed in a miter box where the ends were trimmed. This operation (Fig. 29) was difficult and required hand sawing and scraping. Extreme care was required to obtain precisely plane and parallel ends.

(6) The cylindrical specimens were measured, weighed, and inspected for conspicuous physical features such as stratifications, organic matter, and ice lens formation (Figs. 30, 31). Sampling trimmings were used for mechanical analysis and Atterberg limit tests. The specimens were then wrapped in aluminum foil with an identification tag attached and placed in a labeled canvas sack for storage in the deep freeze.

It is evident that much study is needed to determine the effects of manipulating the frozen material in the way described above. It is known, for example, that the specimens were subjected to a variety of externally applied loads during the specimen preparation.

c. Test procedure. Axial and lateral strains were measured during the tests, using a special type of strain gage developed by personnel of the Technical Equipment and Frozen Ground Applied Research Branches. Preliminary study of past field work indicated that unit strains of the order of 15 to 20% could be anticipated.

The gage adopted for use was of the proving ring type, consisting of an arched, nearly semi-circular shaped section of copper alloy with a thickness of 0.02 in. and a width of 0.50. The gages used for measuring axial strain had a radius of curvature of 0.5 in., which corresponded to a 1-in. gage length, while the lateral strain gages had a radius of curvature of 1.0 in. Strains applied along a plane passing through the gage points produce bending in the element, which results in extension of the outer fibers and compression of the fibers on the inner face. Movement of the gage point can be as great as ± 0.5 in. without causing stresses in excess of the proportional limit. SR-4, type A-3, electric strain gages were cemented to both the inner and outer faces of the

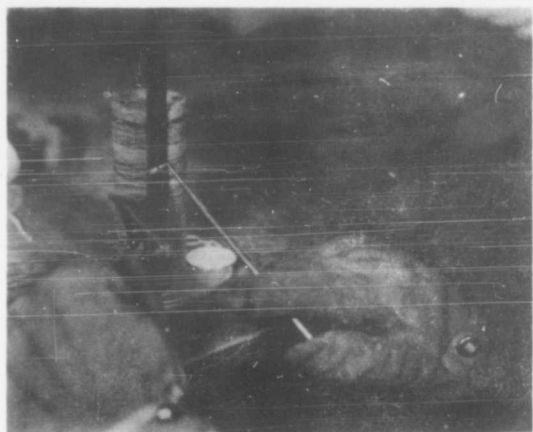


Figure 31. Measuring specimen.

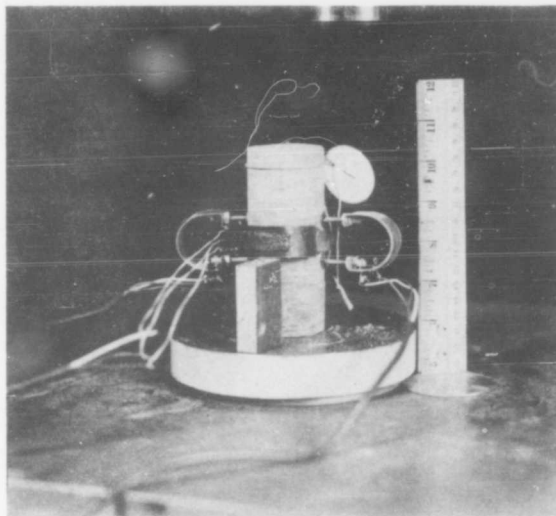


Figure 32. Strain gage details.

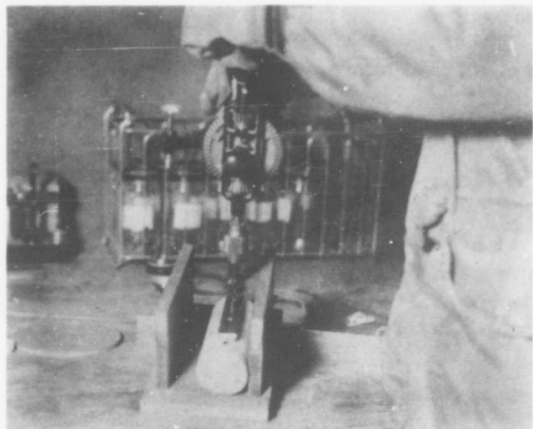


Figure 33. Drilling holes in specimen for gage points.



Figure 34. Placing gage points.

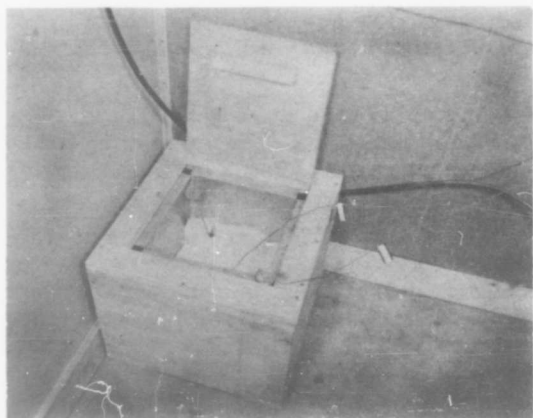


Figure 35. Tempering cabinet.

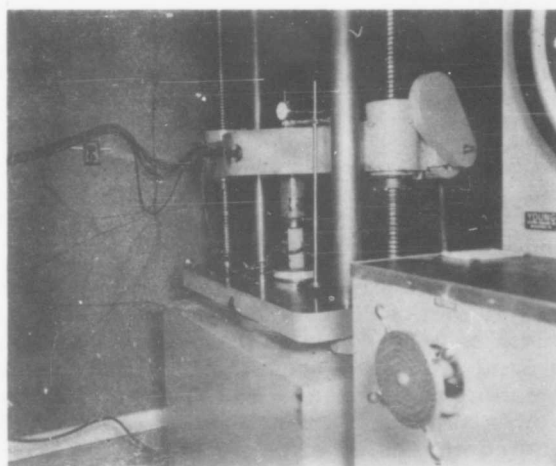


Figure 36. Compression test assembly showing specimen prior to test.

arched metal strips. These electric strain gages were wired to the potentiometer-type bridge in such a way that the recorded strain of the two SR-4 gages would be additive. This type of hook-up eliminated the necessity of applying a temperature correction to the strain readings. Fixtures attached on the ends of the arched metal strips permitted attachment of the gages to the specimens and also added stiffness to the arched sections, which tended to increase the sensitivity of the gages.

The gage points on the specimens consisted of the box portion of a commercial fastener known as the Dritz Dot Snapper. The soil specimens were processed to receive the gage points by drilling holes of $\frac{1}{8}$ -in. diam and approximately $\frac{1}{8}$ -in. depth into the specimen, using a gage block to maintain the proper gage length. The drilled holes were then filled with water and the metal box portion of the fastener was seated in the drilled holes and frozen into the specimen. The fixtures on the ends of the strain gage were designed to provide a snug fit when inserted into the gage points. Figures 32-34 show details of the strain gages and the method of mounting them on the specimens. It will be noted that two axial strain elements, spaced 180° apart, were used to provide a measure of the mean axial deformation, since it was anticipated that the strain would not be equal on the two sides except under abnormal conditions. Only one lateral strain gage was used owing to lack of space on the specimen.

The temperature in the cold room in which the specimens were tested was controlled manually to maintain a temperature of approximately 30°F . This temperature was selected as representative of the average ground temperature during the explosion tests. Six thermocouples, located at random positions throughout the cold room, were read by an electronic recorder. Prior to testing, a thermocouple was inserted in a drilled hole in the center of each cylinder. The specimen was then placed in a tempering cabinet (Fig. 35) near the testing machine, which permitted the specimen temperature to reach the selected test temperature at a rate of approximately 1°F per hr.

The compression tests were conducted in a 120,000-lb capacity hydraulic testing machine. An electronic recorder was used to record the two axial strains, the lateral strain, and the applied load. The total strain was measured in 500-lb load intervals with an Ames dial mounted so that the exact movement of the loading head could be measured. The applied load was read directly on the testing machine indicator dial and was recorded on the same chart as the strain measurements by use of a 6000-lb Baldwin SR-4 load cell.

Calibration of the strain gages and load cell and standardization and range adjustment of the electronic recorder were made prior to each test. Each gage was flexed in a mechanical extensometer to a maximum strain of 0.25 in. During calibration, the axial strain gages decreased from 1.00 to 0.75 in. in length, and the lateral strain gage increased from 2.00 to 2.25 in. long. The recorder was standardized and the range adjusted so that each of the 100 divisions on the recorder corresponded to .0025 in. The strains were found to be linear throughout the full scale to within less than 1%. The load cell was then calibrated in the testing machine and the values on the electronic recorder were compared to those read directly on the indicator dial of the testing machine. The recorder was standardized and the range adjusted so that each division represented 100 lb of total load. The chart speed of the recorder was set at 10 in./min.

The specimen was placed in position in the testing machine and load was applied at one of the established rates of 400 psi/min or 1000 psi/min. After the test, the cylinder was taken to the soils laboratory for the standard physical tests. Figure 36 shows the test set-up.

d. Results. Figures 37 and 38 show typical gradation curves for the frozen soils used in the compression tests. The relationships between: (a) unit stress and unit axial and lateral strains; (b) unit stress and Poisson's index; (c) unit stress and volume change of the test specimen are shown for typical specimens in Figures 39-43. The unit stress and strain values shown represent true values, since they were calculated from the actual cross section of the specimen at the time the stress or strain occurred. The Poisson's index was computed for specific increments of stress. In general, the increment of stress used was 50 psi. The Poisson's index values represent the ratio of

EXCAVATIONS IN FROZEN GROUND

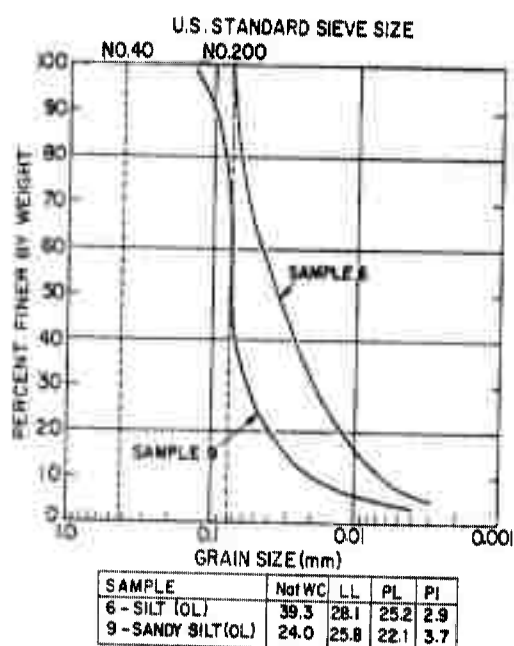


Figure 37. Gradation curves, compression test samples loaded at 400 psi/min.

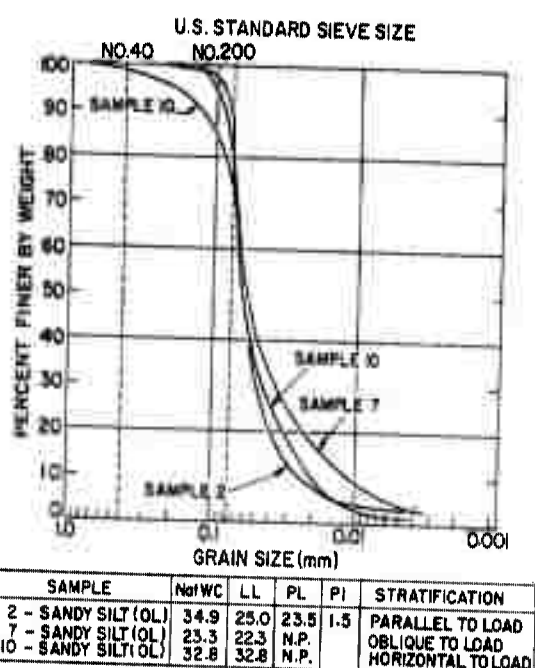


Figure 38. Gradation curves, compression test samples loaded at 1000 psi/min.

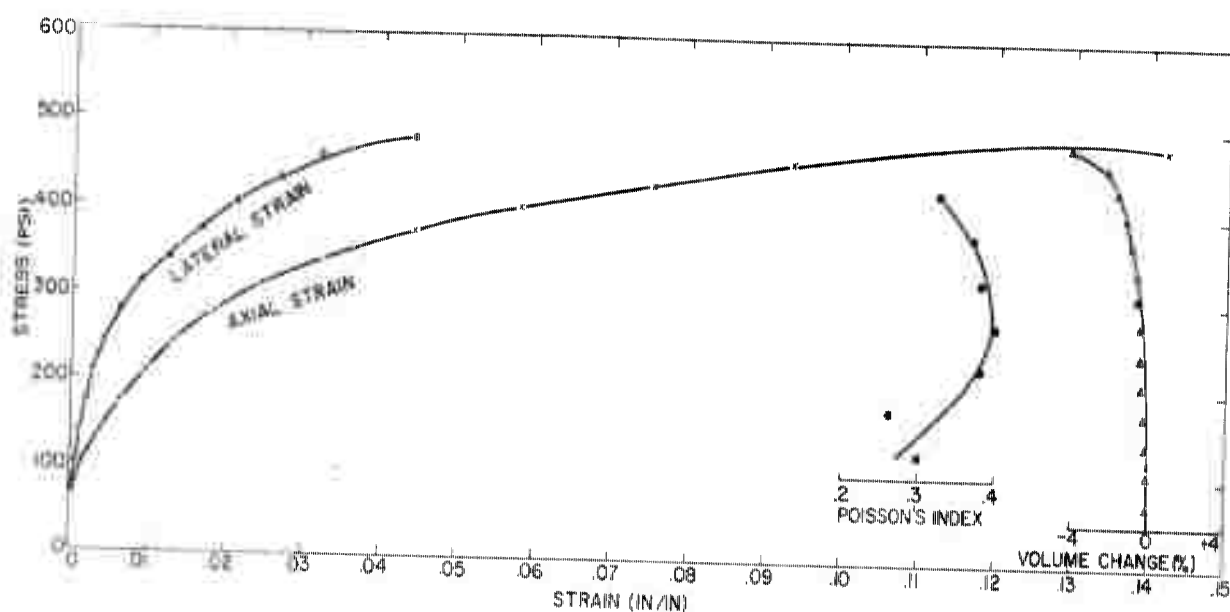


Figure 39. Compression test data, Sample 6. Soil type: silt (OL). Stratification: perpendicular to loading. Rate of loading: 400 psi/min.

the differential lateral strain to the differential axial strain for the specific stress range used. The volume change, expressed as a percent of the original volume of the unloaded specimen, was calculated directly from the unit strain data and represents the change occurring within the center portion of the specimen rather than change of the specimen as a whole. This procedure provided data on volume change for that portion of the specimen in which accurate axial and lateral strains were being measured. Table IX presents pertinent data on the physical properties of each soil cylinder tested and a compilation of all significant results of the unconfined compression tests. The Poisson's index is given for a low and a high stress range because the test data indicated that the

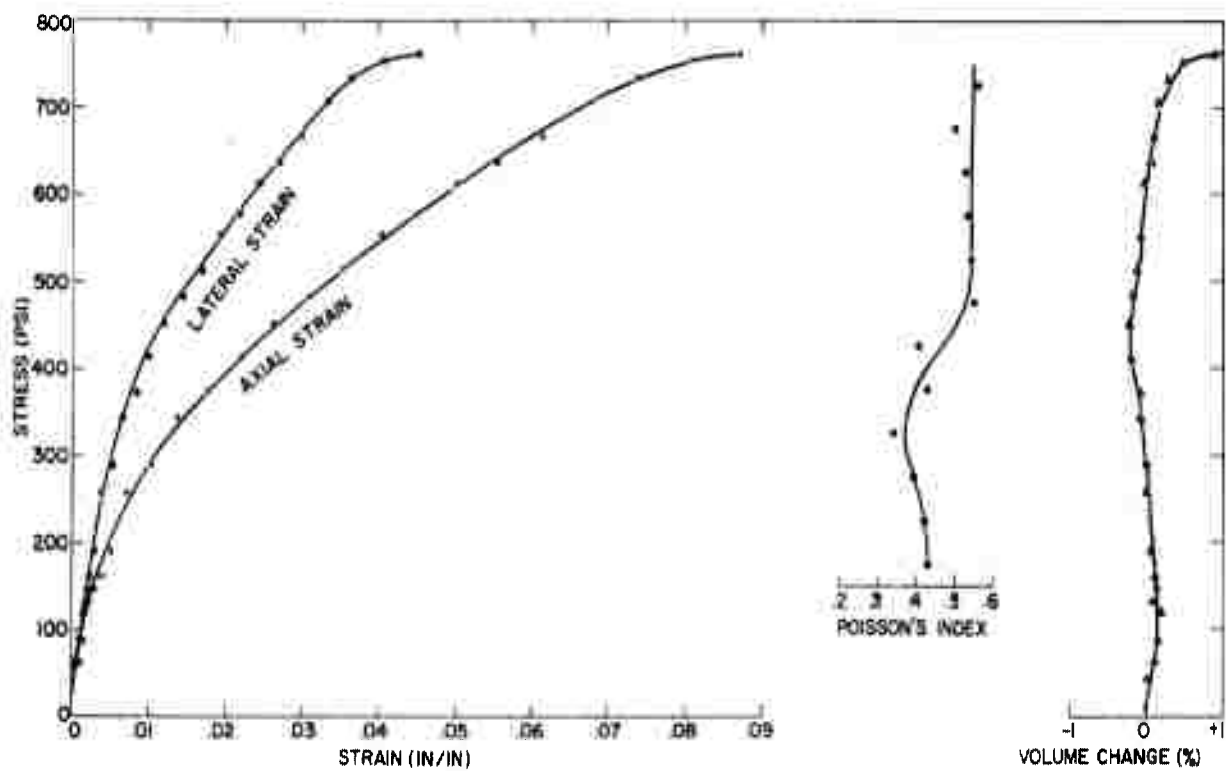


Figure 40. Compression test data, Sample 9. Soil type: sandy silt (OL).
Stratification: parallel to loading. Rate of loading: 400 psi/min.

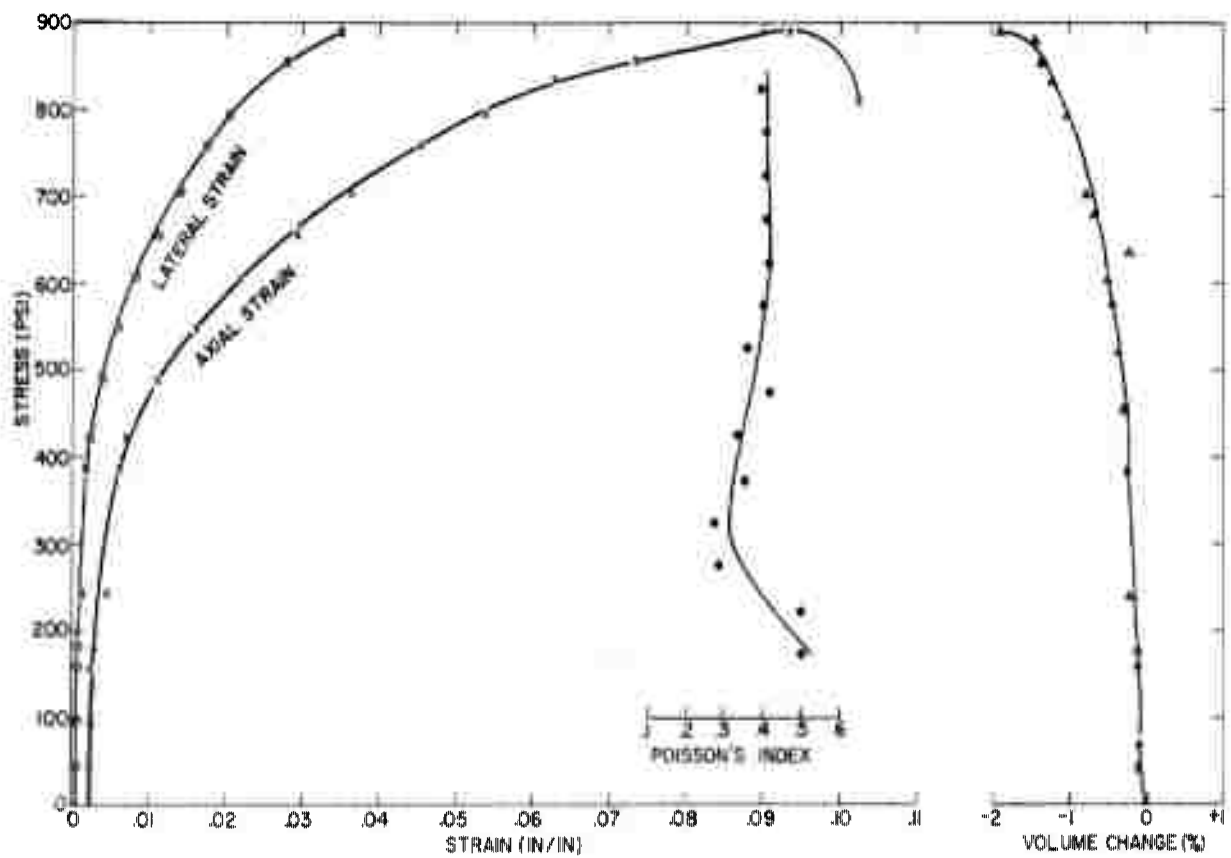


Figure 41. Compression test data, Sample 2. Soil type: sandy silt (OL).
Stratification: parallel to loading. Rate of loading: 1000 psi/min.

EXCAVATIONS IN FROZEN GROUND

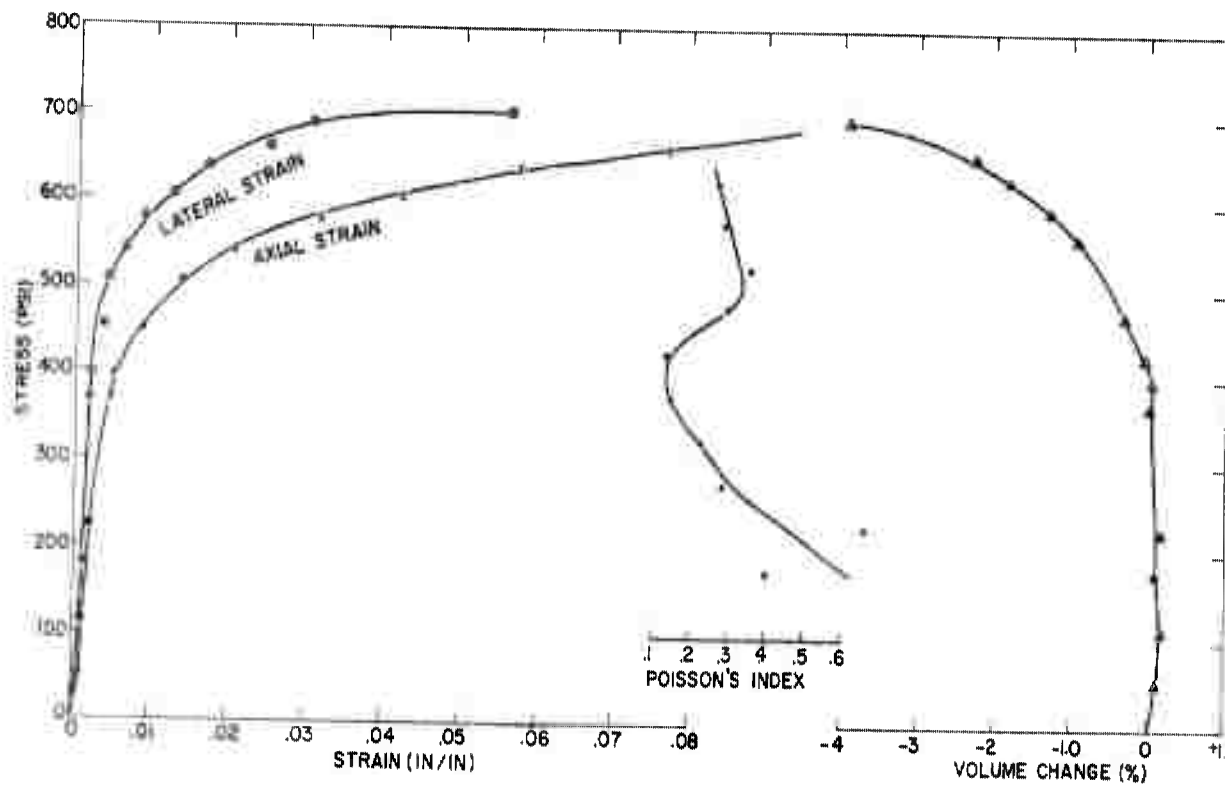


Figure 42. Compression test data, Sample 7. Soil type: sandy silt (OL).
Stratification: oblique to loading. Rate of loading: 1000 psi/min.

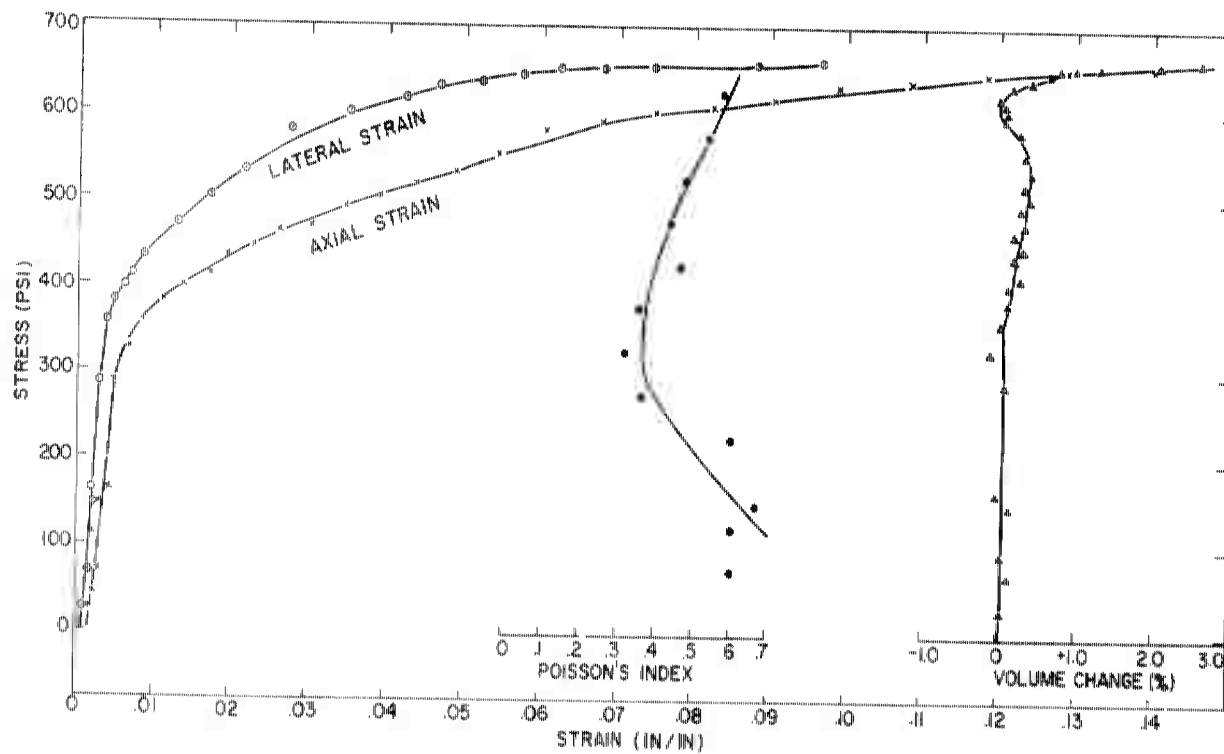


Figure 43. Compression test data, Sample 10. Soil type: sandy silt (OL).
Stratification: perpendicular to loading. Rate of loading: 1000 psi/min.

Poisson's index varied considerably and was dependent on the magnitude of the stress range for which it was computed. The degree of saturation is based on the water content of the test specimen at the beginning of the test in relation to dry unit weight with all water assumed to be in a frozen state. Values computed to be over 100% are presented as 100%. The rate of volume of ice to volume of soil is also based on the assumption that all moisture in the sample is frozen. Table X shows the average unconfined compression test values. Figures 44-49 show core samples before and after testing.

e. **Observations.** Examination of the test specimens indicates that in almost every case failure occurred in the plane of the stratification regardless of the orientation of the stratification to the direction of loading. This strongly indicates that the volume of ice within the specimens which averaged over 100% for the specimens tested, was sufficient to control the strength of the soil-ice mixture, and that the soil itself lost its identity when the pore water froze. The maximum compressive strength values, which range from 237 to 891 psi, fall within the normal range for the compressive strength of ice when tested at temperatures of approximately -2°C .

The data indicate a large scatter among the observed stress and strain values. It is likely that this scatter indicates the extreme sensitivity of the soil-ice mixture to slight variations in the specimen temperature at the time of test, particularly in the near thawing range at which the tests were conducted. As a result of the scatter, it is difficult to establish whether the orientation of the stratification or the rate of loading had a marked effect on the compressive strength, Poisson's index, and tangent modulus. However, the data indicate that the compressive strength was generally higher for the specimens with ice lenses parallel to the direction of loading. This is not borne out by the average values for the specimens tested at a 1000 psi/min rate of stress increase (Table X), since a low compressive strength value of 344 psi (Specimen 5) was included in computing the average value. This trend, if such is the case, appears to be reasonable and in agreement with observations made on unfrozen soil, where it has been demonstrated many times that the shearing strength is usually greater across the strata than parallel to it. When the strata are parallel to the direction of loading, the shearing planes tended to cut across the stratification more than when the strata are perpendicular or oblique to the direction of loading. In the latter cases, failure occurred by bulging (sliding along the horizontal ice strata) or by sliding along the oblique plane, the strata.

With reference to the tangent modulus, it is apparent that the modulus computed from the lateral stress-strain relations is generally larger than those calculated from the axial values. This would indicate that the lateral strains during the initial stages of loading, the so-called elastic range, were somewhat larger than the axial strains. No clear-cut relationship was found between the Poisson's index values and either the orientation of the stratification or the rate of loading. The maximum compressive strength plotted against the ratio of the volume of ice to the volume of soil (Fig. 50) shows a tremendous scatter in the data, and no significant relationship appears evident.



Figure 44. Sample 2 before compression test

Figure 45. Sample 2 after compression test

TABLE IX. UNCONFINED COMPRESSION TEST DATA.

Sample No.	Natural Water Content (%)	Atterberg Limits		Dry Unit Weight (pcf)	Ice Lens Stratification* Orientation*	Specimen Temp. at Time of Test (°C)	Maximum Compressive Strength (psi)	Poisson's Index†		Tangent Modulus (psi/in/in x 10 ³)		Ratio		Degree of Saturation (%)	Strain of Max. Stress (%)	
		L. L.	P. I.					Low Stress	High Stress	Axial	Lateral	Vol. Ice	Vol. Soil		Axial	Lateral
a. Rate of Stress Increase = 400 psi/min.																
1	32.4	38.6	12.9	79.8	Perp.	-2.0	383	.635	.480	142.8	42.1	0.94	89.4		9.1	4.7
2	31.2	21.0	NP	83.8	Parallel	-1.0	728	.251	.279	51.3	125.0	0.91	95.0		10.3	3.5
3	42.7	29.7	3.2	76.9	Perp.	-1.0	642	.388	.436	49.4	67.8	1.24	100.0		13.4	5.6
4	42.3	30.2	4.5	76.6	Perp.	-1.0	269	.679	.982	28.6	43.5	1.24			3.0	3.8
5	38.4	28.3	NP	78.1	Perp.	-1.8	416	.385	.354	80.0	80.0	1.11	100.0		5.3	1.6
6	39.3	28.1	2.9	79.8	Perp.	-1.5	481	.281	.371	80.0	42.1	1.13	100.0		14.2	4.4
7	28.3	23.7	NP	81.6	Perp.	-2.2	411	.514	.557	25.0	28.6	0.82	82.0		13.0	7.2
8	13.1	—	NP	93.7	Parallel	-1.8	223	.491	.341	13.3	22.2	0.38	50.5		8.5	2.2
9	24.0	25.8	1.0	89.6	Parallel	-2.0	760	.397	.508	50.0	66.7	0.70	83.7		8.7	4.5
10	23.0	35.8	2.0	90.3	Parallel	-2.1	735	.532	.607	40.0	33.3	0.67	81.5		8.9	5.7
11	55.1	32.8	9.5	62.3	Perp.	-1.0	—	—	—	—	—	1.59	97.5		—	—
12	40.1	32.8	17.6	63.1	Perp.	-1.8	426	.560	.508	66.7	142.8	1.14	84.3		12.3	6.3
13	50.5	40.3	9.5	63.5	Parallel	-2.1	446	.479	.416	61.5	114.3	1.46	91.0		13.2	5.4
14	52.6	28.3	6.8	58.4	Parallel	-1.5	609	.608	.487	53.3	173.9	1.55	97.0		10.5	3.9
15	67.5	30.4	12.2	58.9	Parallel	-2.0	—	—	—	—	—	1.95	100.0		—	—
16	66.3	37.8	12.5	60.0	Parallel	-2.0	428	.180	.200	50.0	200.0	1.91	100.0		3.8	9.7
17	60.4	37.0	2.0	82.8	Parallel	-2.5	387	.625	.500	69.8	136.4	1.74	100.0		10.8	3.4
18	34.9	25.0	1.3	78.2	Parallel	-2.2	876	.455	.547	100.0	173.9	0.99	100.0		11.0	5.7
19	26.2	36.8	2.1	61.0	Parallel	-2.0	678	.313	.418	70.2	200.0	0.77	69.0		10.4	5.3
20	57.5	29.3	7.4	59.6	Parallel	-2.0	683	1.418	.339	160.0	210.5	1.66	98.0		27.1	7.3
21	58.2	34.4	NP	85.0	Parallel	-1.2	606	.305	.331	111.1	333.3	1.69	94.4		12.0	4.1
22	23.2	29.1	NP	83.6	Parallel	-2.0	237	.048	1.181	66.6	181.8	0.66	72.0		3.0	7.9
23	30.5	26.5	6.2	69.2	Parallel	-2.0	655	.599	.753	58.0	102.6	0.88	92.0		4.6	9.2
24	47.1	28.4	NP	80.9	Parallel	-2.0	851	.368	.379	92.2	121.2	1.36	100.0		31.0	7.6
25	31.3	28.0	NP	76.6	Parallel	-2.0	774	.349	.534	80.0	114.3	0.91	86.5		17.7	8.1
26	31.5	31.4	NP	83.5	Parallel	-2.0	417	.469	1.289	24.7	39.2	0.91	80.0		7.5	9.3
27	31.0	25.0	NP	—	Parallel	-2.0	783	.476	.341	56.3	148.1	0.89	93.0		13.3	4.7
b. Rate of Stress Increase = 1000 psi/min.																
1	35.0	28.9	NP	78.5	Parallel	-1.0	646	.302	.483	60.0	110.0	1.01	92.7		9.5	4.2
2	34.9	25.0	1.5	80.2	Parallel	-1.0	891	.395	.399	80.0	160.0	1.00	97.0		9.3	3.5
3	64.9	30.4	1.3	56.2	Parallel	-1.5	584	.388	.481	50.0	100.0	1.87	97.4		11.6	6.5
4	84.1	31.4	3.8	48.5	Parallel	-3.0	814	.204	.347	70.0	200.0	2.39	100.0		12.9	4.0
5	39.9	26.5	NP	72.9	Parallel	-3.0	344	.500	—	60.0	80.0	1.15	92.0		1.6	2.1
6	54.3	28.4	NP	61.2	Inclined 45°	-2.5	413	.592	.762	40.0	60.0	1.57	93.5		13.8	10.0
7	24.3	22.3	NP	77.4	Inclined 45°	-2.5	703	.343	.265	90.0	160.0	0.70	62.6		18.1	5.6
8	30.6	29.8	3.0	70.4	Inclined 45°	-2.0	168	—	.354	120.0	140.0	0.89	66.0		0.5	0.2
9	66.0	28.8	0.7	55.3	Inclined 45°	-2.0	434	.263	.231	50.0	100.0	1.91	96.5		8.3	1.7
10	32.8	24.7	NP	75.5	Perp.	-2.5	660	.509	.472	90.0	115.0	0.95	81.0		19.5	9.7
11	33.7	23.0	NP	75.4	Perp.	-2.0	766	.434	.430	60.0	140.0	0.97	82.6		20.5	8.3
12	62.3	24.7	2.0	59.3	Perp.	—	754	—	.479	180.0	240.0	1.80	100.0		17.5	9.5

* Orientation given with respect to direction of loading.

† Low stress range includes the lower half of the total stress range — High stress range includes upper half of total stress range.

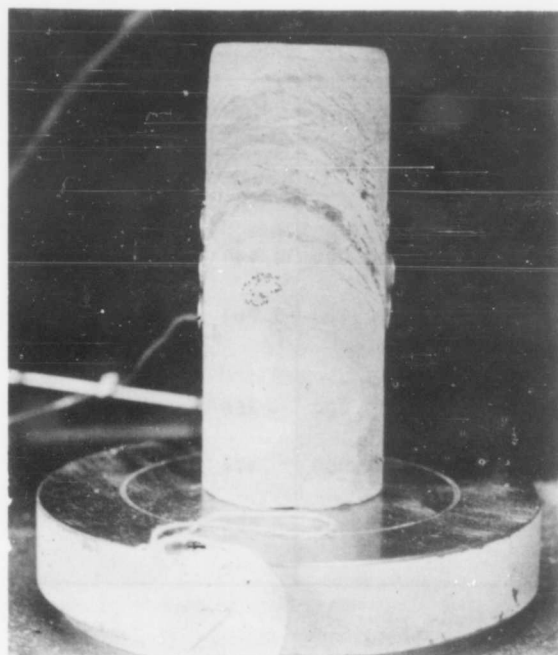


Figure 46. Sample 7 before compression test.

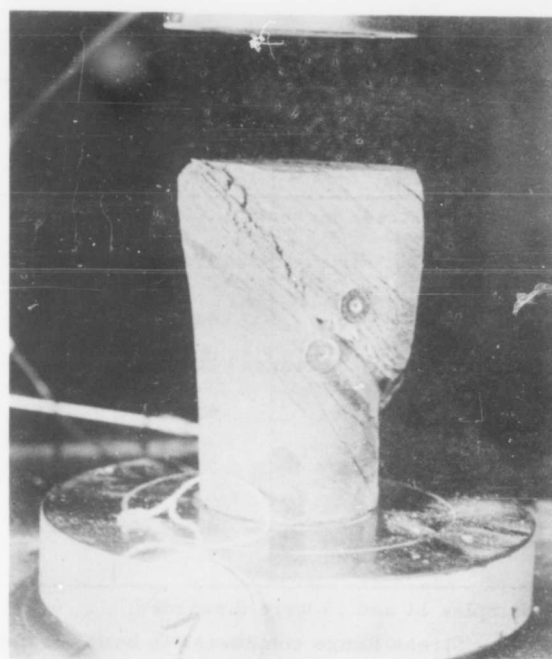


Figure 47. Sample 7 after compression test.

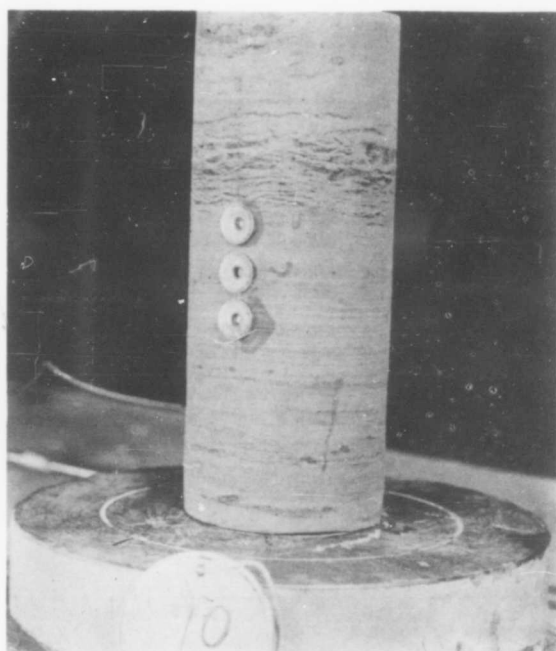


Figure 48. Sample 10 before compression test.



Figure 49. Sample 10 after compression test.

EXCAVATIONS IN FROZEN GROUND

TABLE X. AVERAGE SOIL DATA AND COMPRESSION TEST VALUES

Stratification	Number of Samples*	Compressive Strength (psi)	Moisture Content (%)	Vol. ice Vol. soil	Tangent Modulus (psi)		Poisson's Index	
					Axial	Lateral	Low Stress Range**	High Stress Range ***
a. Rate of stress increase = 400 psi/min.								
Parallel to loading	17	596	45.0	1.14	78,000	140,000	0.490	0.513
Perpendicular to loading	8	432	39.2	1.14	67,000	70,000	0.464	0.531
b. Rate of stress increase = 1000 psi/min.								
Parallel to loading	5	659	51.9	1.58	64,000	130,000	.358	.427
Perpendicular to loading	3	728	42.9	1.24	110,000	165,000	.474	.460
Oblique to loading	4	429	43.8	1.27	75,000	115,000	.400	.403

* Samples 11 and 15 were discarded.

** Low Stress Range considered to be lower half of total stress range.

*** High Stress Range considered to be upper half of total stress range.

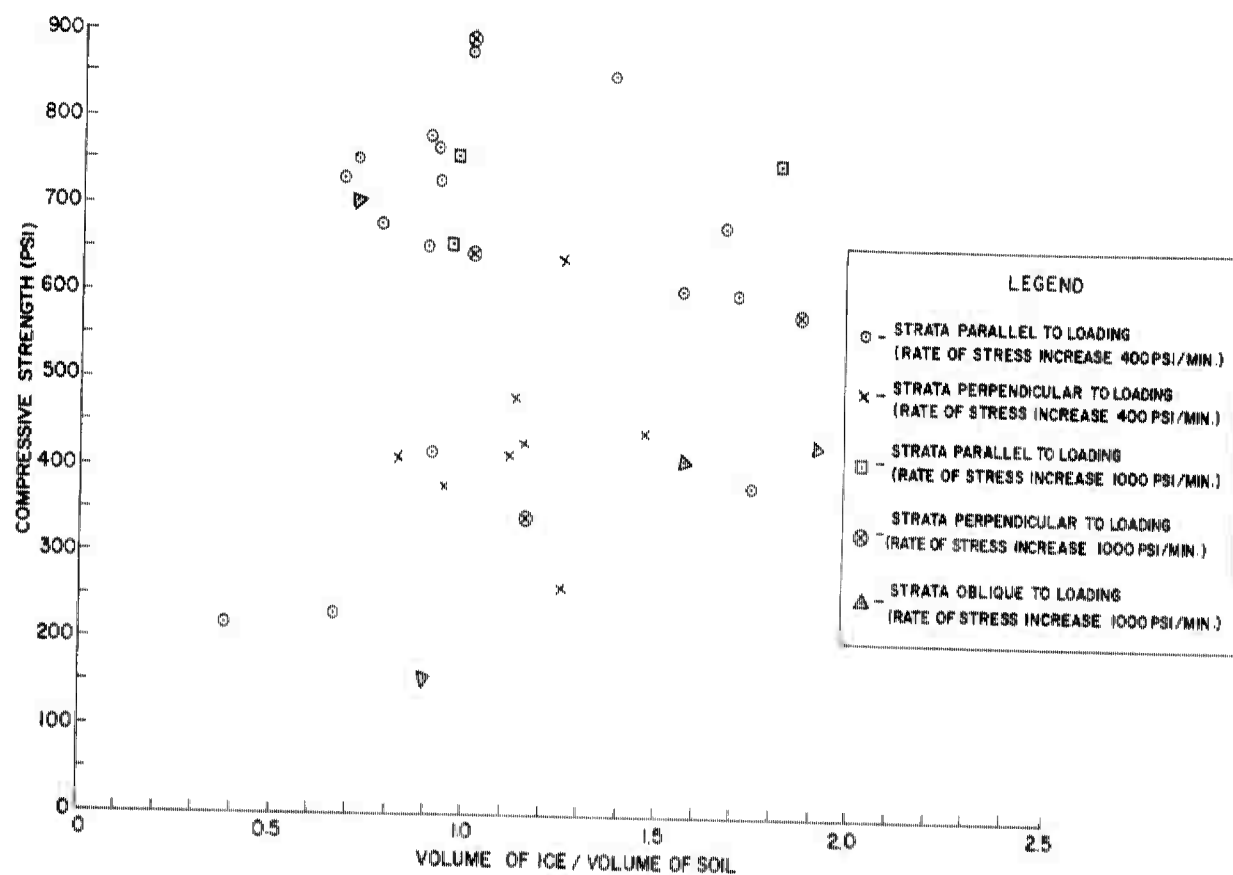


Figure 50. Compressive strength vs. volume of ice/volume of soil.
From compression test data.

CHAPTER III. ANALYSIS OF BLAST TESTS

Section I. Mechanics of Crater Formation in Frozen Keweenaw Silt1. Introduction

As a result of the over-all analysis of blasts in frozen Keweenaw silt, a theory of crater formation has gradually evolved. This theory is essentially a continuation of Livingston's observations on the mechanics of rock failure for crater blasts in various types of rocks and for craters produced by impact and penetration of bombs into rock. It seems desirable to present the theory here, to provide a basis for interpreting the results of the blast tests.

Frozen ground may be considered to be a rock type. The essential differences between frozen Keweenaw silt and rocks such as granite or sandstone are (1) the predominantly plastic behavior of the frozen ground and (2) the influence of the frozen-ground interface and of the underlying unfrozen soil upon the shape and size of crater produced by blasting.

Crater formation may be divided into three phases: (1) shock phenomena; (2) expansion of gases produced by the explosion; (3) rupture of the surface and conversion of the remaining energy of the explosion to forms unrelated to the volume of excavation.

2. Shock phenomena

Shock phenomena are related to the impact produced by detonation of an explosive. The velocity of detonation of commercial explosives is known to increase with the degree of confinement and to vary with the composition of the explosive. Confined and unconfined velocities of explosives used in the Keweenaw Tests are summarized below:

	Velocity (ft/sec)	
	Confined	Open
Atlas 80 Percent Straight Gelatin	21,000	20,000
Atlas 60 Percent Straight Gelatin	20,000	16,000
Gelodyn 1	14,000	10,000
Coalite 7S	10,000	8,000

The reflection of shock waves at an interface or free surface is sometimes thought to explain the rhythmic spacing of the cracks described as "O" (onion) cracks. The cracking is thought to precede ground movement and to be related to the seismic velocity rather than to the velocity of detonation.

Possibly the shock phenomena may be of greater consequence in elastic than in plastic materials, but there is little evidence (as will be shown) to indicate that the shock phenomena are of great importance in frozen Keweenaw silt, which behaves plastically. It is difficult to explain the "I" (inward) cracks and "R" (radial) cracks (which are at right angles to and invariably accompany the "O" cracks) as shock phenomena.

If the shock phenomena are related to the seismic velocity, which is a property of the material, rather than to the velocity of the explosive, then the type of explosive is unimportant.

Results of the Keweenaw Tests establish a definite relation between performance and composition of the various explosives tested. It must follow, therefore, either (1) that shock phenomena are of little consequence in determining the size or shape of a crater in frozen Keweenaw silt or (2) that the shock phenomena are related to the velocity of the explosive. The first explanation is adopted here rather than the second.

The first phase of crater formation therefore is considered to be relatively unimportant in blasts in frozen Keweenaw silt.

3. Expansion of the gas bubble

Upon detonation, the explosive confined within a borehole in frozen Keweenaw silt is converted to gas at high temperature and high pressure. After field study, the conclusion that the gas-filled borehole expands by plastic flow of the frozen Keweenaw silt is inescapable. The walls of the cavity are smooth. Inspection shows that the heat of the explosion does not enlarge the cavity by melting. It is evident also that the cavity is not enlarged by crushing. The gas-filled cavity is henceforth referred to as the "gas bubble."

It is evident that expansion of the gas bubble is not uniform in all directions and that the gas bubble is not spherical. Apparently the shape of the cavity depends both upon the shape of the original column of explosive and upon the resistance of the frozen ground to deformation. Under the conditions of the Keweenaw Tests, the gas bubble probably is pear-shaped. The stem might be erect or inverted depending upon (1) the interface ratio, (2) the depth ratio, and (3) the weight and type of explosive. Expansion of the gas bubble might be likened to the blowing up of a toy balloon. It ruptures prematurely if blown up too quickly; it bulges into odd shapes where the membrane is weak. A delicate balance exists between the energy of the explosion, the direction of displacement of the frozen ground, and the size of the gas bubble before rupture. The frozen ground is displaced outward as the gas bubble expands.

Downward expansion of the gas bubble is a result of downward deflection of the frozen-ground interface and flowage of the unfrozen soil. It is reasonable to assume therefore that the moisture content and the plastic behavior of the unfrozen ground influence the shape of the gas bubble and in turn the shape of the surface crater. If downward expansion proceeds far enough, the frozen-ground interface is ruptured into a series of pie-shaped fragments which radiate outward from the point of maximum deflection. (See Fig. 51.)

Failure planes produced below the explosive charge by downward deflection of the frozen ground interface are, of course, difficult to observe except from within the surface crater. All available evidence indicates that the planes of failure below the charge differ from the surface planes of failure only in that the subsurface crater is much smaller and is inverted.

Apparently rupture occurs in various stages of severity. In the most severe cases, ruptured fragments of frozen ground are shot downward into the unfrozen ground, where they travel as a free body such as a bullet or a bomb.

In many craters formed from charges within the frozen layer, there is a horizontal crack which appears to be a neutral plane or a dividing plane between frozen ground displaced downward and that displaced upward. The width of the crack decreases outward. It may be a 6-in. wedge-shaped opening (as in Fig. 51) or a much smaller opening, depending upon the interface ratio, the depth ratio, and the weight of the charge.

Expansion of the gas bubble (either downward, upward, or laterally) results in surface displacement or bulging. The surface bulge characteristic of craters in rocks and in soils is even more fully developed and preserved in frozen ground because of its plastic behavior.

The surface crater in frozen ground is produced by displacement by the gas bubble and exhibits all the features observed in rock craters except rock-burst phenomena associated with the release of strain energy. This exception is part of the evidence for classifying failure of frozen ground as plastic rather than elastic. The attitude of the planes of failure in surface craters in frozen ground is identical with that of planes of failure in rock craters.

The planes of failure are parallel to the three directions of principal stress. The terms "I" (Inward) cracks, "O" (Onion) cracks, and "R" (Radial) cracks are used

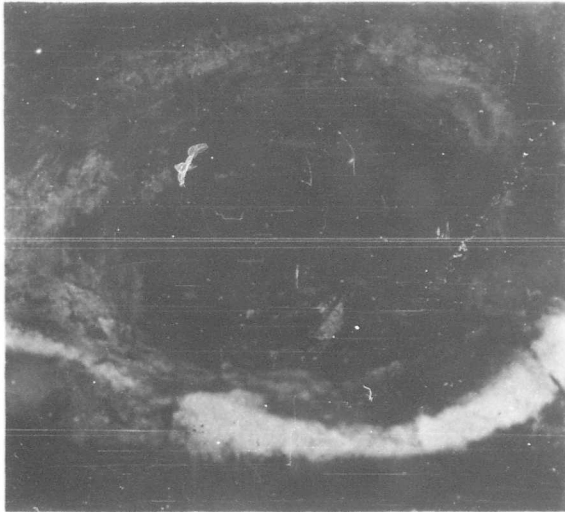


Figure 51. Rupture of the frozen-ground interface due to downward expansion of the gas bubble.



Figure 52. Radial (R) cracks in Keweenaw frozen silt associated with near-critical-depth blast.



Figure 53. Gas-bubble cavern below the frozen layer before removing the debris that has fallen back from the blast.

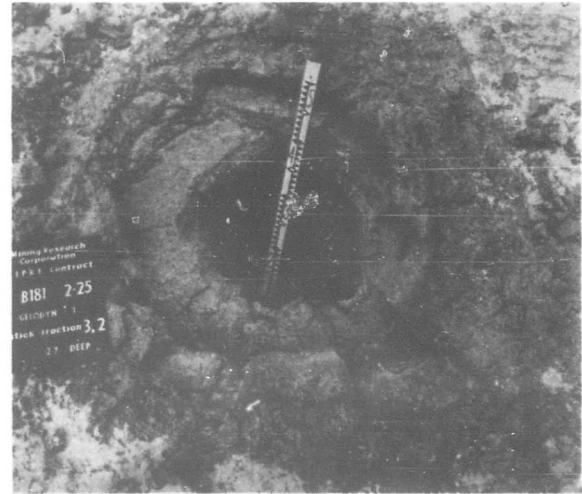


Figure 54. After removal of debris. Concentric layers of "O" cracks (onion) associated with the surface bulge.

to differentiate among the three. Figure 52 shows "R" cracks associated with near-critical-depth blasts. Figure 54 shows all three sets of cracks. The upper layers of the "Onion" have been peeled off during mucking. The "I" cracks are at right angles to the "R" cracks and give a circular outline to the crater in plan view.

The gas bubble, of course, cannot expand downward to rupture the frozen ground interface if the charge is placed in the unfrozen-layer. Under such conditions the gas bubble enlarges to form a cavern underneath the frozen layer, as is evident in Figures 53 and 54. Figure 53 shows the gas-bubble cavern partly filled by debris that has



Figure 55. Surface break-through of the gas bubble at a weight slightly in excess of the critical weight.



Figure 56. Surface break-through of the gas bubble at weight slightly in excess of the optimum weight.

fallen back from the blast. Figure 54 shows the cavern after removal of the debris.

Inspection of the walls of the gas-bubble cavern produced by blasts below the frozen layer proves that the unfrozen material has been thrust laterally aside by plastic flow. Contortions of the original horizontal stratification in the unfrozen silt may be plucked from the soot-blackened walls. The soot is formed of solid particles (smoke) associated with gas in the explosion cavity.

4. Rupture of surface and conversion of pressure head to velocity head

Expansion of the gas bubble is a function of the weight and type of explosive and is related to the number of moles of gaseous product generated by the explosion. The relation between composition and performance of commercial explosives and characteristics of explosives used in the Keweenaw Tests has been discussed in Chapter I. From analysis of the Keweenaw Tests, and consistent with the classification chart (Table I), it seems that two more sets of arrows in the same direction as those shown might be added to the remarks column and labeled "Explosion Pressure Decreases" and "Energy of the Explosion Decreases." Such a classification is here considered to be of greater value in forecasting the performance of explosives than tests made using the ballistic mortar and ballistic pendulum to obtain weight strength, cartridge strength, execution value, or absolute weight strength. A problem arises because of the many different grades of each type of commercial explosive manufactured; but the problem can be overcome mathematically.

The rate of expansion of the gas bubble in frozen Keweenaw silt is here considered to be a function of energy. An increase in energy is thought to be accompanied by a corresponding increase in velocity and in explosion pressure. All three changes are here considered to be interdependent and to be a function of the composition and of the combustion reaction.

At the critical depth, the energy-absorption capacity of the medium equals the energy of the explosion. An increase in weight of explosive ruptures the surface and

produces a crater. At the optimum weight, utilization of energy to produce a crater is maximum. The depth corresponding to the optimum weight is defined as the optimum depth. Optimum depths vary for each type of explosive.

As the weight of explosive (and energy) is increased above the optimum weight, the energy utilization of the explosive decreases. The decrease is here considered to be a result of break-through of the gas bubble to the surface and of conversion of pressure head to velocity head.

Figure 55 is a photograph of break-through of the gas bubble at a weight slightly in excess of the critical weight. Such a blast produces a minimum of noise and flyrock. Under such conditions the gas bubble expands to its greatest possible limits before break-through. A portion of the roof of the cavity remains in place to form an igloo-type foxhole. (See Blast Test B.)

Figure 56 shows break-through at slightly in excess of the optimum weight. Such conditions result in a maximum volume of excavation in frozen Keweenaw silt per unit weight of explosive. Large pie-shaped chunks of frozen ground are thrown into the air, but most of the chunks fall back into the crater. The amount of flyrock, the noise, and the height to which the flyrock rises are greater than at the near-critical-weight condition, but still relatively small. The conversion of energy within the gas bubble from pressure head to velocity head is very slight, but it is apparent that the conversion has started.

As the weight of explosive is increased beyond the optimum weight, the proportion of the energy of the explosion that is converted to velocity head increases. The result is a decrease in volume of excavation per unit weight of explosive, i. e., a decrease in blasting efficiency. As the efficiency is lowered, the noise accompanying the blast increases, fragmentation increases, flyrock travel-height and flyrock travel-distance both increase.

Eventually a point is reached where the efficiency is so poor that the type of explosive used makes little difference in the cratering produced.

It seems reasonable to assume that the principles set forth in preceding paragraphs are applicable not only to blasting in frozen Keweenaw silt but also to blasts in other materials as well. Moreover, there is no reason to assume that the principles are not applicable to military explosives as well as to commercial explosives.

Section II. Blast Test A — Relationships of Explosive, Radius of Crater, Volume of Crater, and Depth of Crater

1. Introduction

The purpose of Blast Test A was to compare crater radii and crater volumes and determine the critical weight of each of four types of commercial explosives for blasts at various depths in frozen Keweenaw silt at the same interface ratio.

At the time blasting was begun in the Keweenaw Tests, the depth of blast holes was 10 in. and the thickness of frozen ground within the proposed test plot ranged from 16 to 18 $\frac{1}{4}$ in. As test work proceeded, the thickness of frozen ground increased slightly, but not sufficiently to permit tests of blast holes deeper than 12 in.

Blast Test A is a composite of Experiment 1 at 10 in. depth of hole (scale 0.55) and Experiments 2 and 8 at 12 in. depth of hole (scale 0.67). The scale of blasts is referred to a prototype blast hole 18 in. deep and 2 $\frac{1}{2}$ in. in diameter. The relation between hole depth and hole diameter for blasts at various scales during the entire period of field work is as follows:

EXCAVATIONS IN FROZEN GROUND

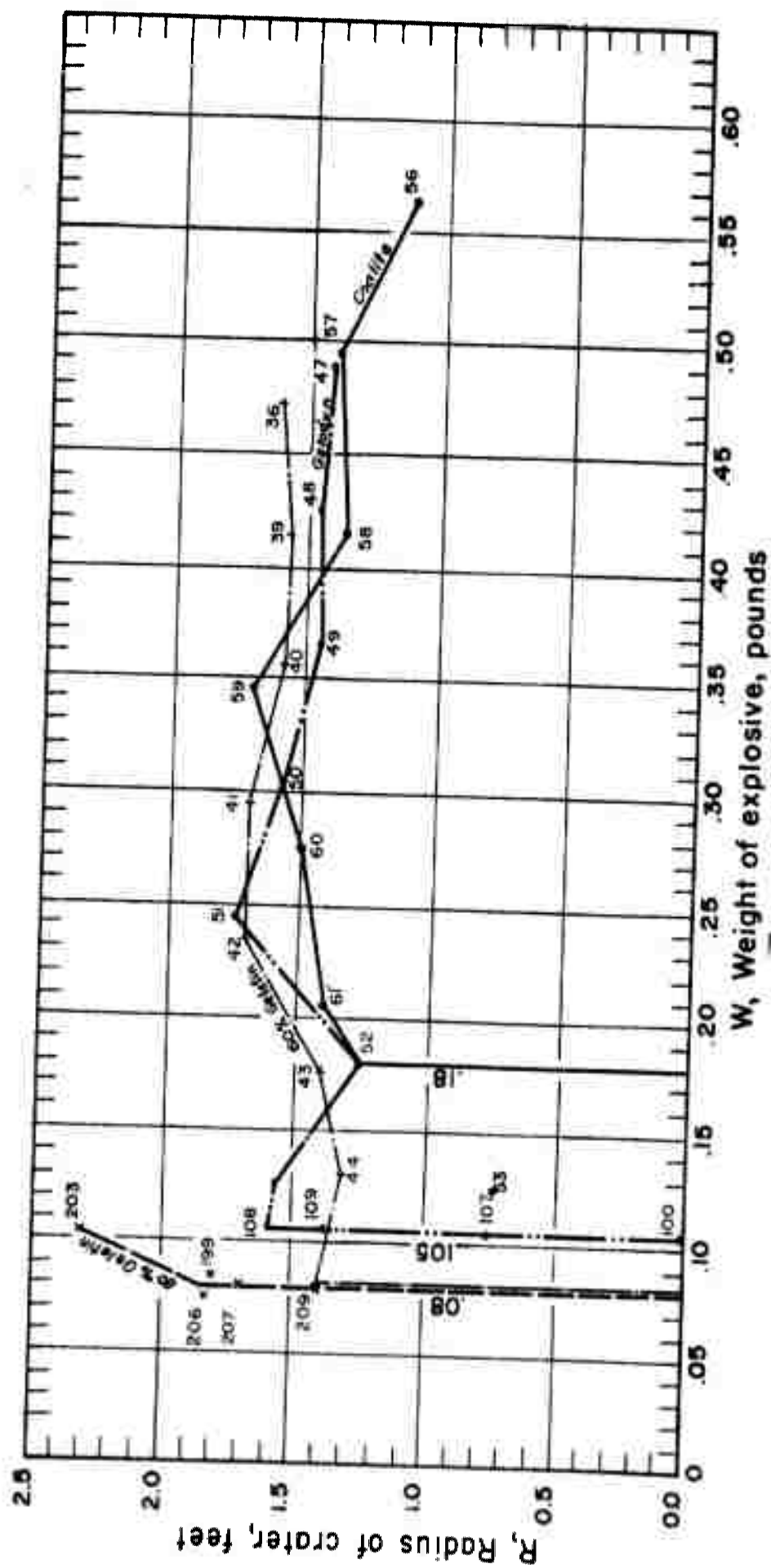


Figure 57. Crater radius vs. charge weight, Keweenaw Blast Test A. Hole depth = 1 ft.

Length-Scale Ratio	Hole Depth (in.)	Hole Diameter (in.)
0.55	10	1 $\frac{1}{2}$
0.67	12	1 $\frac{5}{8}$
0.83	15	2
1.00	18	2 $\frac{1}{2}$
1.17	21	2 $\frac{13}{16}$
1.33	24	3 $\frac{1}{4}$
2.00	36	5
2.50	45	6 $\frac{1}{4}$
3.00	54	7 $\frac{1}{2}$
3.50	63	8 $\frac{3}{4}$

Because of shallow freezing, it was impossible to maintain scale relations and a constant interface ratio for blast holes deeper than 12 in. The interface ratios included in Blast Test A are as follows:

Experiment Number	Hole Depth (in.)	Interface Ratio Range	Number of Blasts	Blast-Hole Numbers
1	10	0.44 - 0.53	28	1-8, 10-31
2	12	0.46 - 0.69	73	38-51, 54-112
8	12	0.51 - 0.59	24	186 - 209

In planning the tests it was concluded (see Ch. II, section 1) that, if an interface ratio of 0.5 or less could be maintained, a reasonable correlation might be possible between critical-depth blasts in frozen ground and critical-depth blasts in other media such as rock or soil.

Ground temperature was recorded at two gage positions (Gages I-1 and I-2) during the field work. Temperatures at 6 in. below surface and at 12 in. below surface are recorded in Figure 6 (Ch. II). The inference is that the ground temperature at a given blast hole is the same as that at the gage position. This is perhaps not true since the ground temperatures at I-1 and I-2 differ.

2. Description

Blast Test A is a composite of three experiments conducted at different times. In Experiment 1, all blast holes were 10 in. deep and 1 $\frac{1}{2}$ in. in diameter. Atlas 80 Percent Straight Gelatin, Atlas 60 Percent Straight Gelatin, Gelodyn 1, and Coalite 7S were used. Blasts were fired with each type of explosive, successively decreasing the weight of explosive uniformly to determine approximately the critical weight.

In Experiment 2, because of the greater thickness of frozen ground, all blast holes were 12 in. deep. It had been observed in Experiment 1 that the critical weight of Gelodyn 1 was less than that of Coalite 7S and that the critical weight of Atlas 60 Percent Straight Gelatin was less than that of Gelodyn 1. The three types of explosives are of different densities and require different volumes of borehole per unit of weight. As a principal objective of Blast Test A was to compare critical weights, it was essential that the depth of center of gravity of charge be the same for all three types of explosive. To vary the depth of hole for each type of explosive and maintain a constant depth of center of gravity would have required a constant weight of explosive, and the weight-depth relations were unknown. It therefore seemed desirable to select a prototype explosive; maintain geometric similarity for the prototype explosive, maintain a constant depth of hole for all types of explosive, but vary the hole diameter so as to maintain a constant depth of center of gravity. Accordingly, in Experiment 2, holes 12 in. deep and 1 $\frac{1}{4}$ in. in diameter were used for blasts of Atlas 60 Percent Straight Gelatin; holes 1 $\frac{7}{8}$ in. in diameter were used for blasts of Gelodyn 1; and holes 2 $\frac{3}{8}$ in. in diameter were used for blasts of Coalite 7S.

The critical weight of Atlas 80 Percent Straight Gelatin at scale 0.67 was found to be very nearly the same as that of Atlas 60 Percent Straight Gelatin. Accordingly, holes of the same diameter were used for blasts of the two explosives.

For each type of explosive, charge weight was reduced uniformly to "straddle" the critical weight. In each experiment, 16 blasts were fired with each of the 4 types of explosives, starting with the weight determined by "straddling" in order to "pinpoint" the critical weight. The procedure was continued until the variation in weight used to "pinpoint" did not exceed the deviation or dispersion due to characteristics of the medium.

Crater data for Blast Test A are tabulated on the data sheets for Experiments 1, 2, and 8. (See Appendix, Fig. A-1 -A-5, and A-11.)

3. Results and analysis

The relation between radius of crater and weight of charge is plotted in Figure 57 for each of three types of explosives. Numbers adjacent to points in the figure are blast-hole numbers. The "curves" have been constructed for each explosive by drawing straight lines between points. Blasts also were made (as shown in Figure 57) with Atlas 80 Percent Straight Gelatin to determine the critical weight, but were not extended to obtain crater dimensions. At the critical weight, the radius of crater drops abruptly to zero.

Because of the small quantity of explosive involved and because of the shallow depth of freezing, it was impossible to determine any difference in the critical weights of Atlas 60 and Atlas 80. At larger length-scale ratios, the critical weight of Atlas 80 was found to be slightly less than Atlas 60.

A characteristic feature of blasts in frozen ground is that a slight increase above the critical weight produces a crater to the full depth of the explosive charge. The term optimum weight (see Terminology) was coined to designate the full-crater condition abruptly produced at near-critical weight. An attempt was made to differentiate between optimum weight and critical weight, using very small increments in weight of explosive (see data sheet, Experiment 3), but the attempt was unsuccessful. Interpolation of data from blasts at larger scales (Experiments 4, 5, 6, 7, 9, 11, and 12) suggests that the optimum weight is slightly greater than the critical weight, but the difference is less than the normal deviation due to variations in physical properties of the medium. Over-all analysis of the blast tests also shows that dispersion increases as the weight of charge approaches the critical weight, which bears upon the inability to differentiate between critical weight and optimum weight in the field.

Critical weight and optimum weight are presented as numerically equal in Figure 57. The weights for various explosives placed 9"-12" from surface to center of gravity are summarized below:

Explosive	Optimum Weight Critical Weight (lb.)
Atlas 80 Percent Straight Gelatin	0.08
Atlas 60 Percent Straight Gelatin	0.08
Gelodyn 1	0.105
Coalite 7S	0.18

For all three types of explosives, an increase in weight beyond the optimum weight does not cause a corresponding increase in radius of crater. The ratio of radius to depth (the r/d ratio) is less than for craters in rocks. In Blast Test A the ratio ranged from 1.36 to 1.69 for Atlas 60, from 1.30 to 1.89 for Gelodyn 1, and from 1.35 to 1.79 for Coalite 7S.

Except in the region of these particular weights, the radius of crater at any given weight is greater for Atlas 60 than for Gelodyn, and greater for Gelodyn than for Coalite 7S.

EXCAVATIONS IN FROZEN GROUND

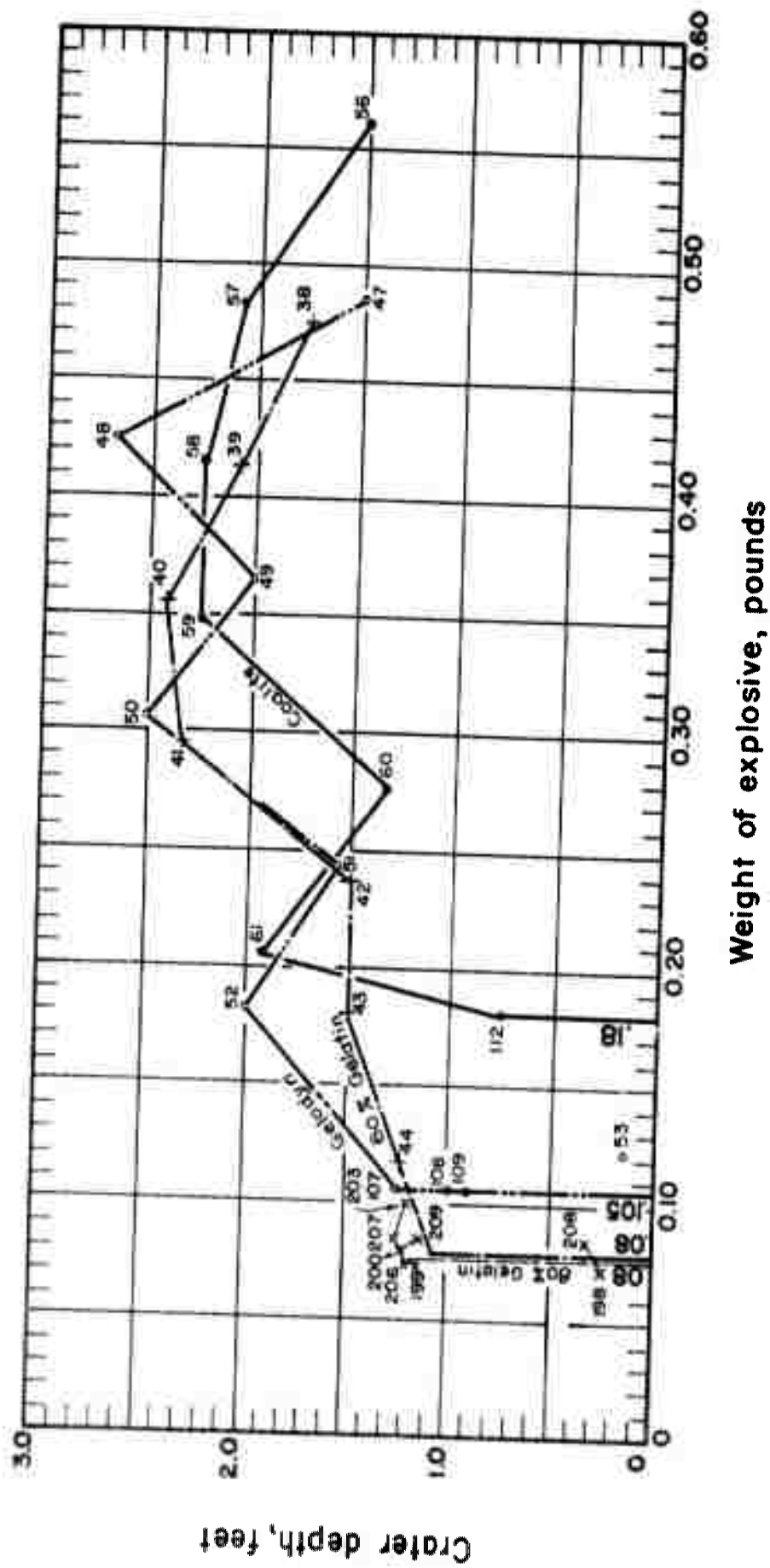


Figure 59. Crater depth vs. charge weight, Keweenaw Blast Test A. Hole depth = 1 ft.

Figure 58 shows volume of crater vs weight of charge. All three curves have the same general shape. All three rise to a peak volume at some intermediate weight and then decline to a volume not greatly in excess of the volume at optimum weight. The weight at the peak volume is designated maximum effective weight (see Terminology). The phenomenon of maximum effective weight has not been observed previously in connection with blasts in rocks or soils. This does not prove that it does not exist in rocks and soils, but it is possible that maximum effective weight (1) may occur only in plastic-acting rocks or (2) may occur only in blasts where the energy of the explosion is greatly in excess of the energy-absorption capacity of the medium. (See also Chapter II, Section IV, Introduction). If the volume of a crater increases measurably as blasts progress from optimum weight to maximum effective weight but the radius of crater remains constant or increases only slightly, the shape of crater must change so as to increase the volume without appreciably changing the radius.

Four measures of crater shape are available: the similitude ratio, the r/d ratio, the ratio of depth of crater to depth of blast hole, and the ratio of the slab volume to the crater volume. (See Terminology.) Inspection of the data sheets Figs. A-1--A-5 and A-11 reveals:

- a) The similitude ratio is negative (depth of crater greater than depth of center of gravity of charge) for all blasts in frozen Keweenaw silt heavier than the optimum weight. The similitude ratio approaches a maximum numerical value near, but not necessarily at, the precise blast that represents maximum volume. The similitude ratio is not as effective for describing craters in frozen ground as for rocks, because of the lack of spread between critical weight and optimum weight.
- b) The r/d ratio of a crater is not an effective measure of shape, because the depth of the crater differs markedly from the depth of center of gravity of the charge owing to expansion of the gas bubble.
- c) The ratio of depth of crater to depth of blast hole is maximum at the maximum effective weight. With Gelodyn 1, the depth of crater may be as much as 2.5 times the depth of the center of gravity of the charge. At this value, the depth of crater is greater in Blast Test A than the depth of frozen ground; this indicates either punching downward or rupture of the frozen-ground interface.
- d) The ratio of chamber volume to crater volume is maximum at maximum effective weight.

Figure 59 shows the relation between depth of crater and weight of charge. An increase in weight of charge in the range between optimum weight and maximum effective weight is accompanied by an increase in depth of crater. The similarity between the depth-weight curves (Fig. 59) and the volume-weight curves (Fig. 58) is apparent. We may conclude, therefore, that, within the range of interface ratios from 0.44 to 0.59, as the weight of explosive charge is increased at constant depth of blast hole, the volume of a crater in frozen Keweenaw silt is increased by a change in shape caused by downward expansion of the gas bubble towards the frozen-ground interface (see also Blast Test B).

4. Summary of observations

From Blast Test A the following characteristics of crater blasts in frozen Keweenaw silt were observed:

- 1) A slight increase in weight of explosive above the critical weight causes a crater to a depth greater than the depth of center of gravity of the explosive charge. The term optimum weight is applied to the minimum weight at which a crater is produced.
- 2) Within the range of interface ratios from 0.44 to 0.59, an increase in weight of explosive charge beyond the optimum weight is not accompanied by a corresponding increase in radius of crater, but is accompanied by an increase in depth and volume of the crater to a weight here referred to as the "maximum effective weight." It is possible that the maximum effective weight is related in some manner to the interface ratio.

3) In the Keweenaw Tests, blasts above the maximum effective weight were considerably fewer than blasts below the maximum effective weight. However, all available evidence for all types of explosives tested indicates that an increase in weight above maximum effective weight, at constant depth of hole, causes both depth and volume to decrease approaching the depth and the volume at the optimum weight. A possible explanation of the phenomenon of "maximum effective weight" is that the gas bubble ruptures in its downward expansion and that the rupture is accompanied by a "gun-barrel" effect in which fragments of frozen ground are "shot" downward into the unfrozen soil.

Section III. Blast Test B — Energy Utilization in Blasting

1. Introduction

Perhaps one of the greatest difficulties in explosion research is to establish a basis for comparing blasts in various materials with various explosives at various length-scale ratios. The difficulty arises because it is usually assumed that the same proportion of the total energy of the two blasts under comparison is expended upon the medium. Actually, the field observer can be positive that the same proportion of the total energy is expended upon the medium only at the critical weight, when all the energy of the explosive is expended upon the medium. The weight of explosive at critical depth (critical weight) is a measure of the energy-adsorption capacity of the medium.

As the weight of explosive is increased beyond the critical weight, a crater is formed, the degree of fragmentation of the broken material increases, flyrock travel-height and flyrock travel-distance increase, and the noise accompanying the blast increases. For an accurate comparison of blast effects at weights other than the critical weight, principles of similitude must be utilized. At different length-scale ratios, the same proportion of the total energy of the explosion must be utilized by the medium or must be lost to the atmosphere in blasts that are comparable and accurately express the model law.

One of two procedures usually is used in field testing: either (1) the charge weight is varied at constant depth of center of gravity or (2) the charge depth is varied at constant weight. In either event the model relations are disturbed if the weight of charge is sufficient to exceed greatly the energy-absorption capacity of the medium and to produce a surface crater. It is impossible by observing the crater or the degree of fragmentation of the broken material to determine visually what proportion of the total energy of the explosion has been utilized by the medium.

An objective of Blast Test B was to determine if possible what changes occur in crater radius, or volume of crater, at constant explosion energy but at various depths in proportion to the critical depth (at various depth ratios). Presumably some relation exists between energy utilization and depth ratio.

Energy utilization might be expressed as a function of either the volume or of the weight of material broken per pound of explosive. In the Keweenaw Tests, the volume basis is used. Energy utilization is calculated on the assumption that the volume of excavation per pound of explosive at the optimum weight represents 100% energy utilization. It should be remembered that the difference between the optimum weight and the critical weight is less than the scatter of the data due to characteristics of the medium, and that the critical weight is a measure of the energy-absorption capacity of the medium. Therefore, the error in estimating energy utilization does not exceed the scatter of the data.

If damage and cracking are due to shock effect rather than to gas bubble expansion, and if the shock effect precedes the displacement caused by gas-bubble expansion, then it would be difficult to establish a relation between loss of energy to the atmosphere and energy utilization or blasting efficiency. But if shock effects are relatively unimportant in blasts in frozen Keweenaw silt, which is the view adopted here, then energy utilization is related to expansion of the gas bubble and to conversion of pressure head to velocity head in the process of surface break-through.

2. Description

Blast Test B was conducted in much the same manner as an "effect-of-depth-experiment," but was preceded by field tests to determine the critical weight of explosive for 1.0-scale blasts using all four types of explosives chosen for the Keweenaw Tests. Thus, the maximum energy-absorption capacity of the medium for each type of explosive and the relation between weight and depth of charge for maximum energy utilization were determined in advance by a series of critical-depth blasts at scale 1.0.

Data sheets for the critical-depth blasts which preceded Blast Test B are summarized in Figures A-12 and A-14. Fifty-five blasts (Blast holes 210-264) were required to "pinpoint" the critical weights of the four types of explosives used. Following results are based upon field observation of blasts summarized in the data sheets.

Explosive	Hole Depth (in.)	Hole Diameter (in.)	Depth of Center of Gravity (in.)	Critical Weight (lb)
Atlas 80 Percent Straight Gelatin	18	2 $\frac{1}{2}$	17 $\frac{1}{4}$	0.20
Atlas 60 Percent Straight Gelatin	18	2 $\frac{1}{4}$	17	0.22
Gelodyn 1	18	2 $\frac{3}{4}$	17 $\frac{1}{8}$	0.38
Coalite 7S	18	3 $\frac{1}{4}$	17 $\frac{1}{4}$	0.66

Hole diameters were calculated using critical weights of explosive for holes 12 in. deep so as to result in an explosive charge of height equal to diameter. It was not expected that the critical weight of Atlas 80 for holes 18 in. deep would be less than that of Atlas 60, but it was. Accordingly, the height of charge for Atlas 80 was less than the hole diameter. (See also Blast Test E — Effect of Charge Shape, and Blast Test C — The Frozen-Ground Interface.)

The procedure followed in Blast Test B was to fire triplicate blasts with each explosive, starting with holes 18 in. deep and successively reducing the depth of hole in 3-in. decrements to a minimum depth of 6 in. The weight of explosive was held constant and equal to the critical weights of each type of explosive for holes 18 in. deep.

The test was conducted as rapidly as possible, but it was found that the depth of frozen ground varied from hole to hole. It was impossible to maintain a constant depth of frozen ground. Moreover, the nature of the test is such that the interface ratio varies, depending upon the hole depth. The depth of frozen ground ranged from 10 to 21 in. The interface ratio ranged from 0.26 to 1.81.

3. Results and analysis

The energy-utilization portion of Blast Test B comprises Experiments 11 and 12, which are summarized on the data sheets (Figs. A-13, A-15, A-16.)

Figure 60 shows the relations between radius of crater and depth of center of gravity of explosive for 0.20-lb blasts of Atlas 80 Percent Straight Gelatin in holes ranging from 18 to 6 in. deep. The critical depth is 1.42 ft. Blasts 232, 233, and 234 are critical-weight blasts.

The difference between weight of explosive required to produce a crater and critical weight is so slight that it cannot be measured. As will be observed from the graph, the dispersion successively decreases as the depth of charges is decreased.

Maximum crater radius was produced by a weight of Atlas 80 equal to the critical weight at 1.42-ft depth at a depth somewhere between 1.22 and 1.42 ft. As the depth of center of gravity of the explosive is decreased from 1.22 to 0.98 ft at constant weight of explosive, the radius of crater decreases almost in direct proportion to the change in length-scale ratio. At less than 0.98 ft the radius remains nearly constant (or decreases less rapidly).

EXCAVATIONS IN FROZEN GROUND

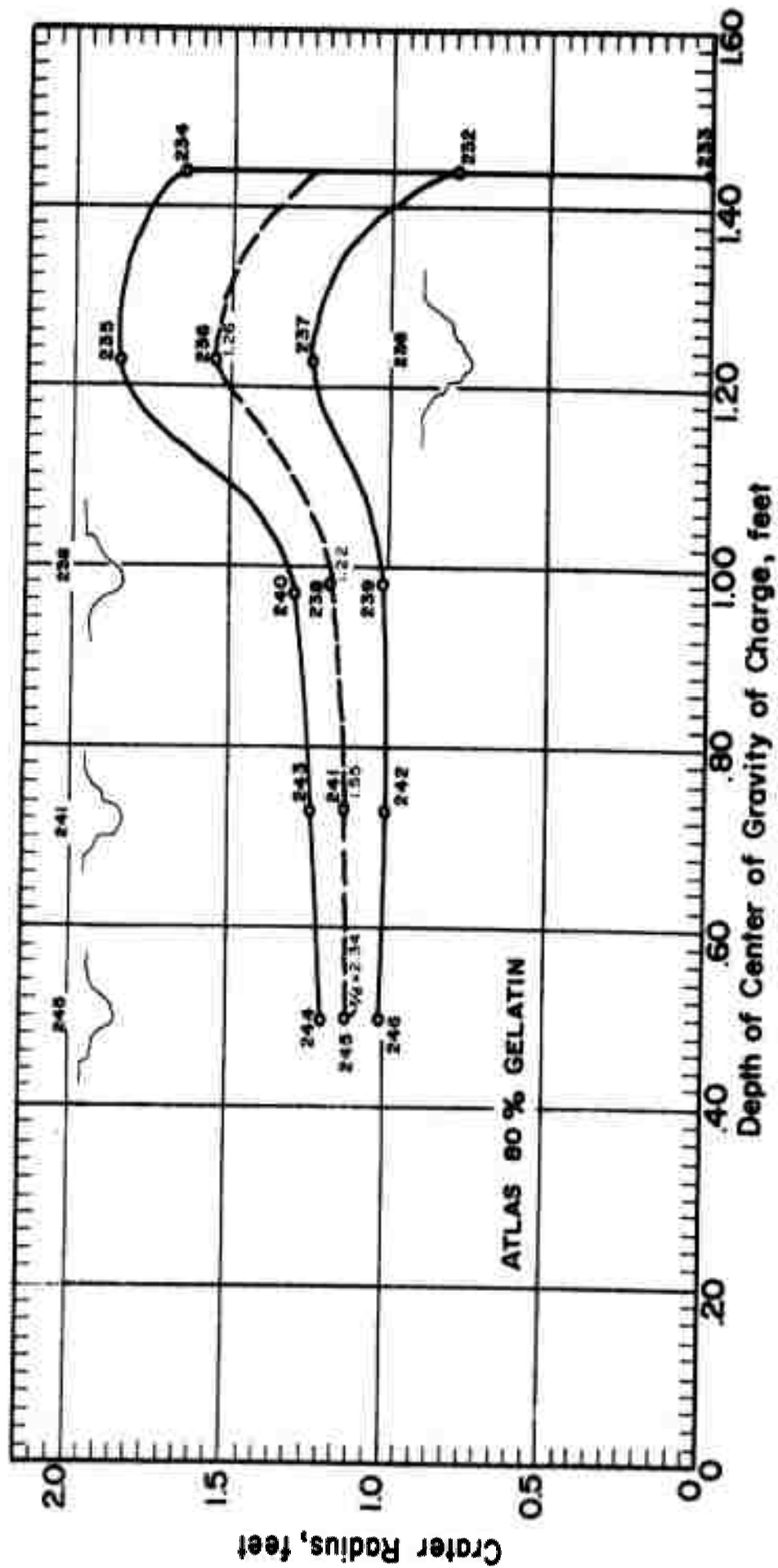


Figure 60. Radius of crater vs. depth of charge. 0.20 lb Atlas 80% Gelatin.
Blast Test B

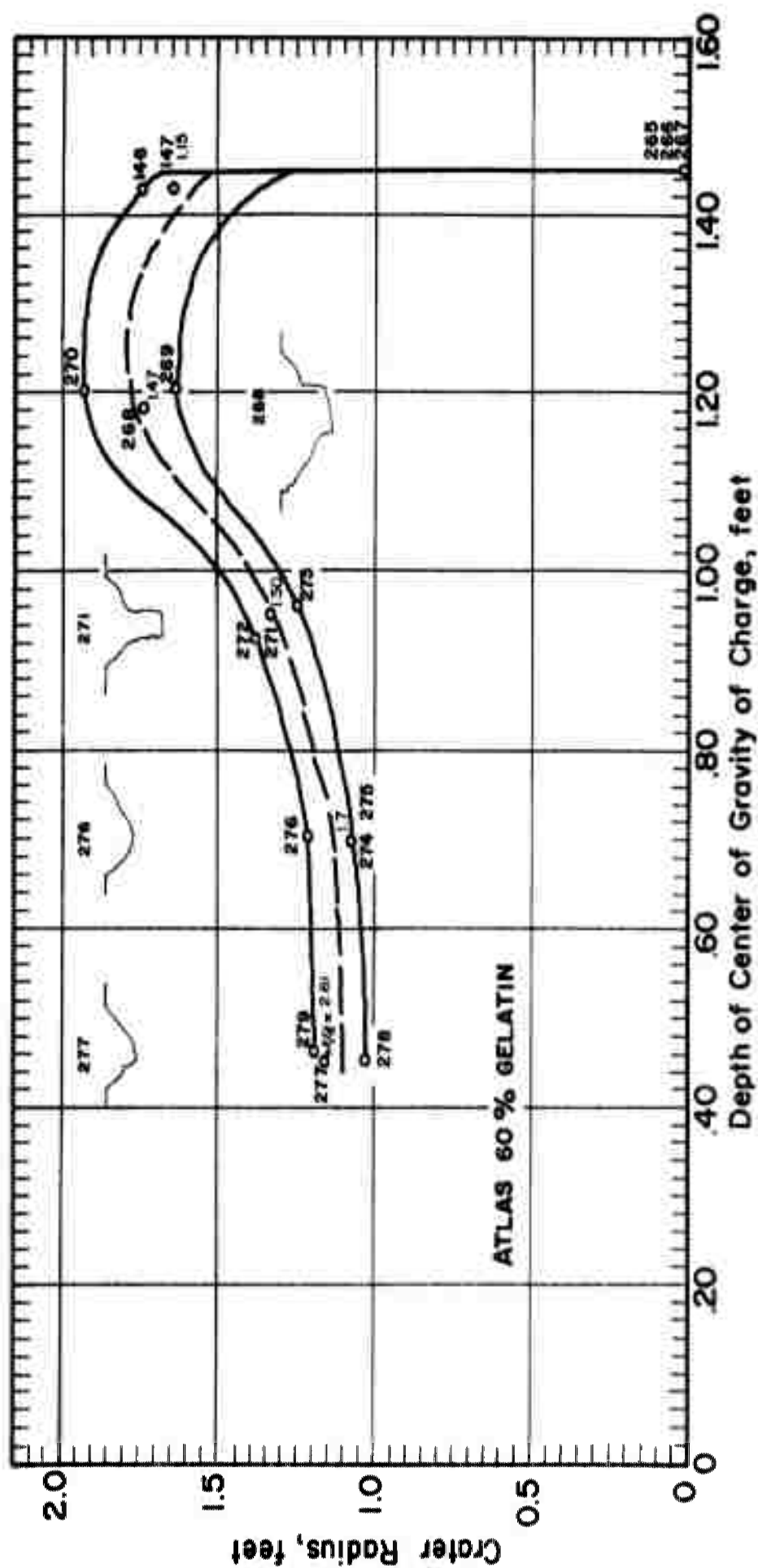


Figure 61. Radius of crater vs. depth of charge. 0.22 lb Atlas 60% Gelatin.
Blast Test B

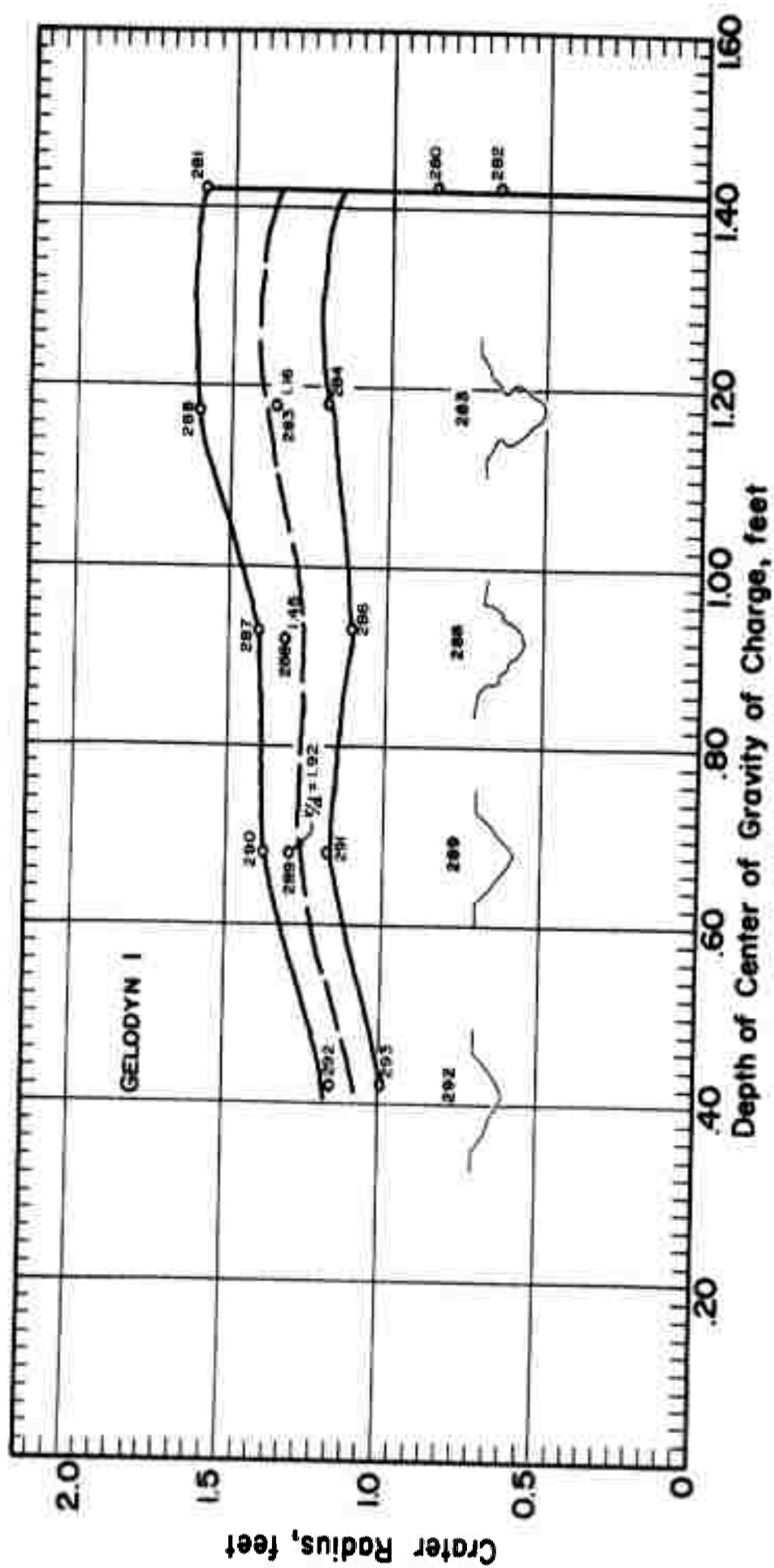


Figure 62. Radius of crater vs. depth of charge.
0.38 lb Gelodyn I. Blast Test B.

Shapes of craters produced by blasts 245, 241, 238, and 236 (which represent average conditions) are shown in the figure. The radius and depth of crater are maximum at 1.22-ft depth of center of gravity and r/d ratio 1.26. The decrease from 1.22- to 0.98-ft depth of center of gravity shows no corresponding change in the r/d ratio of the crater. At 0.98 ft the r/d ratio for crater 238 is 1.22. With a decrease from 0.98 to 0.50-ft center of gravity, the radius remains nearly constant, but the r/d ratio increases from 1.22 to 2.34. As the radius increases, the depth of crater is increased so that the shape change is less apparent than the r/d ratio indicates.

With depth of center of gravity ranging from 1.42 to 1.22 ft, craters are characterized by minimum fragmentation. The fragments are pie-shaped, with "I" cracks, "O" cracks, and "R" cracks coinciding with the 3 directions of maximum principal stress. Flyrock travel-height and flyrock travel-distance are usually less than 50 ft. Figures 55 and 56 accurately represent conditions associated with break-through of the gas bubble. The noise accompanying a cratering blast of this type is minimum.

Fragmentation, noise, and flyrock travel-height and travel-distance all increase as the depth of the charge is reduced. The horizontal distance of flyrock travel may be as much as 300 ft as the depth of center of gravity of the charge approaches 0.50 ft.

Figure 61 shows the relation between crater radius and depth of center of gravity for blasts of Atlas 60 Percent Straight Gelatin, and also the shapes of the resulting craters. The form of the curve is the same as that for Atlas 80 (Fig. 60). As the depth of center of gravity of explosive is reduced from 1.2 ft to 0.9 ft, the radius decreases rapidly, but the r/d ratio remains nearly constant. The radius decreases as the depth of center of gravity is reduced progressively from 0.9 to 0.7 to 0.45 ft, but the r/d ratio increases progressively to 2.6.

The shapes of the Gelodyn and Coalite curves (Figs. 62, 63) are similar, but differ from the Atlas 60 and Atlas 80 curves. The r/d ratio increases progressively as the depth of center of gravity decreases. Otherwise, the relations are the same as for Atlas 60 and 80.

The relations suggest that performance is related to composition of explosive (see Table I) and that two explosives of similar composition exhibit similar blasting characteristics. Thus, we may classify Atlas 80 - Atlas 60 into one series, and Gelodyn 1 - Coalite 7S into a separate series.

The relations presented in Figs. 60-63 are summarized in Fig. 64 using points midway between the upper and lower limits of dispersion. The similarity between the curves for Atlas 60 and Atlas 80, and between the curves for Gelodyn and Coalite, is immediately apparent. Moreover, the weakly developed "hump" in the Gelodyn curve upon approaching the critical weight is in contrast to the continued rise of Coalite 7S and suggests that the behavior of Gelodyn is intermediate between that of Coalite and Atlas 80.

As the depth of charge decreases, all four types of explosives tend to produce nearly the same radius of crater. As the depth increases and approaches the optimum depth, the difference in radii approaches maximum. The optimum depth appears to differ slightly for each type of explosive. It appears also that energy utilization for producing a crater of large radius is greatest at the optimum depth and decreases as the depth of charge decreases.

The depth ratio provides a means of comparing energy utilization of various weights and types of explosives at various depths of charge. The depth ratio is the ratio between the depth of charge and the critical depth. In this blast test, the depth was selected and the critical weight determined by experiment. The depth ratio is 1.0 for a charge buried at the critical depth. The depth ratio is zero for a charge placed so that its center of gravity is on the surface. The depth ratio would be negative for a charge placed with its center of gravity above the surface.

Because energy of an explosive is a direct function of weight, it is desirable to compare the performance of explosives on an equal weight basis. The term radius-utilization factor was coined here as a means of expressing energy utilization per

EXCAVATIONS IN FROZEN GROUND

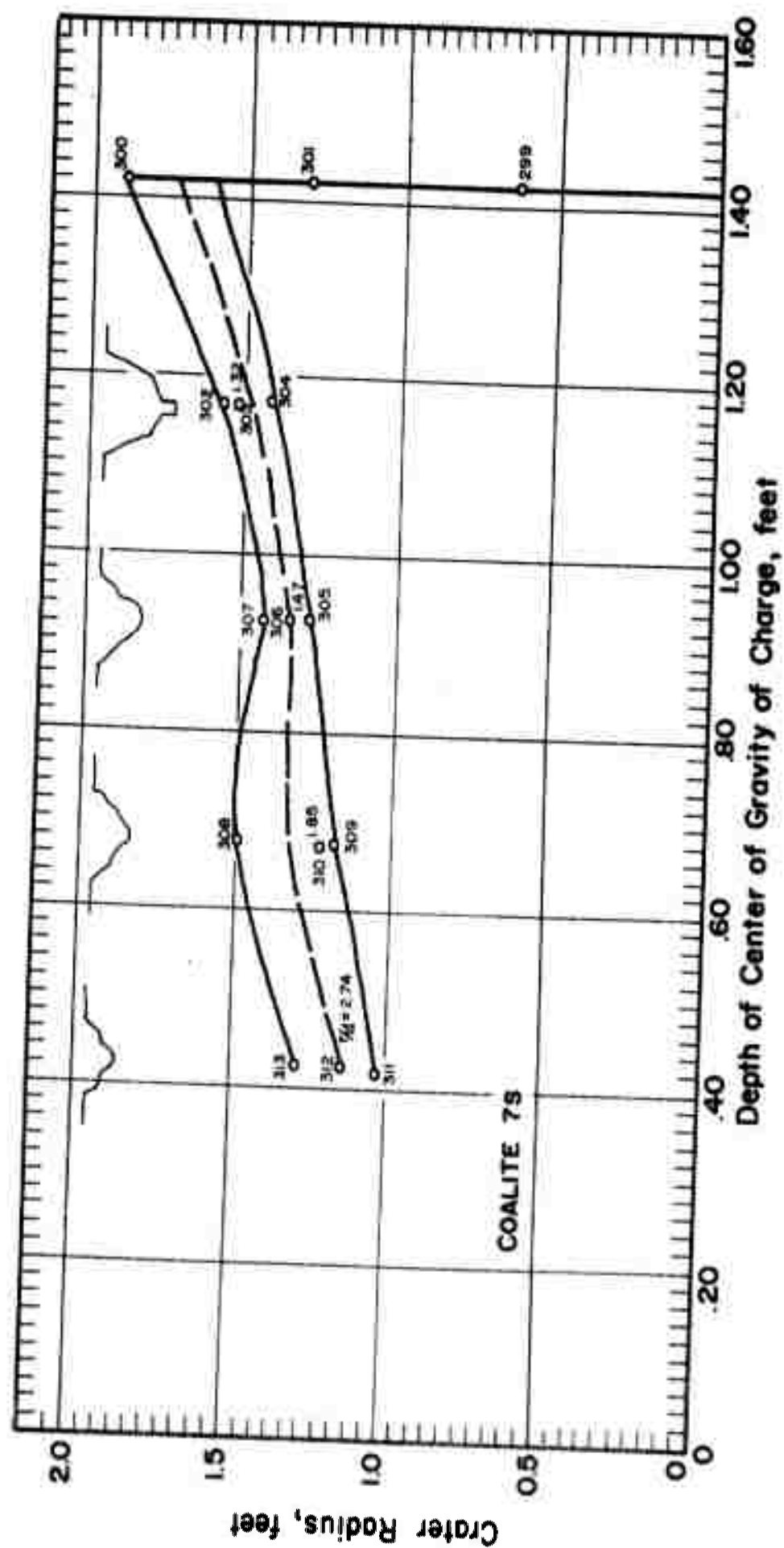


Figure 63. Radius of crater vs. depth of charge
0.66 lb Coalite 7S. Blast Test B.

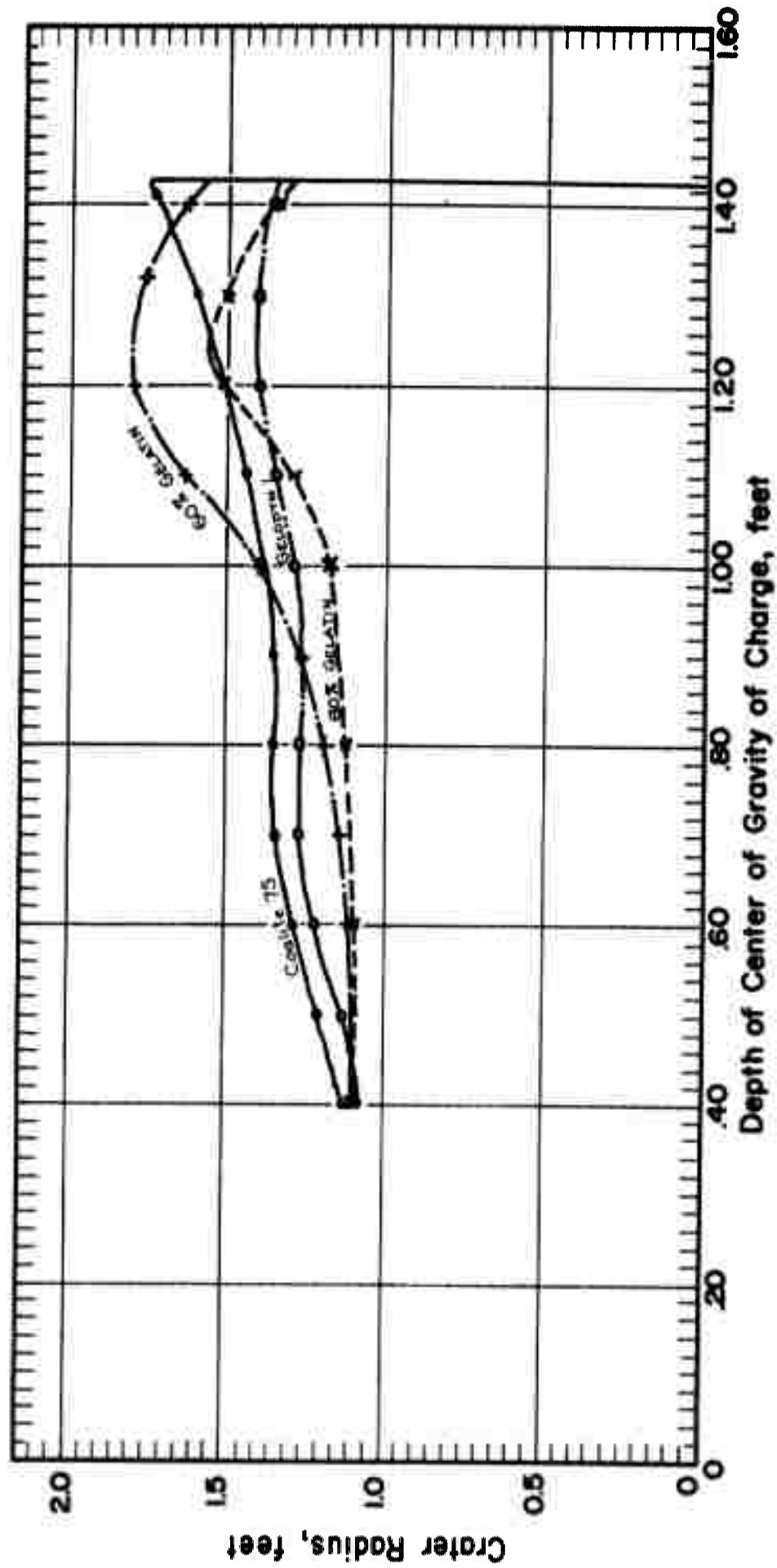


Figure 64. Radius of crater vs. depth of charge, Blast Test B.

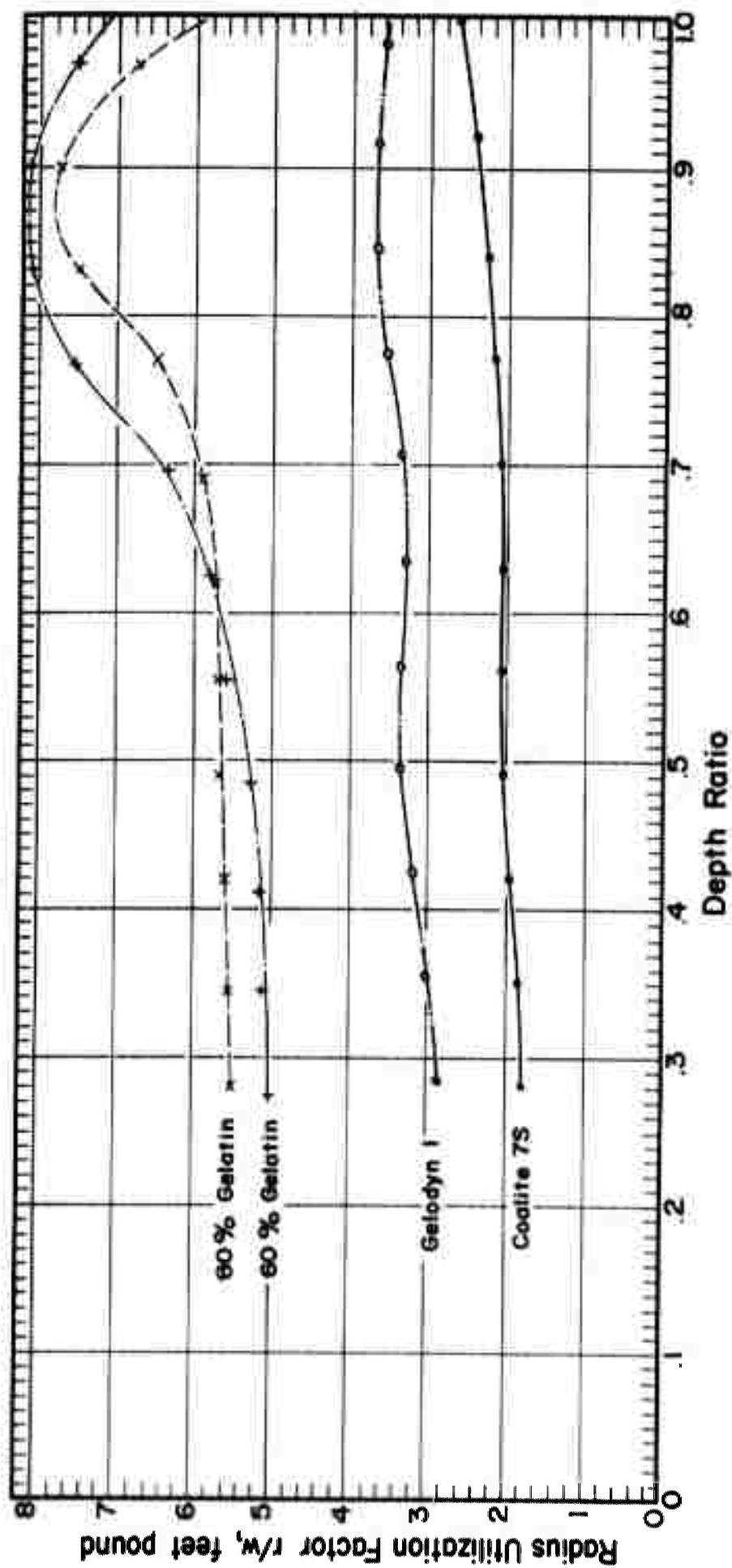


Figure 65. Radius utilization factors vs. depth ratio.
Blast Test B

unit weight of explosive in terms of radius of crater. The radius-utilization factor may be defined as the crater radius divided by the weight of explosive. The units used here are feet and pounds. Therefore, the radius-utilization factor is the number of feet of crater radius obtainable with one pound of explosive.

Fig. 65 was derived from Fig. 64 by expressing depth of center of gravity of charge in terms of depth ratio, and dividing the radius of crater by the weight of explosive to obtain the radius-utilization factor. Radius-utilization factors, at various depth ratios, are different for each type of explosive. The Atlas 60 - Atlas 80 Series of explosives (Straight Gelatins) are much more effective than the Gelodyn - Coalite Series (Semi-gelatin - Ammonia-Base Permissible) in terms of radius produced per pound of explosive. Gelodyn (Semi-gelatin) is more effective than Coalite (Ammonia-Base Permissible). Atlas 60 (Straight Gelatin) is more effective than Gelodyn 1 (Semi-gelatin). Atlas 80 is more effective than Atlas 60 at depth ratios less than 0.62, but less effective at depth ratios above 0.62.

The reason for the anomalous behavior of Atlas 80 with respect to Atlas 60 is not understood at this time. Possibly, (1) some relation exists between interface ratio and radius-utilization factor or (2) the optimum rate of expansion of the gas bubble is related in some manner to the physical properties of the frozen ground. Aside from the above exception, the behavior of the various explosives is consistent with the Classification Chart, (Table I). Criteria such as weight strength, cartridge strength, execution value, and absolute weight strength appear unrelated to performance in frozen Keweenaw silt, which behaves plastically. Velocity appears to be an indication of energy. Calculations based upon the combustion reaction appear to offer promise as a basis upon which performance may be predicted.

Inspection of Figure 65 reveals that the radius-utilization factor is maximum for the Atlas 60 - Atlas 80 Series (Straight Gelatin) in the range of depth ratios from 0.86 to 0.91. The peak is broader, but possibly at a slightly higher range for Gelodyn 1. The peak for Coalite 7S occurs at a depth ratio of 1.0. It follows by inference that the relation between optimum weight and critical weight depends upon the type of explosive. As deviation is greatest for all types of explosives within the range under discussion, and because of restrictions imposed upon the Keweenaw Tests by the shallow depth of frozen ground, it seems desirable to continue the investigation at greater depths of frozen ground.

Blast data are analyzed in following paragraphs with respect to changes in volume of crater. Figure 66 presents the relation between depth of charge and volume of crater for Atlas 80, Atlas 60, Gelodyn 1, and Coalite 7S. The dispersion obtained using triplicate blasts and the increase in dispersion approaching the critical depth may be observed.

Interpretation of the trend of the curves upon approaching the critical depth is difficult. Accordingly, it seems desirable in future tests both to increase the scale of the blasts and to reduce the depth interval between blasts. Rather than using triplicate blasts, it seems desirable to fire at least 5 shots at each depth.

Figure 67 summarizes the data of Fig. 66 using points for each explosive midway between the lower and upper limits of dispersion. Volume-utilization factors for each type of explosive may be obtained from Fig. 67 in the same manner that radius-utilization factors were obtained from Fig. 65. Volume-utilization factors are plotted against depth ratio in Fig. 68.

The volume-utilization-factor curves are different in shape from the radius-utilization-factor curves because of the manner of construction. Because of lack of detail in the interval between holes 15 and 18 in. deep, the volume-utilization-factor curves were projected ahead to critical depth using the trend observed at lesser depths.

The relative positions of the curves for the various explosives is the same as for the radius-utilization-factor. The volume of excavation per pound is less for Coalite than for Gelodyn, less for Gelodyn than for Atlas 60, less for Atlas 60 than for Atlas 80 at depth ratios less than 0.47, but greater at depth ratios above 0.47.

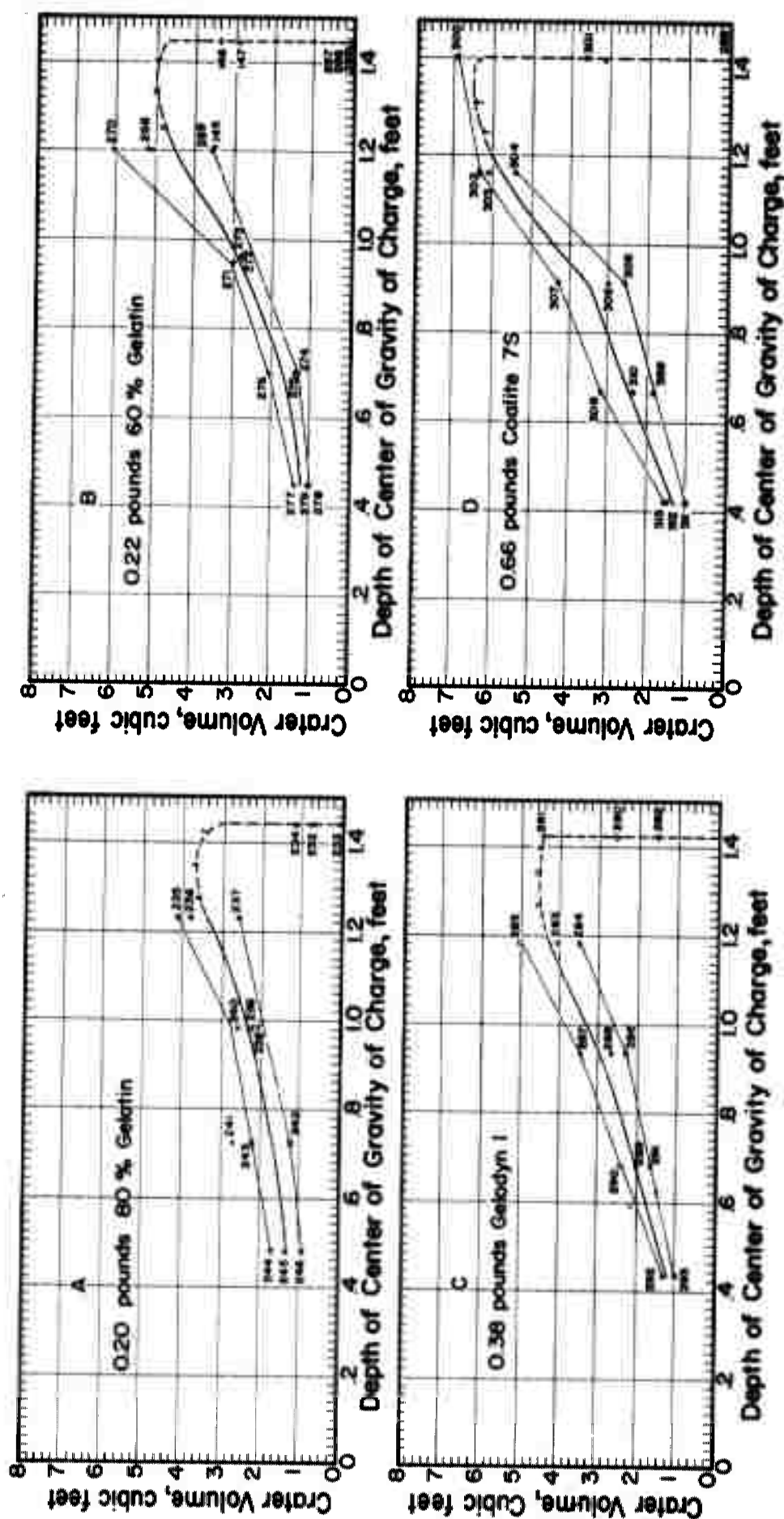


Figure 66. Volume of crater vs. depth of charge, four types of explosives.

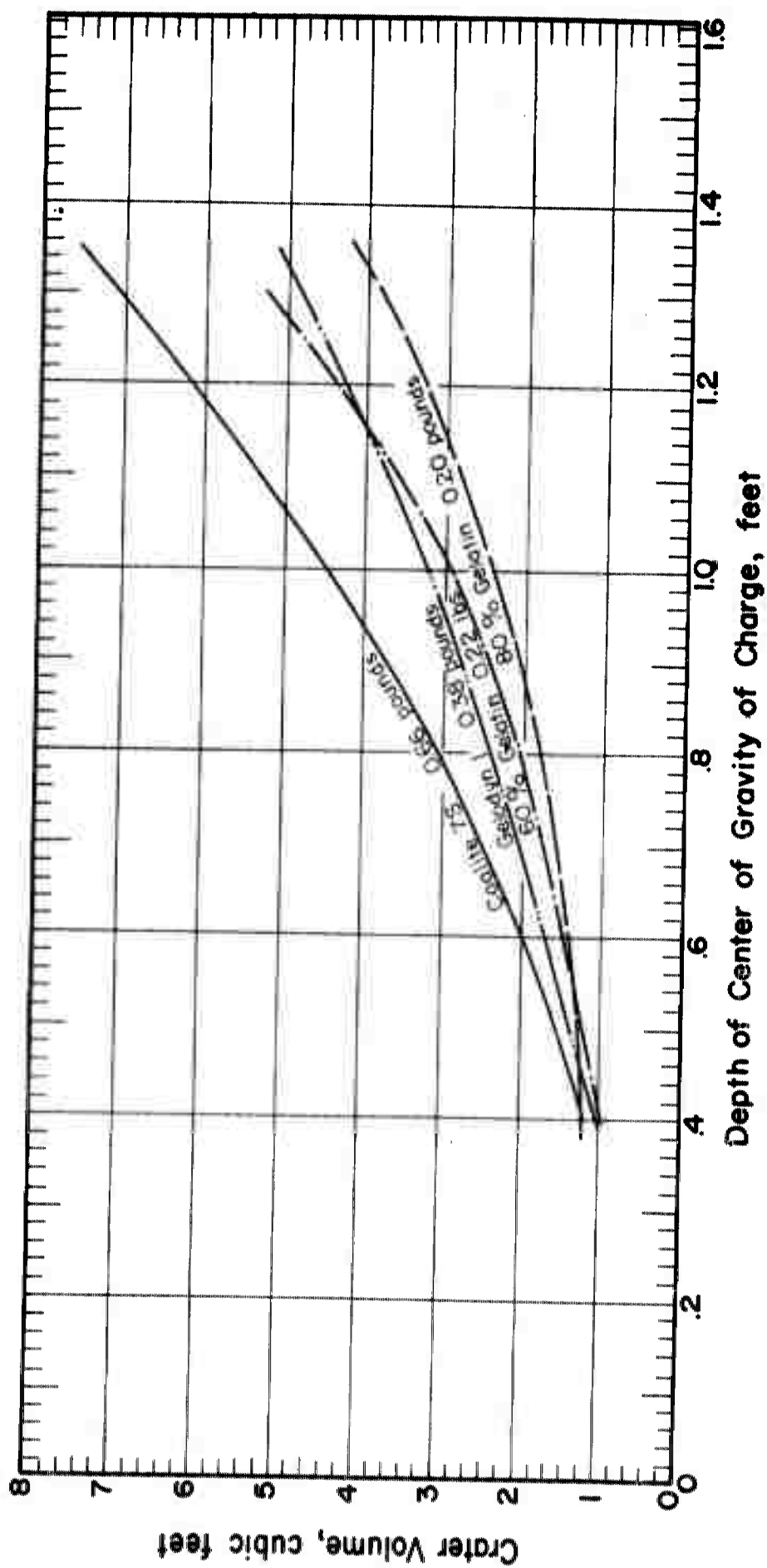


Figure 67. Summary curves, Keweenaw explosives.
Crater volumes at various charge depths.

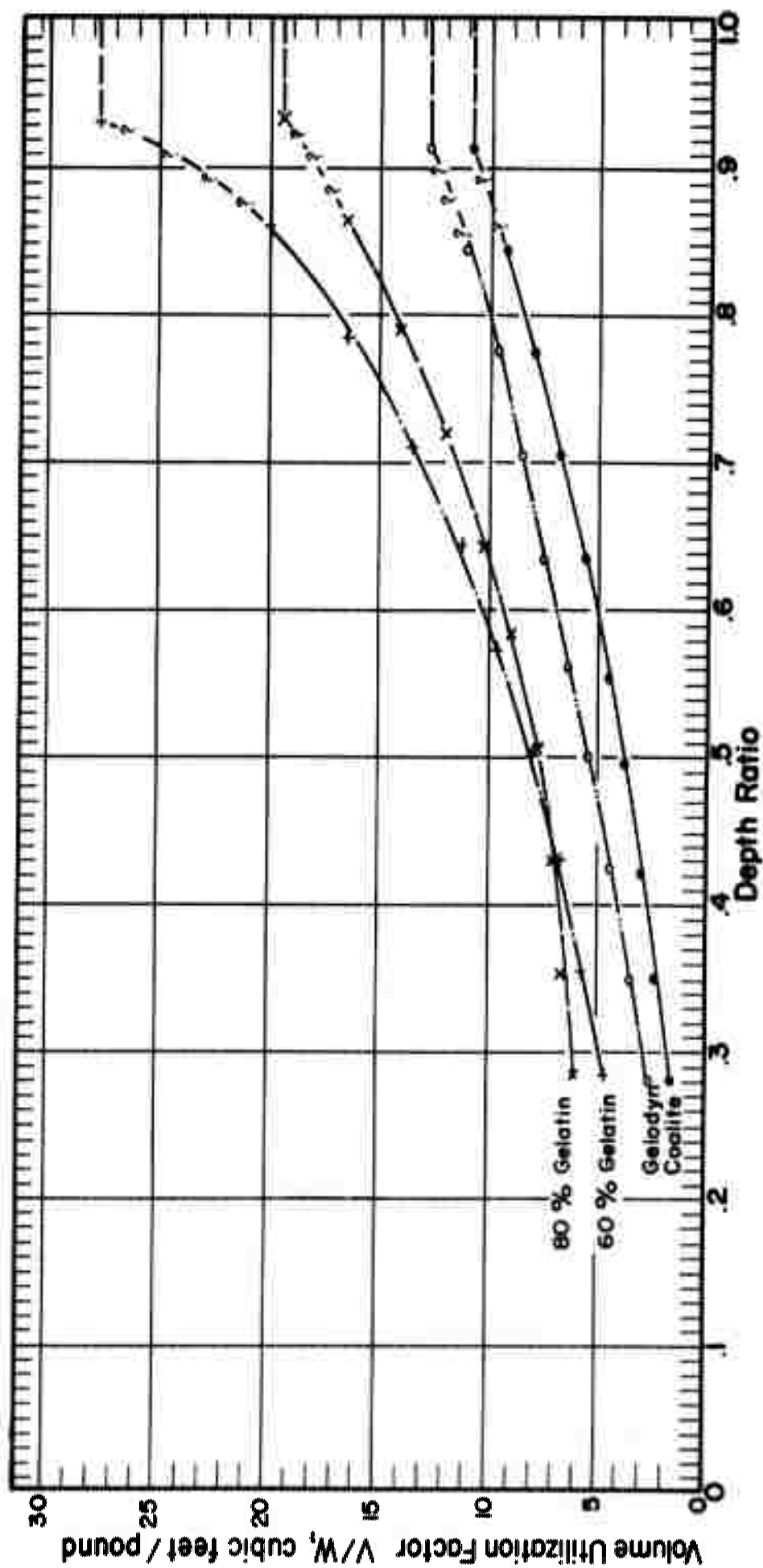


Figure 68. Volume utilization factor vs. depth ratio, Blast Test B.

Neglecting for a moment the anomalous behavior of Atlas 80, it is of interest to note that at a depth ratio of 0.6 the volume-utilization factor multiplied by 2000 equals the confined velocity in feet per second. Moreover, at a depth ratio of 0.5 the volume-utilization factor multiplied by 2000 equals the unconfined velocity in feet per second. The relations are summarized in the following table.

Explosive Type	Depth Ratio	Volume-Utilization Factor (ft ³ /lb)	Volume-Utilization Factor Times 2000	Confined Velocity (ft/sec)	Unconfined Velocity (ft/sec)
Atlas 60	0.60	10.0	20,000	20,000	
Gelodyn 1	0.60	6.8	13,600	14,000	
Coalite 7S	0.60	5.1	10,200	10,000	
Atlas 60	0.50	8.0	16,000		16,000
Gelodyn 1	0.50	5.25	10,500		10,000
Coalite 7S	0.50	3.80	7,600		8,000

As depth ratio is a measure of confinement and standardized tests for measuring velocity of detonation show that velocity increases with confinement, it is not unreasonable to assume that the velocity of detonation increases with the depth ratio.

The peculiar property exhibited by Straight Gelatin explosives of detonating at a much lower rate when unconfined than when confined has been mentioned previously. Probably various grades of Straight Gelatin differ in velocity in a manner not directly in proportion to the blasting gelatin content, but depending also upon the percentage of sodium nitrate present. Sodium nitrate in various combinations with blasting gelatin must be responsible for the anomalous behavior. More sodium nitrate is added to Atlas 60 Percent Straight Gelatin than to Atlas 80 Percent Straight Gelatin. As another grade of Straight Gelatin might have a higher confined velocity than Atlas 60, it might be desirable to investigate blasting action of Straight Gelatins containing more and less sodium nitrate than Atlas 60.

As the depth of burial of explosive is decreased at constant weight or as the weight of explosive is increased at constant depth, the volume-utilization factor decreases. The decrease is accompanied by an increase in fragmentation, but the increase is not as much as one might assume. Flyrock travel-distance, flyrock travel-height, and noise of the explosion increase as the depth of burial is decreased at constant weight (as the depth ratio decreases). From these observations several important conclusions may be drawn:

- 1) The use of explosive greatly in excess of the optimum weight increases the hazard to a soldier constructing a foxhole of being struck by flyrock. To reduce the hazard, the distance between the blast firing point and the foxhole must be increased.
- 2) Because of the greater noise, greater flyrock travel-height, and greater flyrock travel-distance, the use of explosives greatly in excess of the optimum weight increases the likelihood of the enemy's spotting the position where foxholes are being dug.
- 3) From the standpoint of logistics it is undesirable to use explosives greatly in excess of the optimum weight for blasting foxholes in frozen ground because much of energy of the explosion is wasted at shallow depths of burial. Atlas 60 is preferable to other types of explosives used in the Keweenaw Tests because of its greater volume-utilization factor and because of the small weight that must be supplied to the soldier and transported on the battlefield.

Figure 69, a cost comparison of the various test explosives, based upon 1954 prices of Atlas explosives, shows that Atlas 60 is less expensive than the other types used. The explosives were manufactured within 25 mi of the Keweenaw Test Site.

EXCAVATIONS IN FROZEN GROUND

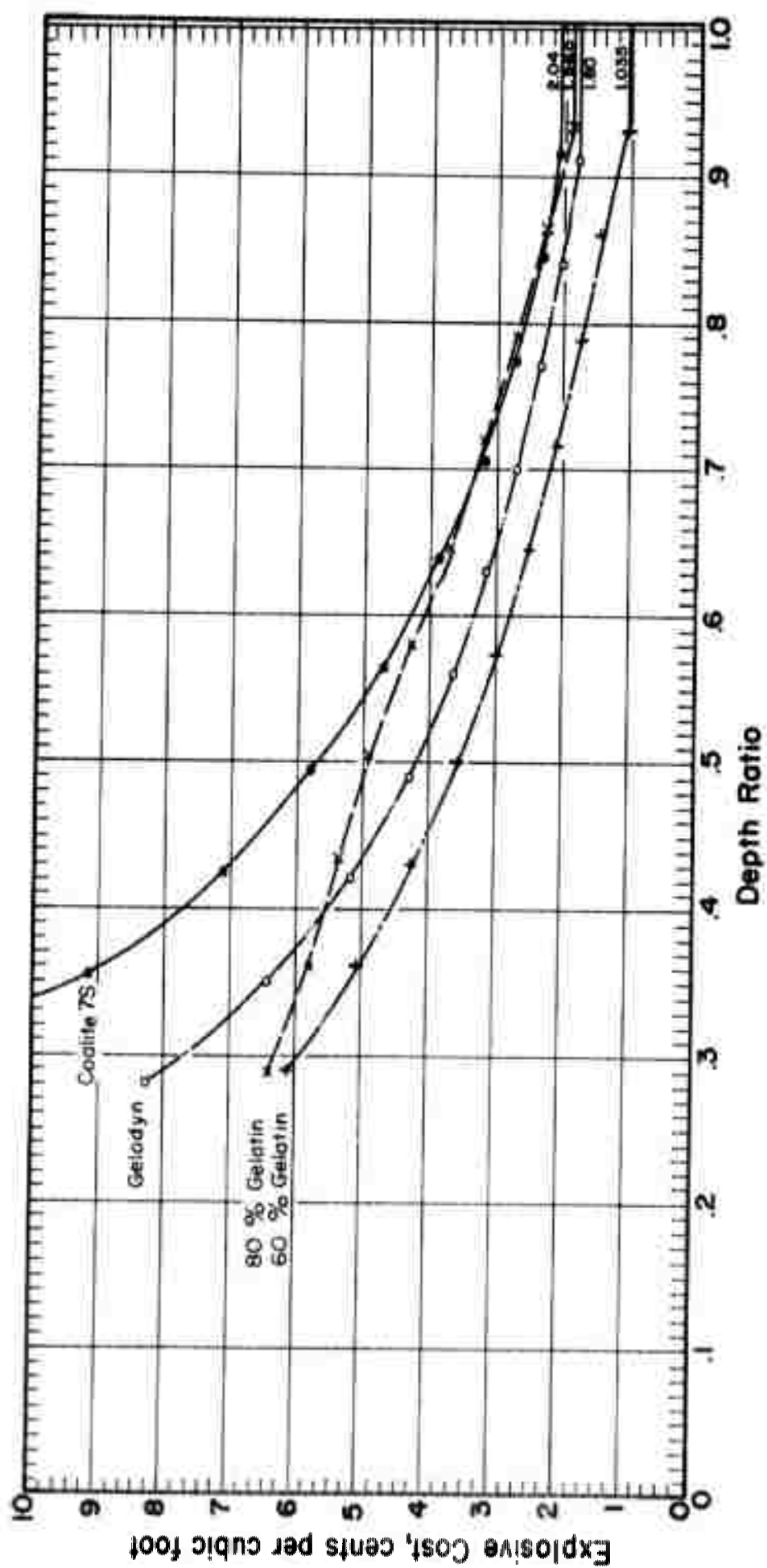


Figure 69. Explosive cost at various depth ratios.

Under the most ideal conditions of controlled blasting, the lowest possible explosives costs obtainable per cubic foot broken are as follows:

	Explosives Costs per Cubic Foot Broken (cents)
Atlas 60	1.035
Gelodyn 1	1.80
Atlas 80	1.96
Coalite 7S	2.04

4. Summary of observations

Energy utilization in the sense of producing a crater of large radius or of large volume is greatest at optimum weight. At optimum weight the depth ratio appears to differ slightly for each type of explosive, but ranges from 0.9 to 1.0. In order to determine accurately the depth-ratio range, additional blasts must be fired in ground frozen to a greater depth than obtained during the Keweenaw Tests.

The term radius-utilization factor is used here to express energy utilization per unit weight of explosive, and is equal to the number of feet of crater radius obtainable with one pound of explosive. The volume-utilization factor is the number of cubic feet of crater excavated per pound of explosive.

Fig. 65 shows the relation between the radius-utilization factor and the depth ratio for each of the Keweenaw Test explosives. As the depth ratio decreases, the radius-utilization factor decreases also. The form of the curves suggests a definite relation between performance and composition of explosive. It is apparent that the Atlas 60-Atlas 80 Series (Straight Gelatin series) differs from the Gelodyn - Coalite Series, and that the behavior of Gelodyn is intermediate between that of Ammonia-Base Permissibles (Coalite 7S) and of Straight Gelatin explosives.

Figure 68 relates volume-utilization factor to depth ratio. The relative position of the curves for the Keweenaw Test explosives is the same as in Figure 65. Each type of explosive seems to exhibit a "characteristic curve." Perhaps the form of the characteristic curve is a property of the material as well as of the explosive.

The energy-utilization effect present in blasts at various length-scale ratios and at various depths using various types of explosives may be expressed by an "energy-utilization number." (See Blast Test C, Section IV, Item 2) Blasts in which the same proportion of the total energy of the explosion is utilized by the medium would have the same energy-utilization number. The energy-utilization number can be calculated using the volume-utilization factor and the model-law equations.

Costs of blasting are directly related to energy utilization. It is most difficult to establish a basis for comparing the efficiencies of various blasts. Efficiencies might be compared on a basis of volume broken per pound of explosive (volume-utilization factor) relative to the volume broken at optimum weight, but it is difficult at present to establish a true standard of comparison because the energy of the explosion cannot be measured and the true relation between impulse and energy utilization is uncertain. The relation between explosives cost and depth ratio (Fig. 69) shows that costs of blasting frozen ground increase as the depth ratio decreases. The lowest possible cost (and perhaps the greatest possible blasting efficiency) is achieved at optimum weight.

The conclusion is inescapable that the performance of an explosive is related to composition. Using the classification of commercial explosives based upon composition (Table I), it is possible to predict the relative effectiveness of the Keweenaw Test explosives at maximum energy utilization (at optimum weight).

EXCAVATIONS IN FROZEN GROUND

The order of the explosives in the chart is inconsistent with energy measurements obtained using a ballistic mortar and ballistic pendulum. A probable explanation is that, because of mechanical limitations, the ballistic mortar and ballistic pendulum cannot measure the energy of an explosion in the regions where the co-volume of the molecules is responsible for deviation from the Perfect Gas Law. Undoubtedly co-volume of the molecules must be taken into account for blasts in the region of optimum weight.

Section IV. Blast Test C—The Frozen-Ground Interface

1. Introduction

The interface between frozen and unfrozen ground is not a sharp boundary, nor is it a plane surface. Moreover, the depth of freezing depends upon many factors, including composition and moisture content of the soil. During the Keweenaw Tests the maximum thickness of frozen ground was 24 in. At the time of maximum depth of freezing, parts of the test site were frozen to a depth not greater than 10 in.

Because of limitations of the test site, it was impossible to measure the effect of the frozen-ground interface or to separate such effect from energy-utilization effects as presented in Blast Test B. It is necessary to know what the effect of the frozen-ground interface is and how to measure it. According to the theory evolved from all the Keweenaw Tests (Ch. II, 1), we may assume that expansion of the gas bubble and the utilization of energy are related in a complex manner: (1) to properties of the unfrozen material below the interface; (2) to the depth ratio; and (3) to the interface ratio. The depth ratio depends both upon the explosive and upon the depth of burial. The interface ratio is the ratio of the depth of burial to the depth of frozen ground. Depth ratio, interface ratio, and explosive type are within control of the blaster, provided the depth of freezing is great enough. The specific properties of the frozen and of the unfrozen ground that should be measured are a matter for conjecture at present.

The Keweenaw Tests suggest that energy-utilization experiments (1) at various length-scale ratios (various depths of frozen ground using scaled charges), (2) at various depth ratios in deeply frozen ground, and (3) at various interface ratios are necessary in order to separate the effects of the frozen-ground interface from the effects of the ground surface for blasts within the frozen layer.

We may conclude as a result of the Keweenaw Tests that one effect of the frozen-ground interface is to change the volume-utilization factor and the radius-utilization factor, possibly by shifting the center of pressure of the gas bubble and by increasing the time (impulse) that the energy of the explosion is exerted upon the medium. Possibly the seeming phenomenon of "maximum effective weight" is related entirely to rupture of the frozen-ground interface (see also Section II, Item 4).

2. Relation of frozen-ground interface to scaling laws

To compare craters produced by blasts at various length-scale ratios, principles of similitude must be employed. The following equation is adopted here as accurately expressing the model law:

$$R = K \sqrt[3]{W}$$

where,

R is radius of rupture

K is a constant

W is weight of explosive.

From information obtained in the Keweenaw Tests and elsewhere, perhaps K can be broken down into three parts and the formula rewritten. In the cases studied here, R becomes N , and $K = ABC$:

$$N = ABC \sqrt[3]{W}$$

where

\underline{N} is the normal distance, in ft from the center of the charge to the damage surface

\underline{A} is an energy-utilization number, which depends upon the type of explosive and the depth ratio. (See Summary of Observations - Blast Test B)

\underline{B} is a rock factor. (See Terminology p. 4)

\underline{C} is a stress-distribution factor, which depends upon the interface ratio and the number of free-faces

\underline{W} is weight of explosive, in lb.

From the data from critical-depth blasts at interface ratios of 0.5 or less, the \underline{ABC} product can be calculated for each of the various explosives used in frozen Keweenaw silt. At interface ratios less than 0.5 we may assume that \underline{C} is 1.0. Then the value of \underline{B} is also constant. Because it was impossible to distinguish in the Keweenaw Tests any difference between critical weight and optimum weight, the same energy-utilization numbers may be used for optimum weight as for critical weight.

Fig. 70 (top) shows graphically the model-law equations for blasts in frozen Keweenaw silt in holes less than 15 in. deep. Within that depth range, the influence of the interface ratio is minimized. The \underline{AB} product is 2.27 for Atlas 60, 2.05 for Gelodyn 1, and 1.70 for Coalite 7S. The model-law equations for critical or for optimum conditions are written adjacent to the curve for each explosive.

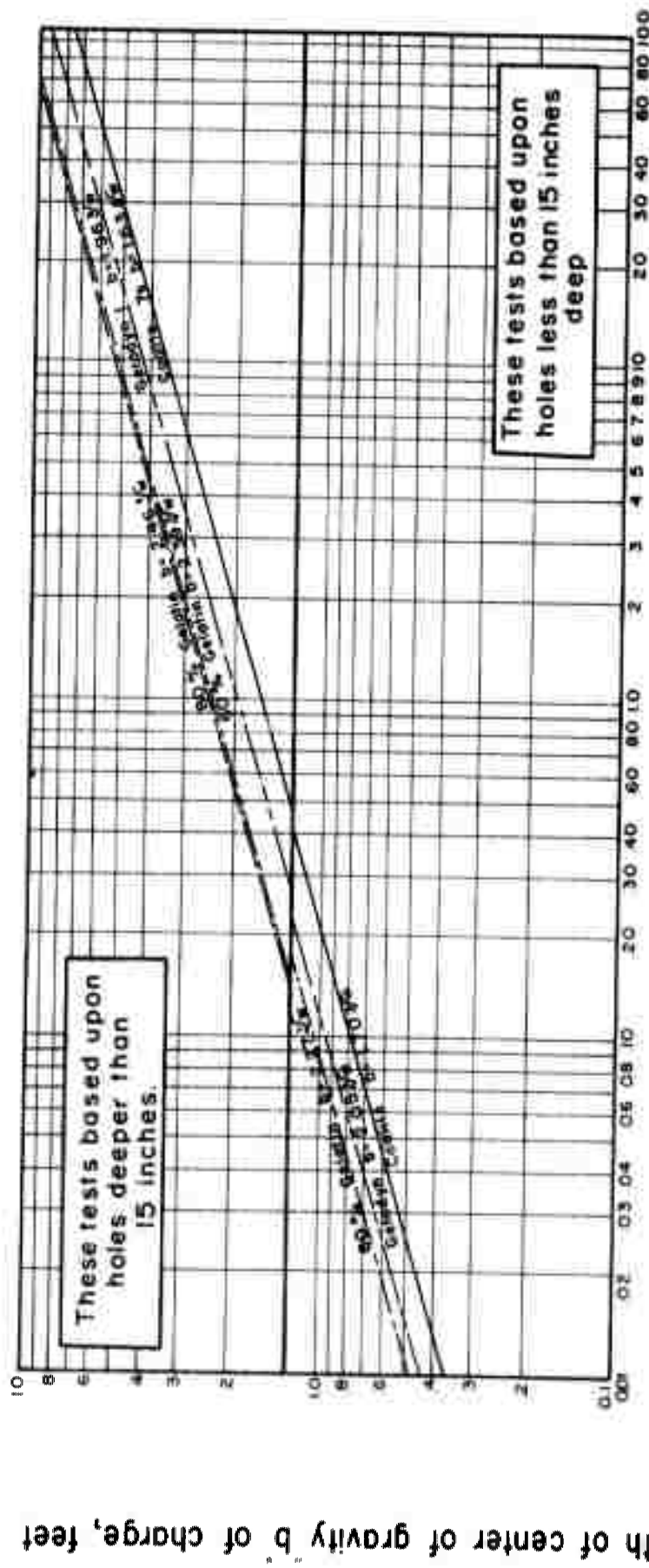
Fig. 70 (bottom) shows graphically model-law equations for blasts in frozen Keweenaw silt as determined using holes 18 in. deep. \underline{AB} products are 2.39 for Atlas 60, 1.96 for Gelodyn 1, and 1.63 for Coalite 7S. Whether the difference in constants in the two sets of equations is due to the interface ratio, to the rock factor, or to the experimental error is unknown at present because the difference is small (approximately 5%), the weights of explosives are small, and the scale of the blasts is small.

One approach used in the field to provide information on the effect of the frozen-ground interface was to calculate the critical weight of explosives for blasts in holes 12, 18, 27, 36, 45, 54, and 63 in. deep (Blasts 155-185; see Appendix A-9, A-10), using the model-law equations, and visually compare results at the various scales. A larger crater was produced for the deep blasts than had been anticipated, but because the difference between optimum weight and critical weight was less than the dispersion, because of the wide limits of dispersion in the region of optimum weight-critical weight, and because blasts over 21 in. deep were below the frozen layer, it was assumed that loss of energy at the interface was negligible. According to the shock-effects theory, one would expect a loss of energy due to reflection at the interface. It is most evident that a loss does not occur. As such evidence was accumulated, the true significance of the gas bubble became apparent.

3. Relation between the ratio of chamber volume to crater volume and the volume-utilization factor

Craters produced by blasts within the frozen layer show the following features, not previously observed in blasts in soils and rock and presumably related in some manner to the interface ratio:

- 1) Neither heavy nor light charges of explosives detonated within the frozen layer broke through the frozen-ground interface, but charges of intermediate weight did. (See Chapter III, Section II, 4.)
- 2) The frozen-ground interface was displaced downward by "bulging" or plastic flow before scabbing. The diameter of the downward bulge was less than the diameter of the surface crater.



Weight of explosive, pounds

Figure 70. Critical weights of explosives for blasts in frozen Keweenaw silt.

- 3) The shape of the surface crater was related in some manner both to the weight of charge and to the interface ratio. Failure of the frozen-ground interface tended to produce an hour-glass-shaped crater. Downward plastic flow of the frozen ground deepened the crater to as much as twice the depth of the charge. The resulting crater was entirely within the distorted frozen layer, but was deeper than the thickness of frozen ground before distortion.

From field observations and measurement of craters, the ratio of chamber volume to crater volume (see Data Sheet Computations, Chapter II, Section I, 2k) appears to be one possible measure of gas-bubble expansion. Figure 71 shows this ratio vs. volume-utilization factor for the Keweenaw Test explosives. Interface ratios and depth ratios are shown adjacent to the points on the curves. The curves are based upon points midway between limits of dispersion presented in Figure 66 (Blast Test B) summarized from the data sheets (Figs. A-13, A-14, and A-15).

Some rather interesting and pertinent observations can be made:

- 1) Each of the curves reverses its slope, perhaps as a result of the influence of the frozen-ground interface.
- 2) Curves of the Straight Gelatin Series (Atlas 60, Atlas 80) resemble each other very closely. Curves of the Semi-Gelatin - Ammonia-Base Permissible Series (Gelodyn-Coalite) resemble each other closely. Curves of the two series differ from each other.
- 3) The plateau for each of the explosives occurs at a different interface-ratio range. The ranges are as follows:

Explosives	Interface-Ratio Range
Coalite 7S	0.26 to 0.72
Gelodyn 1	0.26 to 0.67
Atlas 60	0.60 to 1.50
Atlas 80	0.83 to 1.74

- 4) The width of the plateau and the spread in interface ratio are accompanied by a corresponding spread in volume-utilization factors as follows:

Explosives	Volume-Utilization Factor Range
Coalite 7S	2.0 - 11.0
Gelodyn 1	3.0 - 13.0
Atlas 60	7.5 - 22.5
Atlas 80	7.5 - 19.5

The observed relations are interpreted with respect to gas-bubble expansion in the following paragraph.

Velocity, energy, and pressure all are related to composition of explosive. An increase in velocity is accompanied by an increase in pressure, and an increase in pressure is accompanied by an increase in energy. The energy of Coalite per unit weight of explosive is lower than that of the other types of explosives. As the energy decreases, the gas-bubble pressure decreases also, so that the gas bubble expands more slowly before rupture and increases the chamber volume relative to the crater volume.

Volume-utilization factors of each explosive rise in the "plateau" region. The explosive having the greatest energy shows the greatest rise, and the rise is in proportion to energy. Inasmuch as the increase in volume-utilization factor is associated (possibly in a complex manner) with the interface ratio, variation must be due to failure of the frozen-ground interface. Perhaps as a result of failure, the effective center of pressure of the gas bubble is lowered, thus increasing the depth ratio. An increase in depth ratio is accompanied by a corresponding increase in the

EXCAVATIONS IN FROZEN GROUND

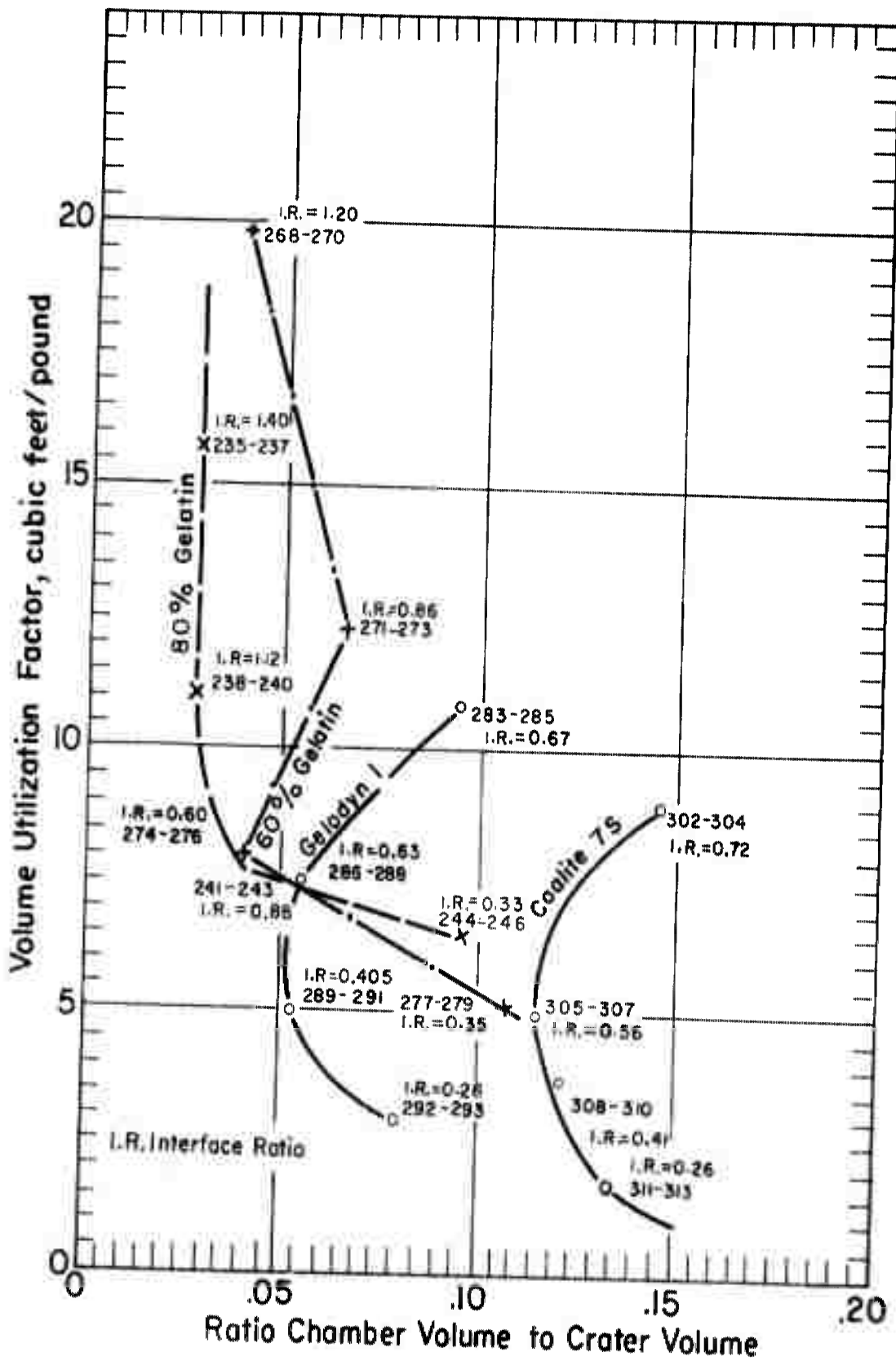


Figure 71. Volume utilization factor as related to ratio of chamber volume to crater volume.

volume-utilization factor (Fig. 68). It is logical to assume that the total time during which the explosion exerts its energy against the frozen ground is greater where failure of the frozen-ground interface occurs than where it does not occur. Accordingly, an increase in volume-utilization factor is perhaps due to an increase in impulse.

4. Increase in volume-utilization factor for charges placed below the frozen layer

In using the model-law equations, it is commonly assumed that the ABC product is the same for blasts at different length-scale ratios. Blast Test B (Fig. 68), shows that the energy-utilization number, A , depends not only upon the type of explosive, but also upon the depth ratio. Because a deep crater is produced in frozen Keweenaw silt as soon as the critical weight is exceeded, the energy-utilization number at optimum depth is the same as at critical depth. Therefore, the ABC product at the optimum weight is the same as at the critical weight. Thus, we have an accurate means of comparing crater volumes at the optimum weight.

Let us assume that a charge with center of gravity 1.0 ft below the surface represents a prototype blast. From field data for blasts at interface ratios of 0.5 or less and the scaling laws, it is possible to determine both the weight of explosive and the volume of the prototype crater.

Using data obtained from the Energy Utilization Experiments (Blast Test B), volumes at various depth ratios have been computed for each type of explosive (Fig. 72). These volumes represent variations of the volume of the prototype crater at various depth ratios and are henceforth referred to as "prototype volumes." Values of A , the energy-utilization number, can be calculated from the graphs for each type of explosive and at any depth ratio, but it appears preferable to wait for additional field data at larger length-scale ratios.

From Figure 72 and the scaling laws, the volume of crater in frozen Keweenaw silt at any depth ratio and any scale ratio for each of the four explosives can be predicted. As the prediction assumes (1) a constant ABC product at both scales and (2) a constant value of A at both scales, any departure from the predicted volume must be due either to C , the stress-distribution factor, or to B , the rock factor.

Thus we can appraise the effect of the interface ratio in a preliminary manner, but final appraisal is impossible until variations in the energy-utilization number and the rock factor are determined at larger scales. Ultimately, after expanding the field data, it should be possible to calculate values of C at various depth ratios and for various types of explosives. The following calculations illustrate an application of the scaling law to this problem and indicate that blasts below the frozen layer give larger crater volumes than blasts within the frozen layer.

Example 1. For a blast using 0.66 lb of Coalite 7S at 8 in. depth of center of gravity in frozen Keweenaw silt 19 $\frac{1}{2}$ in. thick.

- (a) What is the interface ratio?
- (b) What volume of broken material will be produced?

Solution:

$$(a) \text{ Interface ratio} = \frac{8}{19.5} = 0.41$$

- (b) To obtain the volume of excavation:

1. From Fig. 70A,

$$\text{Critical depth} = 1.44 \text{ ft.}$$

$$2. \quad \text{Depth ratio} = \frac{\text{Actual depth of center of gravity}}{\text{critical depth}} = \frac{Cg_A}{Cg_c} = \frac{0.666}{1.44} = 0.463.$$

EXCAVATIONS IN FROZEN GROUND

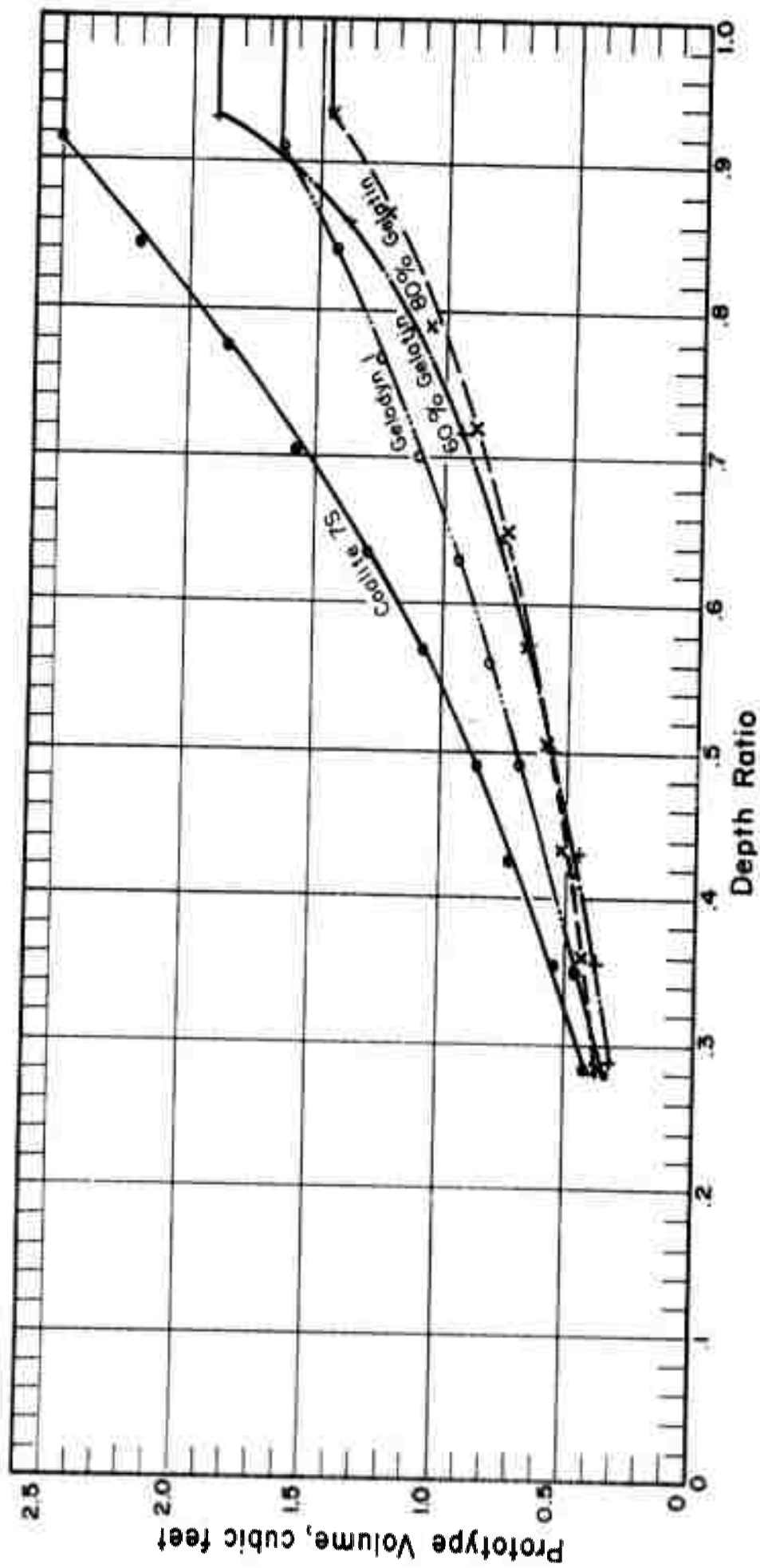


Figure 72. Prototype volumes at various depth ratios,
Blast Test C.

3. From Fig. 72.

Prototype volume V_o (with weight of Coalite equal to the critical weight for 1.0-ft depth) = 0.82 ft³.

4. Obtain volume at 8-in. depth with 0.66-lb charge (V_A) by multiplying V_o by the cube of the critical depth for a 0.66-lb charge of Coalite.

$$V_A = V_o \frac{(Cg_c)^3}{(Cg_o)^3} = V_o (Cg_c)^3$$

$$V_A = 0.82 (1.44)^3 = 2.45.$$

The problem was taken from an actual blast in frozen Keweenaw silt (Hole 310). The actual crater volume obtained by the blast (see Fig. A-15) is 2.37 ft³. The calculated value and the true value are in reasonable agreement.

Example 2: Compare the actual volume obtained from a crater blast of Coalite 7S placed below the frozen layer with the predicted volume for blasts within the frozen layer. The following data are obtained from Blast Hole 168. (See Appendix A-9.)

Weight of explosive	1.40 lb.
Depth of frozen ground	19 in. = 1.58 ft.
Depth of C. G. of charge	22 ¹ / ₈ in. = 1.84 ft.
Actual volume of crater	39.15 ft ³ .

Procedure:

1. From Fig. 70B, for 1.40 lb of Coalite 7S,

$$\text{Critical depth, } Cg_c = 1.83 \text{ ft.}$$

$$2. \quad \text{Depth ratio} = \frac{Cg_A}{Cg_c} = \frac{1.84}{1.83} = 1.005.$$

3. From Fig. 72, prototype volume at 1.00 depth ratio (no data available beyond 1.00),

$$V_o = 2.50 \text{ ft}^3.$$

4. The volume at 1.84-ft depth with 1.40-lb charge (V_A) is:

$$V_A = V_o (Cg_c)^3 = 2.5 (1.83)^3 = 15.4 \text{ ft}^3.$$

In this calculation the stress-distribution factor C is assumed to be constant, 1.0 for charges not affected by the frozen-ground interface. Comparison of the computed volume (15.4 ft³) and the actual volume (39.15 ft³) shows that the volume of excavation per pound of explosive is 2.3 times as great as expected.

We may assume, therefore, that blasts below the frozen layer (interface ratio greater than 1.00) are much more effective than blasts at interface ratios ranging from 0.44 to 0.59.

EXCAVATIONS IN FROZEN GROUND

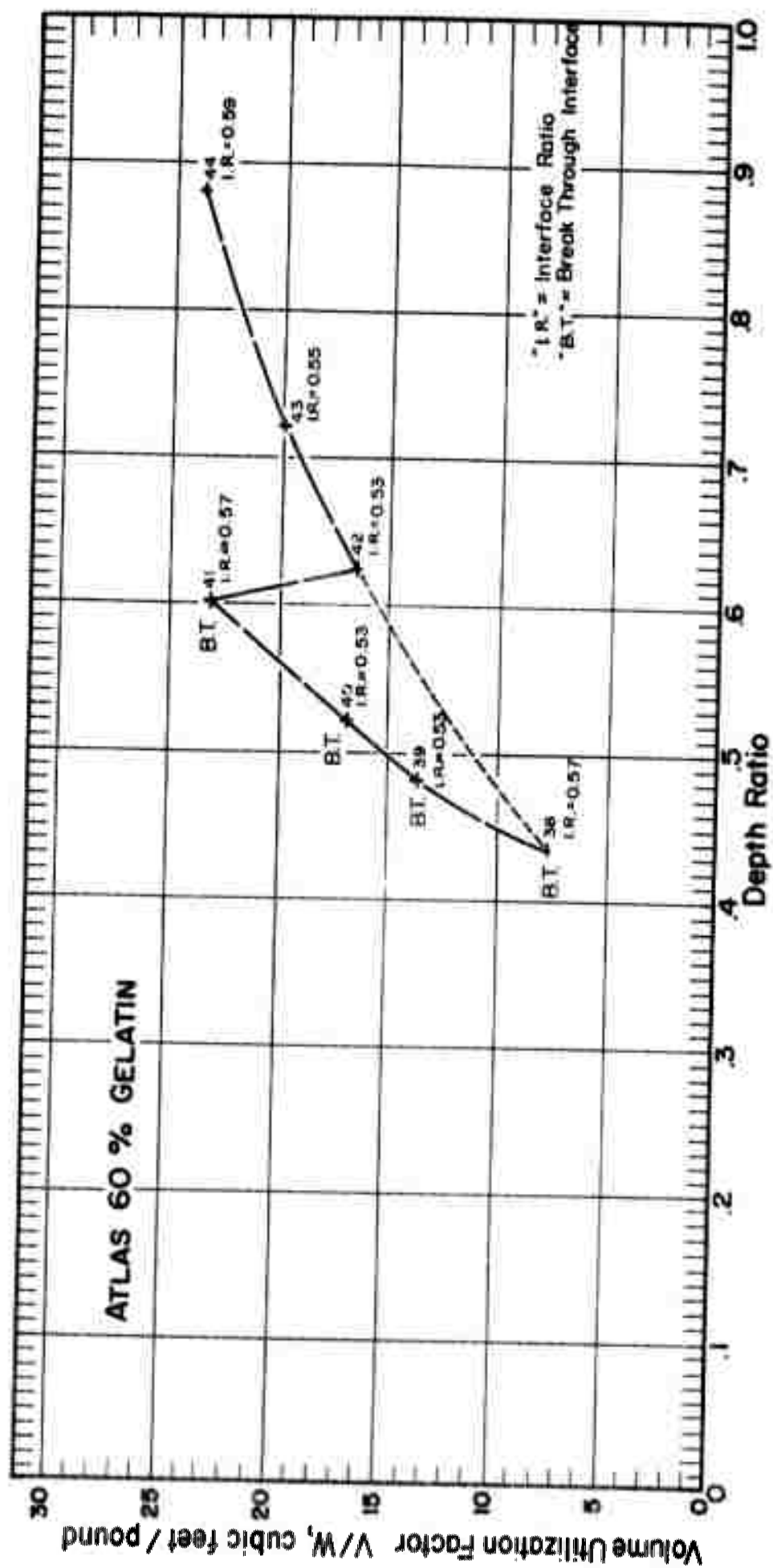


Figure 73. Effect of frozen ground interface at breakthrough.

5. Position of the gas bubble relative to the frozen-ground interface

The evidence concerning the effect of the interface ratio may imply that the energy-utilization number and the stress-distribution factor are related only to the depth ratio, and that a simple series of values of A and of C can be derived ultimately. Unfortunately, there appears to be a delicate balance between the interface ratio, the depth ratio, and the weight and type of explosive. Until these relations can be determined and measured separately, values of C , the stress-distribution factor, cannot be computed accurately. The complex relation is due apparently to the shape and volume of the gas bubble and its position relative to the frozen-ground interface.

In Figure 73, showing blasts at nearly constant interface ratio but at variable depth ratio, the volume-utilization factor rises abruptly at a depth ratio of 0.60. This increase is due to rupture of the frozen-ground interface by the gas bubble. The interface is ruptured in producing Craters 38, 39, 40, and 41, but not in Craters 42, 43, and 44. The condition described is not an isolated example, because the same thing happens with each of the other types of explosives, but the depth ratio at which rupture occurs is different for each.

It may be observed that the decrease in volume-utilization factor with decrease in depth ratio is more rapid following than preceding rupture. Moreover it appears that, following rupture, the volume-utilization factor approaches a value that would be obtained by projecting Curve 44, 43, 42 ahead. In other words, rupture of the frozen-ground interface produces its greatest effect at that particular depth ratio at which rupture is initiated, but as the weight of explosive is increased beyond that required to rupture the frozen-ground interface, the stress-distribution factor, C , approached 1.0.

Even though the volume utilization factor rises for each type as a result of rupture of the frozen-ground interface, in no instance does it exceed the factor at the optimum weight. It is apparent, therefore, that the product of the energy-utilization number, A , and the stress-distribution factor, C , cannot be greater than 1.0 at any given depth ratio for blasts within the frozen layer.

The explanation adopted here of the greater volume obtained in Crater Blast 168 (see Example 2) than predicted is that blasts below the frozen layer are equivalent to blasts in a weaker rock than frozen Keweenaw silt. As Blast 168 is at a depth ratio of 1.005, it may be defined as an optimum-depth shot. Under such conditions the AC product cannot exceed 1.0, regardless of the position of the frozen-ground interface. It follows, therefore, that the increased volume-utilization factor for blasts below the frozen layer is due to the rock factor, B . Accordingly, we may expect a difference of as much as 2.3 to 1.0 between the rock factor for blasts entirely within the frozen ground and the rock factor for blasts below the frozen layer.

For a blast below the frozen layer, part of the rock factor is contributed by the frozen layer and part by the unfrozen layer. Therefore, we might expect that the value of B would range between the value for frozen ground and the value for soil, depending on the relative thickness of each.

6. Igloo-type foxhole construction

A useful and very practical application of the theory of crater formation presented at the beginning of Chapter III is the construction of igloo-type foxholes. An igloo-type foxhole is made by a gas-bubble cavity below the frozen layer; the frozen layer is domed up so that it breaks at the top of the dome, producing an opening large enough for a soldier to crawl into the cavity but leaving the remainder of the dome intact.

Figure 74 shows an igloo-type foxhole (Blast No. 229) produced by a critical-weight blast of Atlas 80 Percent Straight Gelatin placed below the frozen layer. The frozen ground was 16 in. thick. The center of gravity of the charge was placed 53 in. below the surface, using a blast hole $7\frac{1}{2}$ in. in diameter and 4.5 ft deep. The weight of the explosive charge was 3.02 lb. The gas-bubble cavity was 6 ft in diameter and, in this instance, 3.0 ft. high. Additional unfrozen ground can be removed to increase the height of the opening if desired. Only the muck which had fallen through the hole in the roof of the igloo was removed in this case.

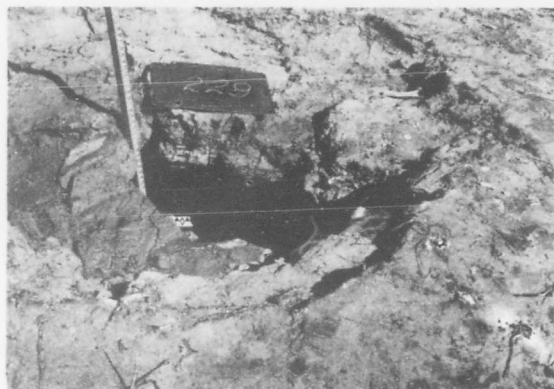
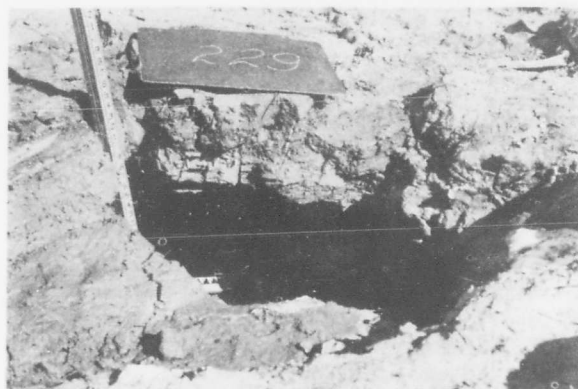


Figure 74. Igloo-type foxhole produced by blast of Atlas 80 Percent Straight Gelatin at critical weight below the frozen layer.

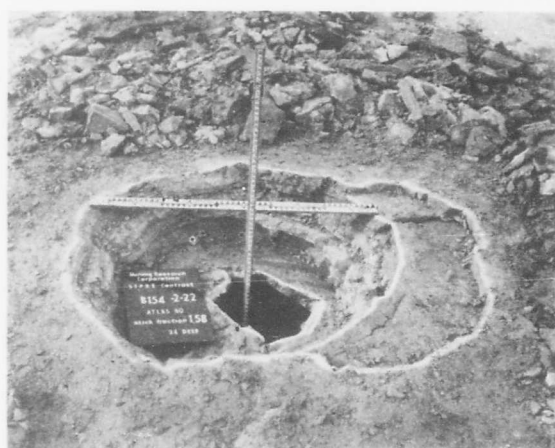
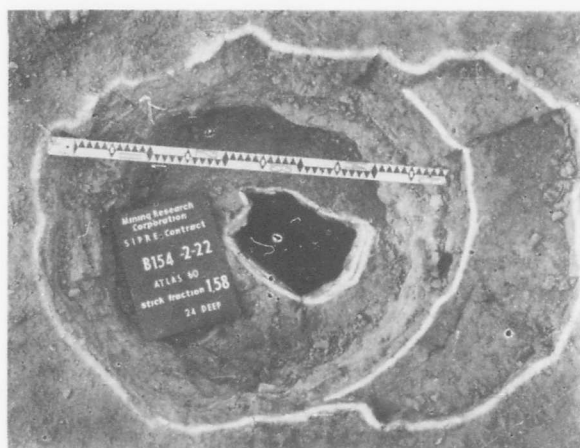


Figure 75. Igloo-type foxhole produced by blast of Atlas 60 Percent Straight Gelatin at critical weight below the frozen layer.

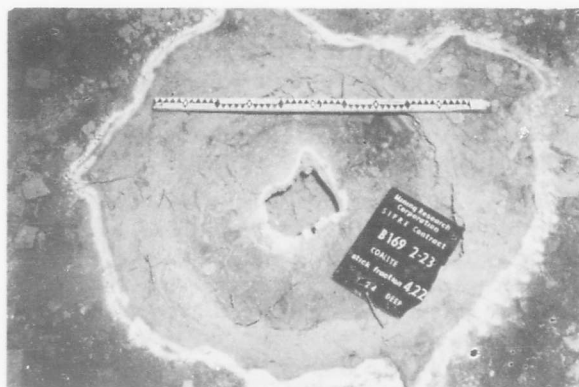


Figure 76. Igloo-type foxhole produced by blast of Coalite 7S at critical weight below the frozen layer.

The domed-up igloo roof is strong enough to be safe without supports. So long as the ground remains frozen, there is little danger of caving.

Figure 75 shows a foxhole made by Atlas 60 Percent Straight Gelatin. More broken material was removed from the crater to expose the roof of the igloo and the hole in the roof. The doming of the frozen ground and the dimensions of the crater are apparent from the level rod and the stadia rod. Weight of explosive was 0.75 lb. Depth of center of gravity of charge was 23 in. The frozen ground was 21 in. thick. The drill hole was 24 in. deep, $3\frac{1}{4}$ in. diam. Diameter of the gas-bubble cavity below the domed roof was 4 ft. No broken material was excavated from the walls of the cavity, which are blackened by soot from the explosion and show contortions in the stratification of the natural dredge-fill Keweenaw silt due to expansion of the gas bubble.

Figure 76 shows a foxhole made by Coalite 7S. Weight of explosive was 1.77 lb. Depth of center of gravity of charge was $21\frac{1}{4}$ in. Frozen ground was 19 in. thick. Drill hole was 24 in. deep, $3\frac{1}{4}$ in. diam. Diameter of the gas-bubble cavity was $4\frac{1}{2}$ ft.

Igloo-type foxhole construction is possible only if the charge weight is properly chosen. The weight and depth of the charge should be selected from Figure 70. Because of the increased effectiveness of blasts below the frozen layer, the depth of charge might be increased very slightly for improved results.

Additional research work should be done to determine the proper ratio between thickness of the frozen layer and depth of the charge to produce gas bubbles of specified diameter and develop roof arches of proper rise and span.

Since the unfrozen ground below the frozen layer is compacted by plastic flow to enlarge the gas-bubble cavity, igloo-type foxhole construction may be impracticable in some types of soils.

Additional work may be desirable to determine the best type of explosive for igloo-type foxhole construction. The greatest skill is required with high-velocity explosives at small length-scale ratios. Military explosives are dangerous because of toxic fumes which fill the gas bubble and permeate cracks and pore space in the medium.

Section V. Blast Test D — Foxhole Construction

1. Introduction

Blast Test C indicated that a charge is more effective placed below rather than in the frozen layer. However, foxholes may be needed in places where depth of freezing is so great that placing the charge below the frozen layer would be impracticable.

Obviously, the problem of drilling a hole and placing a charge to produce a foxhole is not simple under combat conditions. The proper selection of drilling equipment to produce a hole of proper diameter and depth depends upon the physical properties of the material. Various procedures are required under various conditions. It seems impossible to develop a single piece of equipment suited to all the various conditions that can be expected.

Igloo-type foxholes are possible only in certain types of frozen ground and for comparatively shallow depths of freezing. Blast Test D is a preliminary experiment with conventional open-top foxholes produced by "home-made" shaped charges in combination with "stage" blasting, or by hand augers and "stage" blasting.

2. Application of shaped charges to foxhole construction

The scope of the Keweenaw Tests did not include the investigation of shaped charges as a means of producing a borehole in frozen ground. Accordingly, standard military shaped charges were not available. The results described here are of preliminary nature.

Various stand-off distances, diameters of cavity, and various weights of the highest velocity explosive obtainable (Atlas 80) were tested, using a "home-made" 60°-cone-angle shaped charge. Nothing significant was learned concerning the design or use of shaped charges. It is doubtful that the performance of standard military shapes would have been greatly superior to that of the shapes tested. A characteristic feature of the shaped-charge blasts in frozen Keweenaw silt is the terrific air-blast effect compared to the insignificant depths of penetration.

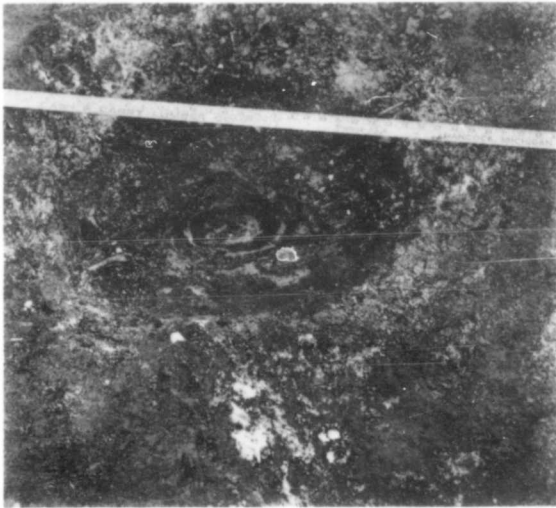


Figure 77. Hemispherical depression produced by 10-lb shaped charge.

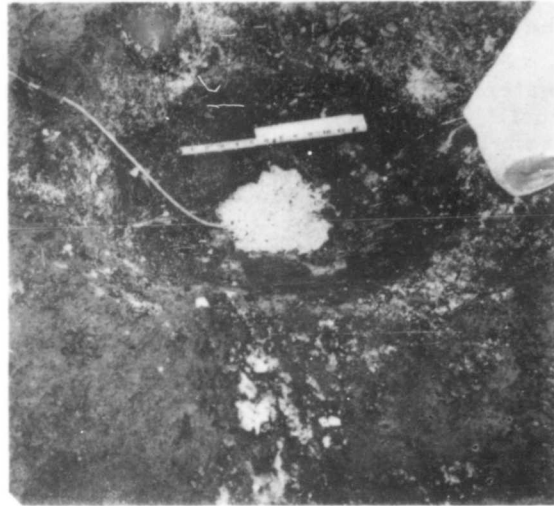


Figure 78. "Plaster shot" of 2.5 lb of Gelodyn 1 before detonation. ,



Figure 79. Crater produced by first "plaster shot".



Figure 80. Foxhole produced by second "plaster shot".

The increase in depth of penetration of a 10-lb shaped charge over a 5-lb shaped charge was so slight that it could not be detected without careful measurement. Penetration appears to occur by downward deflection of the frozen ground (as if it had been struck by a large ball-peen hammer) rather than by a punching or boring effect. The depth of the depression for a 10-lb shaped charge was 11 in. Figure 77 shows the crater-shaped circular depression punched downward into the frozen ground. The absence of broken material in the "crater" and the soot-blackened walls may be observed.

Figure 78 shows the same depression charged with a "plaster shot" of 6 sticks (2.66 lb) of Gelodyn 1 primed with Primacord. The charge was covered with sand stemming tamped to fill the crater before the charge was detonated electrically. The blast deepened the crater from 11 in. to 30 in. (Fig. 79). The bottom of the crater is in

frozen ground, but the frozen-ground interface was bent downward, because the thickness of the frozen ground (21 in.) is less than the depth of crater.

A second "plaster shot" of 2.66 lb of Gelodyn, using the muck from the previous blast for stemming deepened the foxhole as shown in Figure 80. The frozen-ground interface is visible. Excavation below the frozen ground is a matter of shoveling. It is a simple matter to widen the excavation below the frozen ground to accommodate 2 men, or to tunnel under the frozen layer to an adjacent foxhole.

3. Application of hand-auger drilling to foxhole construction

Although penetration of conventional military shaped charges into frozen ground may be better, it is doubtful that the improvement will alter materially the fact that an excessive quantity of explosive is required to produce a borehole in frozen ground with a shaped charge.

It is entirely practical to drill a small-diameter shallow hole into frozen Keweenaw silt with a hand auger. With a charge less than the critical weight, the hole can be sprung to accommodate a heavier charge. If the first charge is small, the second charge can be loaded in the hole immediately and blasted. As may be observed from Figure 59, the second blast can deepen the crater up to 2.5 times the depth of the center of gravity of the charge (up to 2.2 times the depth of the auger hole). The crater may be deepened further by using successive "plaster shots" as described and illustrated in connection with the shaped charge experiments.

Following is an example of results obtained using the preceding technique.

Example A. A hole 6 in. deep and 1 in. in diameter was drilled with a hand auger and sprung with 0.025 lb of Coalite 7S. The sprung hole was immediately re-charged with 0.75 lb of Gelodyn 1 and blasted. The resulting crater greatly resembled that produced by a 10-lb shaped charge but was 1 in. deeper. A "plaster shot" of 2.66 lb of Gelodyn 1 was molded into the bottom of the crater, then covered with muck from the previous blast and fired. The first "plaster shot" deepened the crater from 1.0 ft to 3.6 ft and produced a conical-shaped crater. The process was repeated using a second Gelodyn "plaster shot" of the same weight. The blast resulted in a bulb-shaped cavity 4.5 ft in diameter at the bottom and 3.5 ft in diameter at the top. The foxhole broke through the frozen layer, which was 20 in. thick but was distorted downward by the first "plaster shot." The unfrozen material can be excavated to any depth desired by shoveling.

Example A illustrates that, by use of simple hand-auger technique and stage blasting with "plaster shots", it is possible to construct a foxhole with 6.09 lb of explosive. The foxhole has approximately the same dimensions as one produced using the shaped-charge technique but requiring 15.3 lb of explosive.

In the following example, a deeper hole was drilled with the hand auger (the drilling took longer and dulled the auger), but a foxhole of dimensions comparable to that of Example A was produced with 5.5 lb of explosive.

Example B. A blast hole 1 in. in diameter and 14 in. deep was drilled with a hand auger. The first blast was at optimum weight (0.18 lb of Coalite 7S) and produced a crater 1.1 ft deep and 2.3 ft in diameter. A "plaster shot" of 2.66 lb of Gelodyn 1 deepened the crater to 3.2 ft and produced a conical-shaped crater. A second "plaster shot" of the same weight produced a bulb-shaped crater 4.6 ft in diameter below the frozen-ground interface which tapered from 4.4 ft in diameter at the surface to 2.2 ft in diameter at the interface.

4. Conclusions

It appears that the use of shaped charges for producing boreholes in frozen Keweenaw silt results in excessive air-blast, excessive noise, and poor penetration. By use of a hand auger and stage "plaster" blasting, it is possible to produce a crater with 6 lb of explosive that is comparable to one produced with 15.3 lb of explosive using shaped charges and stage blasting.

EXCAVATIONS IN FROZEN GROUND

It is doubtful that penetration of 24 in. of frozen Keweenaw silt can be accomplished with less than a 20-lb shaped charge.

The use of "plaster shots" consisting of 2.66 lb of Gelodyn has no scientific basis. It is probable that the technique described in Blast Test D can be improved.

The use of hand augers for foxhole construction shows definite promise, but the type of augers employed in the Keweenaw Tests can be improved upon.

Further specific application of data developed in Blast Tests A, B, and C to foxhole construction will be deferred pending field tests in ground frozen deeper than in the Keweenaw Tests.

Section VI. Blast Test E — Temperature Effect

1. Introduction

The formula derived by Livingston for penetration of projectiles into rocks includes a rock factor that relates penetration to the elastic properties of the medium. The Keweenaw Tests indicate that craters in frozen Keweenaw silt are a result of plastic deformation. Lacking evidence to the contrary, it was assumed that the rock factor in frozen ground is related to the ratio of the lateral strain to the longitudinal strain in the material subjected to stress. Accordingly, measurements of this ratio were taken in the laboratory. To avoid confusion in terminology because of the plastic rather than elastic behavior of frozen Keweenaw silt, the term Poisson's index rather than Poisson's ratio is used.

Crater blasts in sandstone and granite¹ have shown a substantial difference between the critical weight of explosive and the weight which produces a crater to the full depth of the explosive charge. The Keweenaw Tests show a very slight difference between the two weights. Inspection of the data for sandstone and for granite reveals that the difference in weight of explosive is much greater for granite, which is a brittle-acting rock, than for Navajo sandstone, which is less brittle-acting. Moreover, inspection of the data of the Bomb Penetration Project² reveals that Zuni granite, which is comparable to Unaweep granite, has a lower Poisson's ratio at the failure stress than does Dakota sandstone, which is comparable to Navajo sandstone. It is probable, therefore, that the difference in weight is a function of Poisson's ratio and that rocks with a low Poisson's ratio (brittle-acting rocks) will show a greater spread between critical weight and optimum weight than rocks with a high Poisson's ratio (plastic-acting rocks) at the same stress range.

The plastic behavior of frozen Keweenaw silt is derived from ice or from moisture in the pore space. It is reasonable to assume, therefore, that the relative proportions of ice and moisture influence Poisson's index and, in turn, the rock factor.

The effect of temperature upon the rock factor in frozen Keweenaw silt was discovered quite by accident while using extremely small increments in charge weight in an effort to measure the difference between the critical weight and the weight which produces a crater to the full depth of the explosive charge. As the temperature effect was not anticipated in planning the Keweenaw Tests, the exact ground temperature at the blast hole at the time of blasting is unknown. It must be assumed that the ground temperatures at Gages I-1 and I-2 (Fig. 6) are representative of temperatures at the blast hole.

2. Description

Twelve holes, $1\frac{5}{8}$ in. in diameter and 12 in. deep were drilled in Keweenaw silt frozen to a depth of 18 in. The interface ratio was 0.65; the scale of blasts was 0.67. Atlas 60 Percent Straight Gelatin was used, starting with slightly less than the critical weight at scale 0.67, and increasing uniformly in increments of 0.004 lb ($1\frac{1}{16}$ in. cartridge length) to 0.103 lb.

1. Livingston, C. W. (1949) Series I and II Experiments, Underground Explosion Test Program, Report of the Colorado School of Mines, Figs. 28, 114. RESTRICTED
2. Livingston, C. W., and Smith, F. L. (1951) Bomb Penetration Project, Colorado School of Mines Research Foundation Inc., CONFIDENTIAL

All blasts were fired on February 17. At that time, a local thaw had melted 1 in. of the surface of the frozen ground, leaving mud and small puddles of water. The ground temperature at Gage position I-1, 6 in. below the surface, was 30.6. At a point 12 in. below the surface, the ground temperature was 30.9. The higher temperature at the greater depth is due to time lag between surface and underground temperature changes.

3. Results and analysis

The data for Blast Test E are summarized in Figure A-6.

Figure 81 shows the depth of crater vs. charge weight. The relations are most erratic. Through a range equal to almost twice the critical weight, it is impossible to predict whether or not a crater will be formed. The range from 0.063 to 0.103 lb of explosive might conceivably represent the dispersion due to variations in physical properties of the frozen ground. Such a dispersion was not encountered in blasts made in colder weather, and the most plausible explanation of the dispersion is that thawing is responsible.

Figures 82 and 83 illustrate ground-surface conditions at the time of blasting. Footprints are visible in the mud in both pictures. Figure 82 is a blast at critical weight which produced a crater. Observe both the sandy nature of the broken material and the muddy surface. Figure 83 is a blast at nearly double the critical weight. Radial cracks may be observed at the collar of the borehole, and the blast may be described as a "critical blast."

The following observations made in the field at the time of blasting are pertinent to the problem.

Temperature and moisture are variables which influence the rock factor. In general, less explosive is required for blasting at low temperatures than at temperatures approaching the melting point. A near-melting-point temperature causes the frozen ground to behave more plastically. At the melting point, moisture is drained from once-frozen sandy soils and accumulates in pools of water, drains through open fractures produced by previous blasts, or remains in the pore space of silty soils.

At near melting-point temperatures in silty soils, the energy of the explosion is absorbed at the charge elevation by plastic flow, thus dissipating the energy and increasing the quantity of explosive required for failure. A noticeable increase in the "surface bulge" is produced without appreciable fragmentation. The bulge is more pronounced in silts, which hold moisture, than in sands, which do not. Fragmentation varies with the moisture content. As the moisture content increases, the ground yields plastically, and little fragmentation is accomplished. At a temperature near the melting point, local sandy areas of high permeability within the frozen Keweenaw silt behave more like a soil than a rock. Less explosive is required for blasting than at lower temperatures. On the contrary, blasting silt areas requires more explosive at near melting-point temperatures than at lower temperatures.

The above observations imply that the quantity of explosives required for blasting is related to the plasticity of the material. As the plasticity increases, the quantity of explosives required increases also. At near melting-point temperatures, local sand areas within the Keweenaw silt are less influenced by the ice particles that cement the sand grains and the frozen sandy soil begins to lose its identity and assumes properties approaching those of an unfrozen soil. At near melting-point temperatures, silt areas become more plastic and assume properties more closely approaching those of viscous materials such as wet clay.

By inspection, the quantity of explosive required for blasting frozen Keweenaw silt at near-melting-point temperature may be as much as 30% greater in high-silt areas and as much as 30% lower in low-silt areas, than at lower temperatures.

4. Summary of observations

Temperature and moisture are variables that influence the rock factor for blasts in frozen ground. The frozen ground is in a process of continuous change, and all of

EXCAVATIONS IN FROZEN GROUND

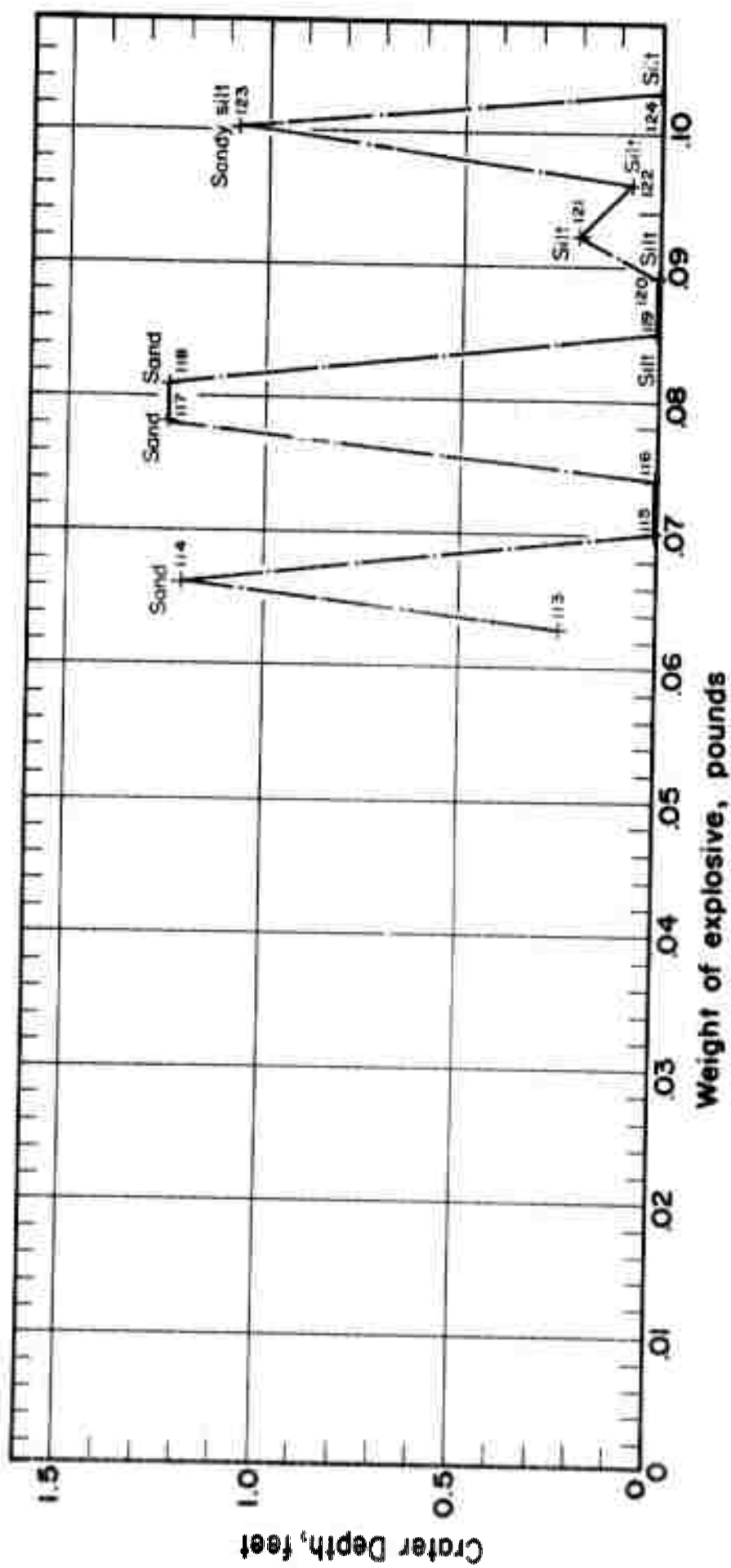


Figure 81. Temperature effect (February 17).
Crater depth vs. charge weight,
Atlas 60% Gelatin.



Figure 82. Blast using critical weight at lower temperatures produced a crater in sandy soil at near-melting point.



Figure 83. Blast using nearly double critical weight at lower temperatures did not produce a crater in silt at near-melting point.

the events that have occurred before blasting influence the rock factor at the time of the blast. In contrast to the viscous behavior of high-silt areas at near melting-point temperatures, which increases the quantity of explosive required for blasting, low-silt areas behave in a manner similar to moist sand, which decreases the quantity of explosive required. Under near melting-point conditions, an extreme variation in the rock factor may be expected. The range of variation is such that the rock factor might be either that for moist sand, wet clay, or frozen silt or that for a composite of all three.

A surface thaw to a depth of a few inches complicates the results of blasting much in the same manner that the presence of the frozen-ground interface complicates the rock factor for blasts below the frozen-ground interface.

It is suggested that the temperature effect be recognized and studied. It seems desirable also to appraise variations in the rock factor resulting from variations in temperature and moisture of frozen ground by extending the field experiments to include blasts in summer before the ground is frozen. It seems desirable also to determine the limiting temperatures of frozen ground above which temperature and moisture effects begin to exert an influence.

Section VII. Blast Test F — Effect of Charge Shape

1. Introduction

The purpose of Blast Test F was to determine the effect of charge shape upon blasts in frozen Keweenaw silt. Crater blasts in rock have shown that a given quantity of explosive produces a larger volume of excavation from blast holes of the same depth as the diameter of the hole is increased. It is generally assumed that a charge of spherical shape is more efficient than any other shape, and it is generally assumed that shape influences the results of blasting.

The results of Blast Test B suggest an explanation for the increased volume of excavation as the diameter of the hole is increased, or as the charge approaches a spherical shape, that differs from the explanation implied in the preceding paragraph. As the shape of a charge approaches a sphere or a cylinder of height equal to diameter, the center of gravity of the charge is lowered in a hole of constant depth. The lowering of the center of gravity is a function of the shape and results in an increase in the depth ratio. An increase in depth ratio results in an increase in the volume-utilization factor or a decrease in the proportion of the total energy of a blast that is wasted to the atmosphere.

A fundamental difference between the two explanations is that, if improved energy utilization is due to shape alone, various values of C , the stress-distribution factor (see Section IV, Item 2), must be assigned to corresponding shapes. On the contrary, if improved energy utilization is due entirely to the greater depth ratio, then the larger volume of excavation is due to a change in the energy-utilization number, which is solely a function of the depth ratio.

2. Description

Coalite 7S was selected for the test because of its low density. The depth of center of gravity of explosive was held constant for five different charge shapes, using the critical weight of Coalite 7S. Thus, the depth ratio also was held constant at 1.0, the point of maximum energy-absorption capacity of the medium. Starting with a height of charge of $7\frac{1}{2}$ in. and a diameter of 1 in., the height was reduced successively so that the height of any set of triplicate blasts equaled one half of the height of the preceding set. The diameter of the blast hole was increased so that the volume of the explosive remained constant for each of the various shapes of charge and equal to the volume occupied by 0.242 lb of Coalite 7S.

Figure A-17 is a data sheet which summarizes the field data and gives the dimensions of the charges and of the resulting craters.

It is difficult to appraise the shape effect because of the slight difference in blast damage by the various shapes. The possibility exists that the position of the frozen-ground interface may have influenced results and that loss of gas pressure due to the mechanical strength of the stemming material in holes of large diameter might be a factor.

All three blasts in holes 1 in. in diameter (height of charge 7 in.) failed to produce a crater. Likewise, all three blasts in holes 4 in. in diameter (height of charge $7\frac{1}{16}$ in.) failed to produce a crater. A charge of height approximately equal to diameter does not appear superior either to one of height $2\frac{1}{2}$ times the diameter or to one of height $\frac{1}{3}$ the diameter.

One might interpret the results to indicate that neither extremely tall charges nor extremely flat charges are desirable, but that little difference can be detected within the range of shapes from height 4 times the diameter to height one-fourth the diameter.

3. Conclusions

The effect of charge shape is so slight within the range of shapes tested and under the conditions of the test that no substantial error in blasting is introduced within limits of shapes ranging from height 4 times diameter to height one-fourth the diameter. It is possible that the range of charge shapes producing equivalent results may be greater than indicated, but it seems desirable to repeat the tests in greater thicknesses of frozen ground and at a larger length-scale ratio. It seems desirable also to determine whether the observed relations hold at depth ratios other than 1.0; to extend the height-to-diameter ratio in future tests to perhaps 10 to 1, provided sufficient thickness of frozen ground is available; and to repeat Blast Test F with a higher velocity explosive, preferably Atlas 60 Percent Straight Gelatin.

We may conclude that the fundamental effect of changing the shape of a charge in a borehole of constant depth is to change the depth ratio and thus to alter the proportions of energy utilized by the medium or lost into the atmosphere. In any attempt to correlate blasts in holes of various diameters at different length-scale ratios, the energy-utilization number, A , should be applied before an attempt is made to correlate. Unless the contrary is proved by the future tests suggested, the stress-distribution factor, C , seems to be independent of the shape of the charge and dependent only on the interface ratio and the number of free-faces.

CHAPTER IV. SUMMARY OF OBJECTIVES; CONCLUSIONS AND RECOMMENDATIONS

Section I — Summary of Objectives

1. Introduction

Limitations of depth of freezing imposed by the test site and limitations of time available for the analysis prevent a complete analysis. However, more information was gained than was originally anticipated. From the fundamentals disclosed in the analysis of the data, it seems possible to correlate blasts in various materials such as soils and rocks (and possibly underwater explosions) with blasts in frozen ground.

2. Objective 1: Most efficient type of explosive for blasts in frozen ground

The tests were restricted to 4 types of commercial explosives: Atlas 80 Percent Straight Gelatin; Atlas 60 Percent Straight Gelatin; Gelodyn 1; and Coalite 7S. The phrase "most efficient type of explosive" as considered here means the explosive that has the most advantages for blasts in frozen ground in military operations. Of the four types of explosives used in the Keweenaw Tests, Atlas 60 Percent Straight Gelatin was found superior to the other types because:

- 1) Except for Atlas 80 Percent Straight Gelatin, less explosive was required to produce a crater at any given depth (Fig. 70).
- 2) The quantity of material broken per pound of explosive was greater (Fig. 68).
- 3) The cost of explosive per cubic foot of excavation was lower (Fig. 69).

The moisture resistance, fumes, cold resistance, and ease of transporting and handling meet the specifications for blasting in frozen ground as well as any of the other types of explosives. (See Chapter I, Explosives Selection.)

The question immediately arises: Why recommend an explosive that has both a lower weight strength and a lower absolute weight strength than the other three Keweenaw Test explosives? (This question is particularly pertinent since Du Pont, Atlas, and Hercules follow the practice of selecting commercial explosives on an absolute-weight-strength or execution-value basis.)

Straight Gelatin explosives have the peculiar property of detonating at a much lower rate when unconfined than when confined. Probably various grades of Straight Gelatin differ in velocity in a manner not directly in proportion to the blasting-gelatin content, but depending also upon the percentage of sodium nitrate present. Sodium nitrate in various combinations with blasting gelatin must be responsible for the anomalous behavior. More sodium nitrate is added to Atlas 60 Percent Straight Gelatin than to Atlas 80 Percent Straight Gelatin. Possibly some other proportion of ingredients would give a higher confined velocity than Atlas 60. Perhaps the best proportions more closely approach a zero oxygen balance for the combustion reaction at high pressure (high confinement).

The Keweenaw Test data suggest that the performance of an explosive is related to composition. The Commercial Explosives Classification Chart (Table I) is based upon composition. It does not seem to be coincidence that, at any particular depth of charge, the critical weights of the various explosives determined in the Keweenaw Tests are directly related to composition. The weight is least for the explosive that contains the least number of additives to the explosive base and the weight

increases as the number of additives increases or as the percentage of nitroglycerine decreases. It appears that energy, explosion pressure, velocity, fumes, and moisture resistance are interrelated. It appears also that the effect of the co-volume of the molecules is greatest in the region from critical weight to optimum weight. It also appears that the co-volume of the molecules is related both to composition and to performance. Each type of explosive (Table I) and each grade of each type has its own "characteristic curve."*

The difference between the results of the Keweenaw Tests and the results extrapolated from standard explosives testing procedure using a ballistic mortar and a ballistic pendulum is possibly explained as follows:

(1) Ballistic-mortar ballistic-pendulum results do not take into account the physical properties of the medium, particularly its energy-absorption characteristics as related to velocity, energy, and impulse.

(2) Ballistic-mortar construction and standard procedure do not allow testing at high charging densities. At high charging densities, deviations from the Perfect Gas Laws** require correction for the co-volume of the molecules as in the F. W. Brown Equation.***

(3) It is well known that velocity of detonation increases with confinement. The Keweenaw Tests (see Chapter III, Blast Test B) indicate that the depth ratio is a measure of confinement. At a depth ratio of 0.6 in frozen Keweenaw silt, the velocities of the test explosives appear to coincide with velocities determined by standard tests. If this interpretation is correct, the data indicate velocity increase as the depth ratio increases above 0.6. Accordingly, it seems desirable to reappraise present procedure for measuring the confined velocities of commercial explosives.

3. Objective 2: Fundamental relation between weight of explosive and depth of charge

When comparing crater blasts in various materials at various length-scale ratios and with various explosives, it is usually assumed that the proportion of the total energy expended upon the medium is the same for each blast. This assumption results when the model relations are expressed in an equation of the form:

$$R = K \sqrt[3]{W}$$

where,

R is radius of rupture, ft.

K is a constant

W is weight of explosive, lb.

The view adopted here is that K is not a constant but a variable. For a particular blast, the value of K is the product of three variables, referred to here as the ABC product. The author expresses the model relations in an equation applicable to blasts in all types of materials with all types of explosives:

$$N = A B C \sqrt[3]{W}$$

* The "characteristic curve" referred to is a graph of volume-utilization factors at various depth ratios, such as Fig. 68. (See also Figs. 64, 65.)

** For a fuller discussion, see Quarterly of the Colorado School of Mines, vol. 46, no. 1, (Jan. 1951), p. 11-27.

*** F. W. Brown (1942) Theoretical calculations for explosives, part II: U. S. Bur. Mines Tech. Paper 643.

where,

N is the normal distance, ft, measured from the center of gravity of the charge to the damage surface under observation.

A is an energy-utilization number, which depends on the type of explosive and the depth ratio.

B is a rock factor, which depends on physical properties of the material and the energy-absorption capacity of the medium.

C is a stress-distribution factor, which depends on the number of free-faces, the interface ratio, and the depth ratio.

W is weight of explosive, lb.

The maximum value of the ABC product in any given medium (or composite of materials) indicates the maximum energy-absorption capacity of the medium to any given explosive, and may be obtained from critical-depth blasts. The experimental error is greater at small scales than at large scales because of limits of accuracy of weighing, measuring, and placing small charges, and because of surface geologic features.

Figure 70 shows graphs of the model-law equations at maximum values of the ABC product as determined from critical-depth blasts in frozen Keweenaw silt at comparatively small scales. Because of the shallow depth of freezing; because the rock factor is sensitive to temperature changes; and because the rock factor is different for charges placed below rather than within the frozen layer, values of the ABC product should be measured also in deeply frozen ground.

With these limitations, it may be assumed that the following values of the ABC product are a better indication of the relative "strength capacity" of the Keweenaw Test explosives than any other measure yet devised.

ABC Product	
Atlas 80 Percent Straight Gelatin	2.46
Atlas 60 Percent Straight Gelatin	2.39
Gelodyn 1	1.96
Coalite 7S	1.63

If the depth of charge is reduced, all other factors remaining constant, a crater is produced and the numerical value of the ABC product is reduced. The decrease depends both upon the explosive and upon the material, but is due to a decrease in the energy-utilization number, A. Each type of explosive exhibits its own "characteristic curve" as the depth of charge is reduced. (See Fig. 65 and 68.) Accordingly, different sets of numbers must be assigned to values of A in the model equation to calculate depth of crater, volume of crater, or radius of crater. Each set varies as a function of the depth ratio (ratio of depth of charge to critical depth).

Time allotted to this project did not permit calculation of various values of A for various types of explosives at various depth ratios. Moreover, it seems undesirable to do so with limited data because the energy-utilization number may be widely applied to military and commercial uses involving all types of explosives. At present, therefore, changes in the values of A must be inferred from Figures 65 and 68 by comparing the volume-utilization factor or radius-utilization factor at the depth ratio desired with the respective value at critical depth (depth ratio 1.0.)

The fundamental relation between weight of explosive and depth of charge is shown in Figure 69 by comparing blasting costs at various depth ratios. A depth

EXCAVATIONS IN FROZEN GROUND

ratio of 1.0 represents a charge placed at critical depth. One of the characteristics observed in frozen Keweenaw silt is that a slight increase in weight beyond the critical weight causes a crater to be formed. Another characteristic is that dispersion is maximum at critical weight. Accordingly, at the scales dictated by the shallow depths of freezing at the Keweenaw Test Site during the winter of 1953-54, it was impossible to obtain sufficient information to be certain of the exact form of the curves for depth ratios greater than 0.91 to 0.93 (horizontal lines are probably incorrect).

The absolute minimum cost of explosives per cubic foot broken for blasts in frozen ground is a reciprocal measure of the "efficiency" of the various test explosives and is tabulated as follows:

	Cost (cent/ft ³)
Atlas 60 Percent Straight Gelatin	1.03
Gelodyn 1	1.80
Atlas 80 Percent Straight Gelatin	1.96
Coalite 7S	2.04

At a depth ratio of 0.4, the cost of Atlas 80 Percent Straight Gelatin and Gelodyn 1 are the same and the relations are

	Cost (cent/ft ³)
Atlas 60 Percent Straight Gelatin	4.6
Atlas 80 Percent Straight Gelatin	5.5
Gelodyn 1	5.5
Coalite 7S	7.7

As the depth ratio decreases, costs for the low-velocity explosives begin to skyrocket and the decrease in velocity of Atlas 60 at low confinement begins to take effect. Extrapolation of the curves suggests that, at depth ratios less than 0.27, 80 Percent Straight Gelatin becomes more effective than 60 Percent Straight Gelatin.

Extrapolation of the cost curves to depth-ratio zero (the range of "plaster shots," surface contact shots, and airbursts) explains why high-velocity explosives are better for shaped charges than low-velocity explosives. The relations suggest that Atlas 80 should have been used for the foxhole construction "plaster shots" (Blast Test D) rather than Gelodyn 1.

The form of the cost curves causes one to speculate that the "rock-factor effect" upon cost and upon energy utilization may be much the same as the "depth-ratio effect." If so, this explains why practical experience has found low-velocity explosives to be superior for use in "soft rocks" and high-velocity explosives for "hard rocks." It might be desirable in the future to plot rock factor against explosives cost for various types of explosives to determine the limitations of various types of explosives and form a new basis for selecting explosives for both commercial and military applications.

The prototype volume curves (Fig. 72) supplement the cost data and show that at high depth ratio, a low-velocity explosive (Coalite 7S) can produce a larger crater, than a high-velocity explosive. In all instances the critical weights of explosives were used to obtain the information summarized in Figure 72, but the critical weight of the low-velocity explosive is greater than the critical weight of the explosive next higher in velocity (Fig. 70; Table II). The curves also show that, because of its anomalous behavior (increase in velocity with increased confinement), Atlas 60 can produce nearly as large a crater as Coalite 7S (and with considerably less explosive).

Because logistic considerations in military operations make it undesirable to use a large number of different types of explosives, and because toxic fumes are a serious hazard in igloo-type foxhole construction (see Blast Test C, Chapter III), it seems desirable to include Atlas 60 in future igloo-type foxhole experiments.

The fundamental relations between volume of crater, type of explosive, weight of charge, and depth of charge for blasts within the frozen layer in frozen Keweenaw silt are presented in Figure 84. For example, if a 5-lb charge of each of the test explosives is placed with its center of gravity 2.0 ft below the surface, the crater volumes to be expected will be as follows:

Type of Explosive	Volume of Crater (ft ³)
Coalite 7S	35
Gelodyn I	33
Atlas 80	42
Atlas 60	36

These volumes do not measure the effectiveness of the explosive, but only the skill of the blaster. A skillful blaster would increase the volume of excavation with the same weight of explosive by placing the charges at the following depths (See points "O" on curves.):

Type of Explosive	Depth of Charge (ft)	Volume of Crater (ft ³)
Coalite 7S	2.4	48
Gelodyn I	3.0	58
Atlas 80	3.8	100
Atlas 60	4.0	120 (approx.)

Obviously under battle conditions it would be unwise to risk a camouflet by using too small a weight of explosive. Accordingly, a compromise between skill and prudence must be made, and the charge should be placed at a lesser depth, for example at 0.9 optimum. Under such conditions the following size craters may be expected with a 5-lb charge:

Type of Explosive	Battle Design Depth (ft)	Volume of Crater (ft ³)
Coalite 7S	2.2	42
Gelodyn I	2.7	49
Atlas 80	3.4	81
Atlas 60	3.6	96

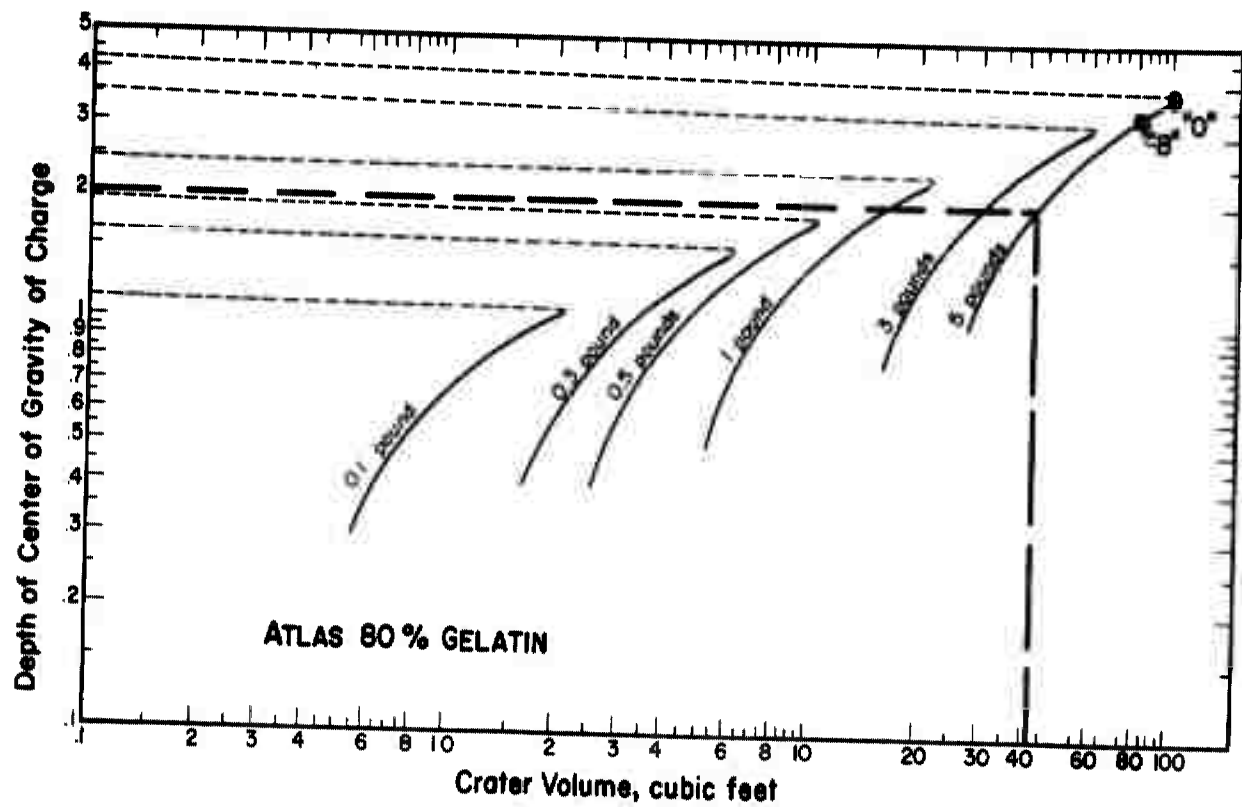
The use of excess explosives in blasting foxholes in frozen ground has the following disadvantages (see Blast Test B, Ch. III, Sec. III):

- 1) The danger of being struck by flyrock is increased. To reduce the hazard, the distance between the blast firing point and the foxhole must be increased.
- 2) The greater noise, flyrock travel-height, and flyrock travel-distance helps the enemy to spot the position where foxholes are being dug.
- 3) From the standpoint of logistics, much of the energy of the explosion is wasted at shallow depths of burial.

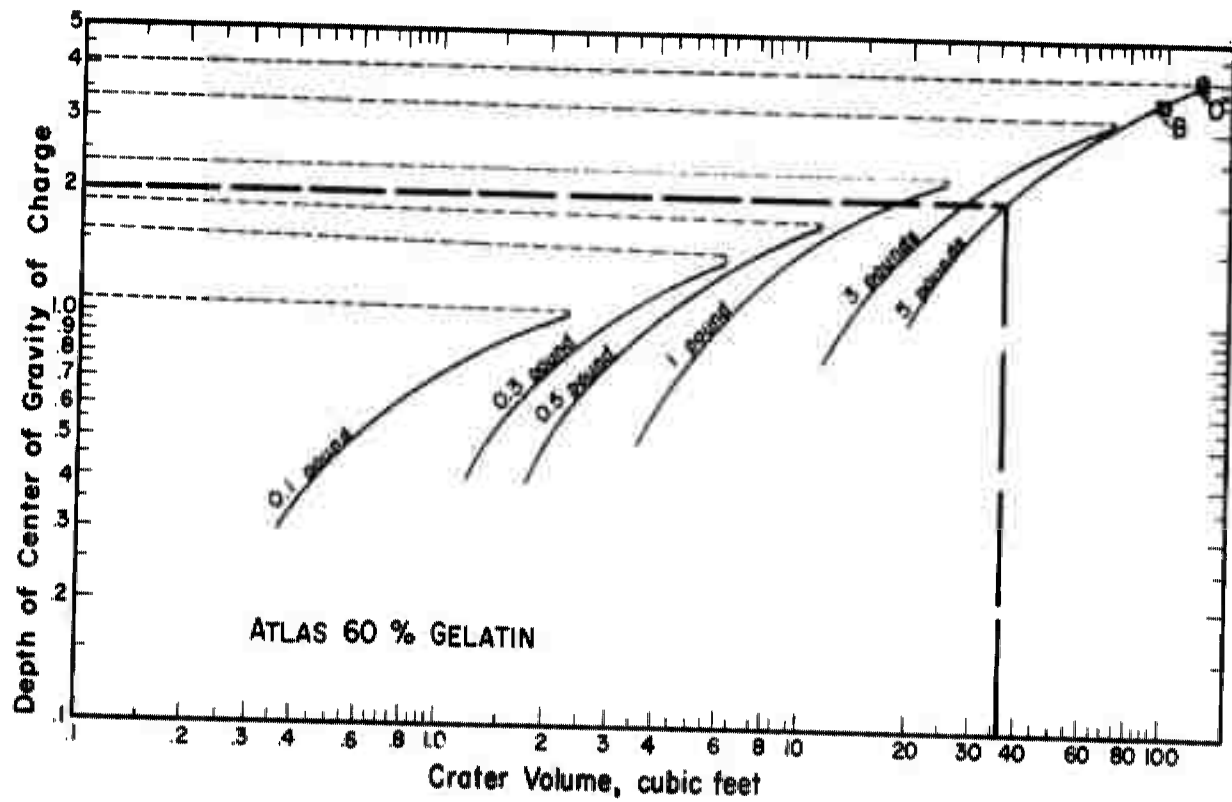
In addition, excess explosive prohibits igloo-type foxhole construction.

If the practice of using two or three times as much explosive as required is followed in spite of these drawbacks, the use of 60 Percent Straight Gelatin Dynamite should not be considered, and experiments should be directed towards determining the characteristics of various high-velocity explosives (Military Explosives) in the

EXCAVATIONS IN FROZEN GROUND

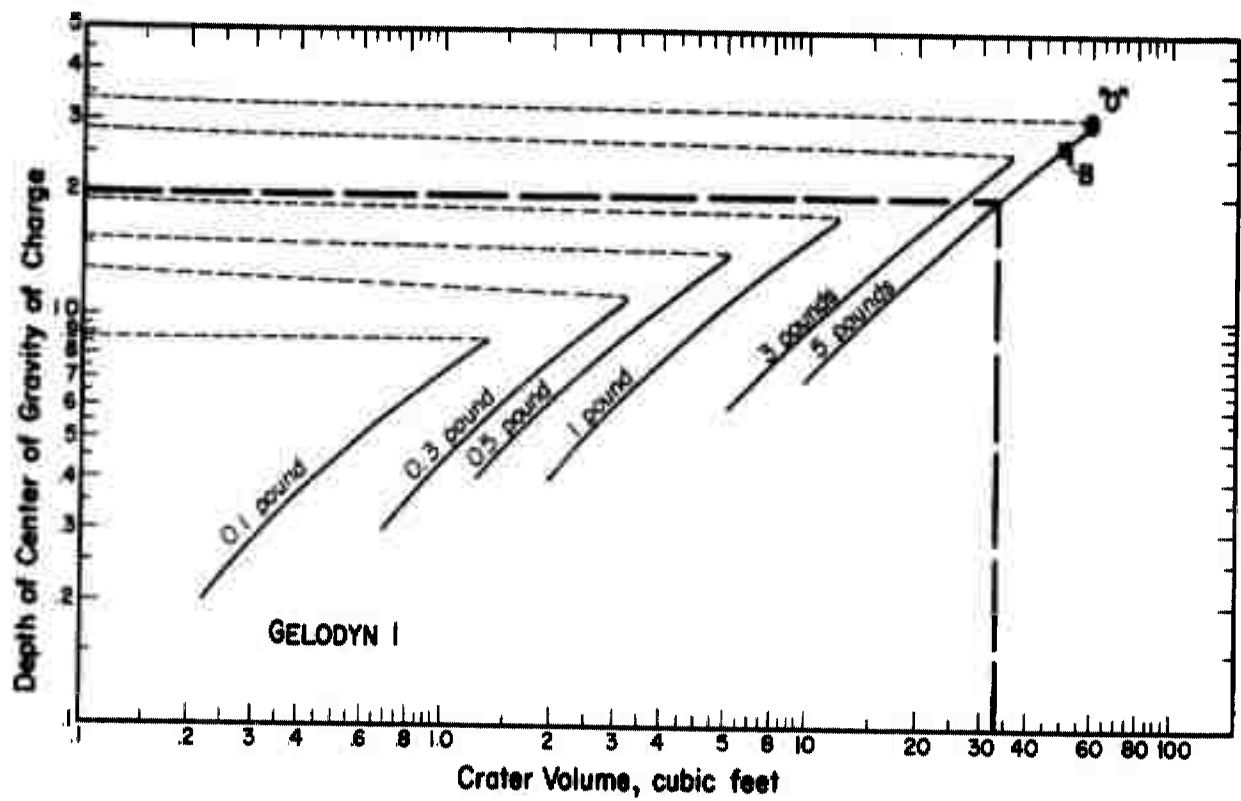


A. Depth of charge vs. crater volume, Atlas 80% Gelatin.

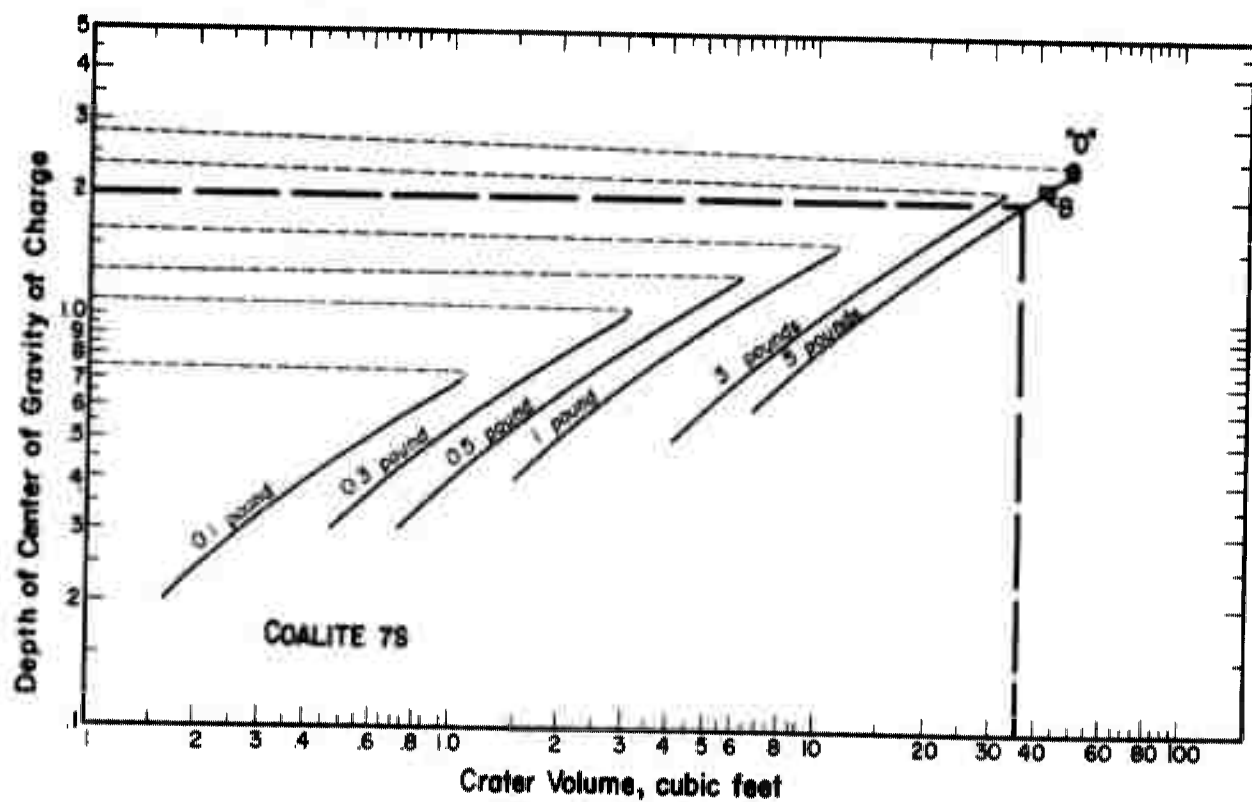


B. Depth of charge vs. crater volume, Atlas 60% Gelatin.

Figure 84. Volume of craters in frozen Keweenaw silt.



C. Depth of charge vs. crater volume, Gelodyn 1.



D. Depth of charge vs. crater volume, Coalite 7S.

Figure 84. Volume of craters in frozen Keweenaw silt.

range of depth ratios less than 0.4. (See Fig. 68 and also opening paragraphs, Chapter I, Section I, Introduction, The Problem.)

4. Objective 3: Proper position of charge relative to the frozen-ground interface

Presumably, the proper position of the charge relative to the frozen-ground interface is that position at which the volume of excavation per unit weight of explosive is maximum. The volume of excavation per unit weight is maximum at the optimum weight (by definition).

At the optimum weight both the ABC product and the energy-utilization number, A, are maximum.

It is difficult to specify the proper position of the charge relative to the frozen-ground interface, because too many factors are involved. The problem must be restated as follows:

What is the proper position of the charge relative to the frozen-ground interface for blasts within the frozen layer?

Field evidence indicates that rupture of the frozen-ground interface is due to downward expansion of the gas bubble and to plastic deformation of the frozen ground below the explosive charge. Expansion of the gas bubble may be compared to the blowing up of a toy balloon. If blown up too quickly, it ruptures prematurely. If weak spots are present, the balloon bulges into odd shapes.

The effect of rupture of the frozen-ground interface is illustrated in Figure 73. Break-through is accompanied by a rise in the volume-utilization factor, due to lowering the center of pressure of the gas bubble and increasing the interval of time that the explosion pressure is exerted upon the medium (impulse). In no instance does the volume-utilization factor increase above that at depth ratio 1.0. Thus, at break-through the product of the stress-distribution factor (which expresses the effect of the frozen-ground interface) and the energy-utilization number approaches, but never exceeds, the value of the AC product at optimum depth.

According to the Keweenaw Test data, statements that the proper position of the charge relative to the frozen-ground interface ranges from an interface ratio of 0.60 to 0.75 are unfounded. Instead, break-through and rise of the volume-utilization factor seem to be related in a complex manner both to the depth ratio and to the interface ratio. Moreover, at constant interface ratio, the depth ratio at break-through appears to differ for each type of explosive. Break-through occurs at higher depth ratios for low-velocity than for high-velocity explosives.

For blasts in shallow depths of frozen ground, as at the Keweenaw Test Site during the winter 1953-54, it is most difficult to separate the effects of break-through of the frozen-ground interface from the effects of break-through of the surface (See Blast Test C, Ch. III). A new series of experiments must be conducted in deeply frozen ground before numbers can be assigned to the stress-distribution factor.

5. Objective 4: Feasibility of fracturing the frozen layer by placing a charge in the underlying unfrozen material

Placing a charge in the unfrozen material below the frozen layer increases the rock factor at constant weight of explosive, thus increasing the critical depth for a charge of given weight. At a given depth and weight of charge (see Example 2, Blast Test C) a charge placed below the frozen layer produces a larger volume of crater than the volume obtained by extrapolating the data for charges placed within the frozen layer.

We consider that the increase in volume is analogous to the difference to be expected between charges placed in rock and in soil. Thus we may attribute the increased volume to an increase in the rock factor, B, rather than to an increase either in the energy-utilization factor, A, or the stress-distribution factor, C.

The statement of Objective No. 4 perhaps implies that the depth of the charge is increased to place it below the frozen layer. Increasing the depth increases the length-scale ratio of the blast and increases the weight of charge as a function of the

cube of the length-scale ratio. The increase in weight of charge would result in an increase in volume of crater independent of any change in the ABC product. The value of A for the two blasts remains constant because the depth-ratio remains constant. The increase in volume can be due only to a change in B or in C or in both B and C. The position of the charge within the frozen layer relative to the interface, to the depth-ratio, and to the type of explosive all influence the value of C. Accordingly, when comparing blasts within and blasts below the frozen layer, all the factors must be specified.

The comparison made here assumes that the blast within the frozen layer does not break through the frozen-ground interface (C remains constant). If break-through did occur, it is doubtful that C would increase appreciably relative to the increase in B for charges placed deeply within the unfrozen material. A charge placed with its center of gravity precisely at the frozen-ground interface presents a problem, as downward and lateral expansion of the gas bubble occur without break-through. Presumably, the rock factor is the same as for a charge slightly above the frozen-ground interface. Presumably also, the energy-utilization number cannot exceed the value at depth ratio 1.0.

6. Objective 5: Effect of diameter of the borehole and shape of charge on results of blasting

The effect of charge shape was explored in Blast Test F (Chapter III, Section VII). It is generally assumed that the shape of charge influences both the stress distribution in the medium and the shock effects. It is sometimes assumed also that the shape of a charge is responsible for the anomalous behavior of measurements of strain, hydrostatic pressure, acceleration, and displacement.

The charge shape must be related either to shock effects or to displacement associated with gas-bubble expansion. It is possible here only to appraise the effect of shape upon gas-bubble expansion, since the shock effect (Chapter III, section I) is considered to be relatively unimportant in frozen Keweenaw silt.

The explanation adopted here is as follows: As the shape of a charge approaches a sphere or a cylinder of height equal to diameter, the center of gravity is lowered in a hole of constant depth and increasing diameter. The lowering of center of gravity is a function of shape, but, more important, results in an increase in the depth ratio. An increase in depth ratio results in an increase in volume-utilization factor (see Blast Test B) or a decrease in the proportion of the total energy of a blast that is wasted to the atmosphere.

According to this explanation, the shape effect can be expressed by the energy-utilization number, which is a function of depth ratio solely. On the contrary, if the increase in energy utilization is due to shape also, different values of C, the stress-distribution factor, must be assigned to corresponding shapes.

From the results of Blast Test F, we consider that the effect of shape is so slight within the range from height = 4 x diam to height = $\frac{1}{4}$ diam, at constant depth of center of gravity, that no substantial error in blasting is introduced by ignoring any possible variations in the value of C due to a shape effect.

It seems desirable to determine whether or not the results are valid at depth ratios other than 1.0; to extend the height-to-diameter ratio to perhaps 10 to 1, if sufficient frozen ground is available; and to compare results using a high-velocity explosive (Military Explosive) with those using a low-velocity explosive (Coalite or equivalent).

Section II. Conclusions and Recommendations

1. Feasibility of using explosives for constructing foxholes in frozen ground

The use of explosives for constructing foxholes in frozen ground can be carried out both safely and economically with proper blasting techniques. Improper placement of the charge and use of excessive quantities of explosives are responsible for the poor results cited in D. A. Pamphlet 20-201¹ and in Exercise Eager Beaver

1. Department of the Army (1951) Military improvisation during the Russian campaign, DA Pamphlet 20-201, Historical Study.

(Combined United States-Canadian Engineer USER Trial 1951-1952).¹

Not only can conventional crater-type foxholes be constructed, but in certain soil types, if the thickness of frozen ground is not too great, igloo-type foxholes can be made. An igloo-type foxhole is one in which the frozen ground is domed up by a controlled explosion, leaving a hole in the roof and a cavity below. (See Chapter III, Section IV, Blast Test C).

Further experiments in foxhole construction should include several varieties of military explosives and at least two types of commercial explosives.

2. Methods of placing the charge

It is perhaps impossible to develop one type of drilling rig that is ideally suited to all the conditions to be found in various types of frozen ground. Various methods of drilling must be used for holes of various sizes and depths. The type of equipment used in the Keweenaw Tests (see Chapter I, Section II, Blast-Hole Drilling) is satisfactory for research purposes but probably can be improved upon in military operations.

Preliminary experiments using shaped charges for constructing a foxhole were discouraging. Before further investigation of shaped charges, it is recommended:

1) that the technique of using hand augers and stage blasting described in Blast Test D, (Ch. III, Section V) be investigated further and that various types of augers be developed and tested;

2) that preliminary inert-bomb drops be made from certain specified altitudes of release, using certain specified sizes of bombs, in order to determine penetration characteristics of frozen ground, with a view toward designing bombs useful in the construction of both conventional and igloo-type foxholes under battle conditions, where conventional drill rigs might be impracticable.

3. Mechanics of crater formation

A theory of crater formation for blasts in frozen ground has gradually evolved. This theory is essentially a continuation of Livingston's observations on the mechanics of rock failure for crater blasts in various types of rocks and for craters produced by impact and penetration of bombs into rock. The theory (Ch. III, Section I) deals with (1) shock phenomena, (2) expansions of the gas bubble produced by the explosion, and (3) rupture of the surface and of the frozen-ground interface, and the conversion of the remaining energy of the explosion to forms unrelated to the volume of excavation. Modifications of the theory are perhaps necessary for application to a multitude of different types of materials, but most future blasting research is perhaps related in some manner to it.

4. The crater equation

The view is adopted here that blasts in various types of frozen ground, and in most types of materials, with various types of explosives are expressed by an equation of the form:

$$N = A B C \sqrt[3]{W}$$

The equation is discussed in Chapter III, Section IV-2 and Chapter IV, Section I-2.

It is recommended that future blasts in frozen ground be directed towards:

(a) expressing the energy-utilization number, A, as a function of depth ratio and possibly of charge shape;

(b) expressing the rock factor, B, as a function of the physical properties of various types of frozen ground at various temperatures and as a function of the thickness of the frozen layer relative to the depth of the charge;

1. See Boyd, W. K. (1953) Minutes, Consultant's Conference, on Excavations in frozen ground, 10 November, 1953.

(c) expressing the stress-distribution factor, C , as a function of the interface ratio and of the depth ratio;

(d) investigating further the effect of the charge shape and of the number of free-faces upon the stress-distribution factor.

5. Future instrumentation

Perhaps as a result of the Keweenaw Tests, sufficient progress has now been made with fundamentals to institute a moderate program of instrumentation directed primarily towards developing suitable equipment and techniques for obtaining measurements of:

- (a) flyrock travel-height and flyrock travel-distance,
- (b) borehole pressure,
- (c) hydrostatic pressure and impulse.

6. Classification of explosives

The conclusion is inescapable that performance of commercial explosives is related to composition. The Commercial Explosives Classification Chart (Table 1) is arranged in order of composition. Present procedure of selecting commercial explosives upon an absolute-weight-strength or execution-value basis and present procedure for measuring the velocity confined are perhaps in error, or unsuitable for our purposes, and should be re-appraised.

A classification procedure based upon oxygen balance and composition should be established for military explosives, to be used as a basis for selecting explosives for various military applications.

A survey of the literature should be conducted, and all information relevant to explosion pressure, explosion temperature, oxygen balance, combustion reactions, velocity of detonation, and energy of explosion should be analyzed.

7. Correlation of blast data

Much information is available from various blasting research projects conducted in soils and rocks. It seems desirable to compute and analyze as much as possible of the available data; much useful information pertaining to variations in the energy-utilization number, the rock factor, and the stress-distribution factor should be obtained.

APPENDIX

Data Sheets, Experiments 1-13
(Figures A1-A17)

BLAST HOLE			TYPE OF EXPLOSIVE	CARTRIDGE STRENGTH	WEIGHT STRENGTH	STICK COUNT 1-1/4 x 8	INCHES OF EXPLOSIVE	CARTRIDGE FRACTION	EXPLOSIVE WEIGHT, LBS. PER CARTRIDGE	WEIGHT OF CHARGE, LBS.	VELOCITY CONFINED	VELOCITY UNCONFINED	HEIGHT OF CHARGE	HEIGHT OF STEMMING	SURFACE TO CENTER OF GRAVITY INCHES	DEPTH OF FROZEN GROUND INCHES	CENTER OF GRAVITY TO INTERFAC INCHES	INTERFAC RATIO	CRATER AREA SQUARE FEET	CRATER RADIUS INCHES	CRATER DEPTH INCHES	DEPTH OF SLABBING INCHES	CHAMBER RADIUS FEET	r/d RATIO	SIMILITUDE RATIO	CRATER VOLUME CUBIC FEET	SLAB VOLUME CUBIC FEET	CHAMBER VOLUME CUBIC FEET	NUMBER	REMARKS
NUMBER	DIAMETER INCHES	DEPTH FEET																												
1	1 1/4	0.83	60% GELATIN	60.0	52.3	97	8	1	.472	472	20,000	16,000	6	4	7	16	9	.44	7.28	1.52	12	7	.60	2.60	-0.63	2.42	2.29	0.13	1	
2	-	-	-	-	-	-	7	.875	-	412	-	-	5 1/2	4 1/2	7 1/2	-	8 1/2	.45	7.09	1.50	30	7 1/2	.65	2.48	-3.03	3.64	3.01	0.63	2	
3	-	-	-	-	-	-	6	.75	-	353	-	-	4 1/2	5 1/2	7 1/2	16 1/2	8 1/2	.46	4.33	1.17	26	7 1/2	.48	1.84	-2.41	3.04	2.19	0.85	3	
4	-	-	-	-	-	-	5	.625	-	294	-	-	2 1/2	7 1/2	9	17	8	.53	6.27	1.41	17	9	.61	1.88	-0.89	2.75	2.44	0.31	4	
5	-	-	-	-	-	-	4	.5	-	236	-	-	2 1/2	7 1/2	8 1/2	-	8 1/2	.51	4.13	1.15	14	8 1/2	.45	1.58	-0.60	1.71	1.57	0.14	5	
6	-	-	-	-	-	-	3	.375	-	177	-	-	1	9	9 1/2	17 1/2	8	.54	2.98	0.97	12	9 1/2	.40	1.22	-0.26	1.45	1.41	0.04	6	
7	-	-	-	-	-	-	2	.25	-	118	-	-	1 1/2	8 1/2	9 1/2	18	8 1/2	.51	4.51	1.20	12	9 1/2	.25	1.56	-0.30	1.41	1.39	0.02	7	
8	-	-	-	-	-	-	1	.125	-	.059	-	-	1 1/2	9 1/2	9 1/2	-	8 1/2	.54	3.93	1.12	11	9 1/2	.08	1.38	-0.13	1.06	1.06	0.0	8	
9	-	-	PRIMACORD	-	-	-	30	-	-	1	-	-	1	9	9 1/2	18 1/2	9	.51	0	0	0	-	-	-	-	-	-	-	9	
10	-	-	GELODYN 1	55.0	64.6	110	8 1/2	1.09	446	488	14,000	10,000	6 1/2	3 1/2	6 1/2	19	12 1/2	.36	5.20	1.54	12	6 1/2	.60	2.29	-0.78	1.89	1.74	0.15	10	
11	-	-	-	-	-	-	7 1/2	.95	-	425	-	-	6	4	7	17	10 1/2	.41	6.47	1.54	11 1/2	7	.73	2.47	-0.64	2.31	2.10	0.21	11	
12	-	-	-	-	-	-	6 1/2	.81	-	362	-	-	3 1/2	6 1/2	8 1/2	18 1/2	10 1/2	.45	3.09	0.99	15	8 1/2	.51	1.46	-0.86	1.51	1.24	0.27	12	
13	-	-	-	-	-	-	5 1/2	.68	-	307	-	-	4 1/2	5 1/2	7 1/2	-	10 1/2	.41	3.77	1.10	17	7 1/2	.65	1.73	-1.23	1.87	1.54	0.33	13	
14	-	-	-	-	-	-	4 1/2	.54	-	244	-	-	4 1/2	7	8 1/2	-	10	.46	3.92	1.12	13 1/2	8 1/2	.51	1.58	-0.59	1.89	1.68	0.21	14	
15	-	-	-	-	-	-	3 1/2	.41	-	181	-	-	1 1/2	6 1/2	8 1/2	-	10 1/2	.45	5.40	1.31	11	8 1/2	.40	1.88	-0.31	1.67	1.64	0.03	15	
16	-	-	-	-	-	-	2 1/2	.28	-	125	-	-	1 1/2	8 1/2	9 1/2	-	9 1/2	.50	4.29	1.17	12	9 1/2	.40	1.52	-0.30	1.69	1.66	0.03	16	
17	-	-	-	-	-	-	1 1/2	.13	-	.063	-	-	1	9	9 1/2	-	9 1/2	.51	.72	0.48	2	2	.06	.61	.79	.04	.04	.0	17	
18	-	-	COALITE 7-S	44.2	61.9	120	11 1/2	1.38	407	560	10,700	8,600	5 1/2	4 1/2	7 1/2	-	10 1/2	.38	9.07	1.70	11 1/2	7 1/2	.71	2.86	-0.61	3.06	2.83	0.23	18	
19	-	-	-	-	-	-	9 1/2	1.18	-	483	-	-	6 1/2	3 1/2	6 1/2	-	11 1/2	.36	4.50	1.20	14 1/2	6 1/2	.60	2.13	-1.15	1.66	1.42	0.24	19	
20	-	-	-	-	-	-	8 1/2	1.02	-	413	-	-	5 1/2	4 1/2	7 1/2	-	10 1/2	.40	6.89	1.48	12 1/2	7 1/2	.60	2.41	-0.69	2.30	2.14	0.16	20	
21	-	-	-	-	-	-	6 1/2	.85	-	350	-	-	3 1/2	6 1/2	8 1/2	-	9 1/2	.44	5.80	1.36	15 1/2	8 1/2	.42	2.01	-0.91	1.92	1.77	0.15	21	
22	-	-	-	-	-	-	5 1/2	.68	-	274	-	-	2	8	9	-	9	.49	5.40	1.31	12 1/2	9	.52	1.75	-0.39	2.10	1.99	0.11	22	
23	-	-	-	-	-	-	4 1/2	.51	-	210	-	-	1 1/2	8 1/2	9 1/2	-	8 1/2	.50	3.40	1.04	14	9 1/2	.38	1.35	-0.51	1.37	1.26	0.11	23	
24	-	-	-	-	-	-	2 1/2	.34	-	140	-	-	2	8	9	-	9	.49	4.93	1.25	13	9	.53	1.67	-0.44	1.87	1.77	0.10	24	
25	-	-	-	-	-	-	1 1/2	.17	-	.070	-	-	1	9	9 1/2	-	8 1/2	.51	-	0.40	1 1/2	1 1/2	.08	.50	.82	.03	.03	0.0	25	

SLIPRE CONTRACT MINING RESEARCH CORPORATION
EXPLOSION TESTS IN FROZEN ROCK
DATA SHEET EXPERIMENT NO. 1
BLAST TEST A FIG. A1 SEP. 30, 1934

NUMBER	DIAMETER INCHES	DEPTH FEET	TYPE OF EXPLOSIVE	CARTRIDGE STRENGTH	WEIGHT POUNDS	STICK COUNT 1/4 L.B.	INCHES OF EXPLOSIVE	CARTRIDGE FRACTION	EXPLOSIVE	EFFECTIVE WEIGHT, LBS.	WEIGHT OF CHARGE, LBS.	VELOCITY CONFINED	VELOCITY UNCONFINED	HEIGHT OF CHARGE	HEIGHT OF STEMMING	SPACE TO CENTER OF GRAVITY INCHES	DEPTH OF FROZEN GROUND INCHES	CENTER OF GRAVITY TO WATERLINE INCHES	INTERFACIAL RATIO	CHARGE AREA SQUARE FEET	CHARGE RADIUS FEET	CHARGE DEPTH INCHES	DEPTH OF SLAMMING INCHES	CHARGE RADIUS FEET	V.R. RATIO	SIMILITUDE RATIO	CHARGE VOLUME CUBIC FEET	SLAM VOLUME CUBIC FEET	CHARGE VOLUME CUBIC FEET	NUMBER	REMARKS	
26	1 1/2	0.82	60% GELATIN	800	55.5	97	1	0.09	1	472	044	20,000	40,000	1	3 1/2	18 1/2	18 1/2	8 1/2	53	-	0.17	2 1/2	2 1/2	0.09	0.00	0.00	0.00	0.00	0.00	26		
27	-	-	GELATIN	50.0	64.6	110	1	11	1	446	049	14,000	30,000	1	3 1/2	18 1/2	18 1/2	8 1/2	51	-	0.00	0	0	0.00	0.00	0.00	0.00	0.00	0.00	0.00	27	
28	-	-	COALITE 7-5	44.2	91.9	120	1	18	1	407	063	10,100	8,000	1	3 1/2	18 1/2	18 1/2	8 1/2	51	-	0.00	0	0	0.00	0.00	0.00	0.00	0.00	0.00	0.00	28	
29	-	-	60% GELATIN	800	82.3	97	1	0.06	1	472	029	20,000	40,000	1	3 1/2	18 1/2	18 1/2	8 1/2	53	1	0.17	2 1/2	2 1/2	0.09	0.00	0.00	0.00	0.00	0.00	0.00	29	
30	-	-	-	-	-	-	-	-	-	-	-	-	-	-	-	-	-	-	-	-	-	-	-	-	-	-	-	-	-	30		
31	-	-	-	-	-	-	-	-	-	-	-	-	-	-	-	-	-	-	-	-	-	-	-	-	-	-	-	-	-	31		
32	-	-	-	-	-	-	-	-	-	-	-	-	-	-	-	-	-	-	-	-	-	-	-	-	-	-	-	-	-	32		
33	-	-	-	-	-	-	-	-	-	-	-	-	-	-	-	-	-	-	-	-	-	-	-	-	-	-	-	-	-	33		
34	-	-	-	-	-	-	-	-	-	-	-	-	-	-	-	-	-	-	-	-	-	-	-	-	-	-	-	-	-	34		
35	-	-	-	-	-	-	-	-	-	-	-	-	-	-	-	-	-	-	-	-	-	-	-	-	-	-	-	-	-	35		
36	-	-	-	-	-	-	-	-	-	-	-	-	-	-	-	-	-	-	-	-	-	-	-	-	-	-	-	-	-	36		
37	-	-	-	-	-	-	-	-	-	-	-	-	-	-	-	-	-	-	-	-	-	-	-	-	-	-	-	-	-	37		

SLIP E. CONTRACT MINING RESEARCH CORPORATION
 EXPLOSIVE TESTS IN FROZEN GROUND SILT
 DATA SHEET EXPERIMENT NO. 1
 BLAST TEST A FIG. 4.2 SEPT. 30, 1954

BLAST HOLE			TYPE OF EXPLOSIVE	CARTRIDGE STRENGTH	WEIGHT STRENGTH	STICK COUNT 1-1/4"	INCHES OF EXPLOSIVE	CARTRIDGE FRACTION	EXPLOSIVE WEIGHT, LBS. PER CARTRIDGE	WEIGHT OF CHARGE, LBS.	VELOCITY CONFINED	VELOCITY UNCONFINED	HEIGHT OF CHARGE	HEIGHT OF STEMMING	SURFACE TO CENTER OF GRAVITY INCHES	DEPTH OF FROZEN GROUND INCHES	CENTER OF GRAVITY TO INTERFACE INCHES	INTERFACE RATIO	CRATER AREA SQUARE FEET	CRATER RADIUS FEET	CRATER DEPTH INCHES	DEPTH OF SLASHING INCHES	CHAMBER RADIUS FEET	1/4 RATIO	SIMILITUDE RATIO	CRATER VOLUME CUBIC FEET	SLAB VOLUME CUBIC FEET	CHAMBER VOLUME CUBIC FEET	NUMBER	REMARKS	
NUMBER	DIAMETER INCHES	DEPTH FEET																													
38	1 1/2	10	60% GELATIN	60.0	52.3	97	8	1	472	472	20,000	16,000	5 1/2	6 1/2	9 1/2	18	8 1/2	51	7.87	1.58	21	9 1/2	0.58	2.05	-1.27	3.70	3.22	0.48	38		
39	-	-	-	-	-	-	7	875	-	413	-	-	4 1/2	7 1/2	9 1/2	-	8 1/2	54	7.12	1.51	25	9 1/2	0.72	1.86	-1.56	5.66	4.40	1.26	39	BROKE THROUGH INTERFACE	
40	-	-	-	-	-	-	6	75	-	354	-	-	4	8	10	19	9	53	7.65	1.56	29	10	0.65	1.87	-1.90	5.95	4.68	1.27	40	-	
41	-	-	-	-	-	-	5	625	-	295	-	-	2 1/2	9 1/2	10 1/2	-	8 1/2	57	9.00	1.69	28	10 1/2	0.60	1.87	-1.57	6.78	5.67	1.09	41	-	
42	-	-	-	-	-	-	4	50	-	236	-	-	3	9	10 1/2	20	9 1/2	53	8.75	1.67	18	10 1/2	0.67	1.91	-0.71	3.95	3.69	0.26	42	-	
43	-	-	-	-	-	-	3	375	-	177	-	-	2	10	11	-	9	55	6.20	1.40	17	11	0.84	1.53	-0.55	3.55	3.18	0.37	43	-	
44	-	-	-	-	-	-	2	25	-	118	-	-	1 1/2	11 1/2	11 1/2	19	7 1/2	59	5.85	1.36	15	11 1/2	0.39	1.39	-0.28	2.78	2.73	0.05	44	-	
45	-	-	-	-	-	-	1	125	-	109	-	-	1	11	11 1/2	-	7 1/2	57	-	-	-	0	-	-	1.0	-	-	-	-	45	NO CRATER
46	-	-	-	-	-	-	1	100	-	100	-	-	1	11 1/2	11 1/2	-	7 1/2	59	-	-	-	0	-	-	-	-	-	-	-	46	-
47	1 1/2	-	GELDYN 1	55.0	64.6	110	8 1/2	1.09	446	486	14,000	10,000	5 1/2	6 1/2	9 1/2	-	9 1/2	46	6.50	1.44	18	9 1/2	0.57	1.89	-0.97	3.08	2.77	0.31	47		
48	-	-	-	-	-	-	7 1/2	95	-	424	-	-	3 1/2	8 1/2	10 1/2	17	6 1/2	59	6.64	1.45	32	10 1/2	1.10	1.72	-2.16	7.17	4.35	2.82	48	BROKE THROUGH INTERFACE	
49	-	-	-	-	-	-	6 1/2	82	-	364	-	-	3 1/2	8 1/2	10 1/2	18	6 1/2	57	6.42	1.43	24	10 1/2	0.60	1.67	-1.34	4.16	3.49	0.67	49	-	
50	-	-	-	-	-	-	5 1/2	68	-	303	-	-	2 1/2	9 1/2	10 1/2	19	8 1/2	57	7.50	1.54	30	10 1/2	0.68	1.70	-1.75	5.83	4.66	1.17	50	-	
51	-	-	-	-	-	-	4 1/2	54	-	242	-	-	1 1/2	11 1/2	11 1/2	17	5 1/2	69	9.51	1.74	19	11 1/2	0.56	1.78	-0.62	5.07	4.80	0.27	51	-	
52	-	-	-	-	-	-	3 1/2	41	-	181	-	-	1 1/2	11 1/2	11 1/2	15	3 1/2	77	4.96	1.26	24	11 1/2	0.34	1.30	-1.15	3.09	2.70	0.39	52	-	
53	-	-	-	-	-	-	2 1/2	27	-	122	-	-	1 1/2	11 1/2	11 1/2	15	3 1/2	77	1.75	0.75	13	11 1/2	0.75	0.77	+0.87	0.11	0.11	0.0	53	-	
54	-	-	-	-	-	-	1 1/2	14	-	106	-	-	1 1/2	11 1/2	11 1/2	-	-	-	0.0	0.0	-	0	-	-	1.0	-	-	-	-	54	NO CRATER
55	-	-	-	-	-	-	1	10	-	106	-	-	1 1/2	11 1/2	11 1/2	-	-	-	0.0	0.0	-	0	-	-	1.0	-	-	-	-	55	-
56	2 1/2	-	COALITE 75	44.2	61.9	120	11 1/2	1.38	407	562	10,700	8,600	3 1/2	8 1/2	10 1/2	17	6 1/2	60	4.06	1.14	18	10 1/2	0.80	1.35	-0.78	2.52	1.97	0.55	56	-	
57	-	-	-	-	-	-	9 1/2	119	-	484	-	-	2 1/2	9 1/2	10 1/2	17	6 1/2	63	6.21	1.41	25	10 1/2	0.67	1.57	-1.32	4.83	3.90	0.93	57	-	
58	-	-	-	-	-	-	8 1/2	102	-	415	-	-	1 1/2	10 1/2	11 1/2	18	6 1/2	63	5.81	1.36	27	11 1/2	0.22	1.45	-1.40	4.54	4.18	0.36	58	-	
59	-	-	-	-	-	-	6 1/2	85	-	346	-	-	1 1/2	10 1/2	11 1/2	20	8 1/2	57	9.04	1.70	27	11 1/2	0.76	1.79	-1.37	6.98	5.72	1.26	59	-	
60	-	-	-	-	-	-	5 1/2	68	-	277	-	-	1 1/2	10 1/2	11 1/2	-	-	57	7.17	1.51	16	11 1/2	0.42	1.59	-0.41	3.83	3.71	0.12	60	-	
61	-	-	-	-	-	-	4 1/2	50	-	205	-	-	1	11	11 1/2	18	6 1/2	64	7.00	1.49	23	11 1/2	0.60	1.55	-1.00	4.48	3.92	0.56	61	-	
62	-	-	-	-	-	-	2 1/2	34	-	139	-	-	1 1/2	11 1/2	11 1/2	-	6 1/2	66	0.0	0.0	0	0	-	-	1.00	-	-	-	-	62	NO CRATER

S. I. P. R. E. CONTRACT MINING RESEARCH CORPORATION
EXPLOSION TESTS IN FROZEN FRODOG SILT
DATA SHEET EXPERIMENT NO. 2
BLAST TEST A F.W. A3 S. I. 30, 1954

NUMBER	BLAST HOLE		TIME OF EXPLOSIVE	CRATERING STRENGTH	WEIGHT STRENGTH	STOCK COUNT STRENGTH	INCHES OF EXPLOSIVE	CARTON FUNCTION	EXPLOSIVE PER CARTON	WEIGHT OF CHARGE, LBS	VELOCITY CONFINED	VELOCITY UNCONFINED	HEIGHT OF CHARGE	HEIGHT OF STEMMING	SURFACE TO CENTER OF CRATER, INCHES	DEPTH OF FRESH GROUND INCHES	CENTER OF CRATER INCHES	CRATER AREA SQUARE FEET	CRATER RADIUS FEET	CRATER DEPTH INCHES	DEPTH OF SLABBER INCHES	DIAMETER RADIUS FEET	V/D RATIO	SIMILITUDE RATIO	CRATER VOLUME CUBIC FEET	SLAB VOLUME CUBIC FEET	CHARGE VOLUME CUBIC FEET		REMARKS	
	DIAMETER INCHES	DEPTH FEET																												
63	2 1/2	10	COALITE 75	44.2	61.9	120	1 1/2	17	407	489	10,700	8,500	1	11 1/2	11 1/2	11 1/2	10												NO CRATER	
64	2 1/2	10	COALITE 75	44.2	61.9	120	1 1/2	17	407	489	10,700	8,500	1	11 1/2	11 1/2	11 1/2	10													NO CRATER
65	2 1/2	10	COALITE 75	44.2	61.9	120	1 1/2	17	407	489	10,700	8,500	1	11 1/2	11 1/2	11 1/2	10													NO CRATER
66	2 1/2	10	COALITE 75	44.2	61.9	120	1 1/2	17	407	489	10,700	8,500	1	11 1/2	11 1/2	11 1/2	10													CRATER-LOW CRITICAL
67	2 1/2	10	COALITE 75	44.2	61.9	120	1 1/2	17	407	489	10,700	8,500	1	11 1/2	11 1/2	11 1/2	10													CRATER-MODERATE CRITICAL
68	2 1/2	10	COALITE 75	44.2	61.9	120	1 1/2	17	407	489	10,700	8,500	1	11 1/2	11 1/2	11 1/2	10													
69	2 1/2	10	COALITE 75	44.2	61.9	120	1 1/2	17	407	489	10,700	8,500	1	11 1/2	11 1/2	11 1/2	10													
70	2 1/2	10	COALITE 75	44.2	61.9	120	1 1/2	17	407	489	10,700	8,500	1	11 1/2	11 1/2	11 1/2	10													
71	2 1/2	10	COALITE 75	44.2	61.9	120	1 1/2	17	407	489	10,700	8,500	1	11 1/2	11 1/2	11 1/2	10													CHARGING ERROR
72	2 1/2	10	COALITE 75	44.2	61.9	120	1 1/2	17	407	489	10,700	8,500	1	11 1/2	11 1/2	11 1/2	10													
73	2 1/2	10	COALITE 75	44.2	61.9	120	1 1/2	17	407	489	10,700	8,500	1	11 1/2	11 1/2	11 1/2	10													
74	2 1/2	10	COALITE 75	44.2	61.9	120	1 1/2	17	407	489	10,700	8,500	1	11 1/2	11 1/2	11 1/2	10													NO CRATER
75	2 1/2	10	COALITE 75	44.2	61.9	120	1 1/2	17	407	489	10,700	8,500	1	11 1/2	11 1/2	11 1/2	10													CRATER
76	2 1/2	10	COALITE 75	44.2	61.9	120	1 1/2	17	407	489	10,700	8,500	1	11 1/2	11 1/2	11 1/2	10													
77	2 1/2	10	COALITE 75	44.2	61.9	120	1 1/2	17	407	489	10,700	8,500	1	11 1/2	11 1/2	11 1/2	10													CRITICAL
78	2 1/2	10	COALITE 75	44.2	61.9	120	1 1/2	17	407	489	10,700	8,500	1	11 1/2	11 1/2	11 1/2	10													CRATER
79	2 1/2	10	COALITE 75	44.2	61.9	120	1 1/2	17	407	489	10,700	8,500	1	11 1/2	11 1/2	11 1/2	10													
80	2 1/2	10	COALITE 75	44.2	61.9	120	1 1/2	17	407	489	10,700	8,500	1	11 1/2	11 1/2	11 1/2	10													
81	2 1/2	10	COALITE 75	44.2	61.9	120	1 1/2	17	407	489	10,700	8,500	1	11 1/2	11 1/2	11 1/2	10													
82	2 1/2	10	COALITE 75	44.2	61.9	120	1 1/2	17	407	489	10,700	8,500	1	11 1/2	11 1/2	11 1/2	10													
83	2 1/2	10	COALITE 75	44.2	61.9	120	1 1/2	17	407	489	10,700	8,500	1	11 1/2	11 1/2	11 1/2	10													NO CRATER
84	2 1/2	10	COALITE 75	44.2	61.9	120	1 1/2	17	407	489	10,700	8,500	1	11 1/2	11 1/2	11 1/2	10													LOW CRITICAL
85	2 1/2	10	COALITE 75	44.2	61.9	120	1 1/2	17	407	489	10,700	8,500	1	11 1/2	11 1/2	11 1/2	10													MODERATE CRITICAL
86	2 1/2	10	COALITE 75	44.2	61.9	120	1 1/2	17	407	489	10,700	8,500	1	11 1/2	11 1/2	11 1/2	10													CRATER
87	2 1/2	10	COALITE 75	44.2	61.9	120	1 1/2	17	407	489	10,700	8,500	1	11 1/2	11 1/2	11 1/2	10													

SLITRE CONTRACT, MINING RESEARCH CORPORATION
EXPLOSION TESTS IN FROZEN REVEREND BILT
DATA SHEET
EXPERIMENT NO. 2
SEPT. 30, 1964
FIG. A-4

BLAST HOLE			TYPE OF EXPLOSIVE	CARTIDGE STRENGTH	WEIGHT STRENGTH	STICK COUNT 1-1/4" x 8"	INCHES OF EXPLOSIVE	CARTIDGE FRACTION	EXPLOSIVE PER CARTIDGE	WEIGHT OF CHANGE, LBS.	VELOCITY CONFINED	VELOCITY UNCONFINED	HEIGHT OF CHANGE	HEIGHT OF STEMMING	SURFACE TO CENTER OF GRAVITY INCHES	DEPTH OF FROZEN GROUND INCHES	CENTER OF GRAVITY TO INTERFACIAL INCHES	INTERFACIAL RATIO	CRATER AREA SQUARE FEET	CRATER RADIUS FEET	CRATER DEPTH INCHES	DEPTH OF SLABbing INCHES	CHAMBER RADIUS FEET	1/4 RATIO	SIMILITUDE RATIO	CRATER VOLUME CUBIC FEET	SLAB VOLUME CUBIC FEET	CHAMBER VOLUME CUBIC FEET	NUMBER	REMARKS
NUMBER	DIAMETER INCHES	DEPTH FEET																												
125	1 1/8	1.0	60 % GELATIN	60.0	52.5	97	1 1/8	.11	.472	.052	20,000	16,000	1	11"	11 1/2	18 ±	6 1/2 ±	.64												CRATER
126	-	-	-	-	-	-	1 1/8	.14	-	.066	-	-	1	11 1/2	11 1/2	-	-	.65												CRATER
127	-	-	-	-	-	-	1 1/8	.18	-	.085	-	-	-	-	-	-	-	-												UPLIFT AREA
128	2	1.25	-	-	-	-	1 1/8	.23	-	.109	-	-	1	15	15 1/2	19 ±	4 ±	.80												NO CRATER
129	-	-	-	-	-	-	2 1/8	.31	-	.146	-	-	1	14 1/2	14 1/2	20 ±	4 1/2 ±	.77												CRITICAL
130	-	-	-	-	-	-	3 1/8	.39	-	.184	-	-	2	13	14	20 ±	6 ±	.70												CRITICAL
131	2 1/8	1.5	-	-	-	-	3 1/8	.41	-	.194	-	-	1 1/2	16 1/2	17 1/2	-	3 ±	.86												NO CRATER
132	-	-	-	-	-	-	4 1/8	.55	-	.260	-	-	1	17	17 1/2	-	2 1/2 ±	.87												NO CRATER
133	-	-	-	-	-	-	5 1/8	.68	-	.321	-	-	1 1/2	16 1/2	17 1/2	21 ±	4 ±	.92												NO CRATER
134	2 1/8	1.75	-	-	-	-	5 1/8	.64	-	.302	-	-	3	18	19 1/2	-	1 1/2 ±	.93												CRITICAL
135	-	-	-	-	-	-	6 1/8	.86	-	.406	-	-	1	20	20 1/2	-	1 1/2 ±	.98												CRITICAL
136	-	-	-	-	-	-	8 1/8	1.07	-	.505	-	-	1 1/2	19 1/2	20 1/2	22 ±	1 1/2 ±	.93												CRITICAL
137	3 1/8	2.0	-	-	-	-	7 1/8	.95	-	.448	-	-	1	23 1/2	23 1/2	23 ±	-1 1/2 ±	1.07												NO CRATER
138	-	-	-	-	-	-	10 1/8	1.26	-	.596	-	-	1 1/2	22 1/2	23 1/2	-	-	1.06												CRITICAL
139	-	-	-	-	-	-	12 1/8	1.59	-	.760	-	-	1	21 1/2	23 1/2	23 ±	-1 ±	1.02												CRITICAL

S.L.P.R.E. CONTRACT MINING RESEARCH CORPORATION
 EXPLOSION TESTS IN FROZEN KEWSENAW SULF
 DATA SHEET EXPERIMENT NO. 4
 September 30, 1954 FIG. A7

NUMBER	BLAST HOLE		TYPE OF EXPLOSIVE	CARTRIDGE STRENGTH	WEIGHT STRENGTH	STICK COUNT 1/4" R	INCHES OF EXPLOSIVE	CARTRIDGE FRACTION	EMPLOYEE WEIGHT LBS PER CARTRIDGE	WEIGHT OF CHARGE LBS	VELOCITY COMPARED	VELOCITY 3000000/SEC	VELOCITY UNCOMPARED	HEIGHT OF CHARGE	WEIGHT OF STEERING	SURFACE TO CENTER-TO-INTERFACIAL INCHES	DEPTH OF PROTRUSION INCHES	CENTER-TO-INTERFACIAL TO INTERFACIAL RATIO	CHARGE AREA SQUARE FEET	CHARGE RADIUS FEET	CHARGE DEPTH INCHES	DEPTH OF FLANGE INCHES	CHARGE RADIUS FEET	VE RATIO	SIMILITUDE RATIO	CHARGE VOLUME CUBIC FEET	FLARE VOLUME CUBIC FEET	CHARGE VOLUME CUBIC FEET	NUMBER	REMARKS	
	DIAMETER INCHES	DEPTH FEET																													
140	1 1/2	1.0	80% RELATIN	80.0	52.5	87	1	11	472	0.51	3000000	4000000	-	1	11	11	23	11	242	0.89	4	4	0	90	78	57	0	140			
141	-	-	-	-	-	-	1	14	-	0.65	-	-	-	-	-	-	-	-	4.65	1.22	14	11	0	124	28	2.23	0.3	141			
142	-	-	-	-	-	-	1	18	-	0.65	-	-	-	-	10	11	-	11	4.65	1.22	14	11	0.36	124	28	2.23	0.3	142			
143	2	1.25	-	-	-	-	1	25	-	1.1	-	-	-	-	14	14	-	8	84	0.80	0.50	8	14	0.34	133	27	2.04	0.3	143		
144	-	-	-	-	-	-	2	31	-	1.47	-	-	-	-	-	-	22	71	87	0.0	0	0	-	0	0	10	-	0	144		
145	2 1/2	1.5	-	-	-	-	3	39	-	1.84	-	-	-	-	14	14	-	71	88	5.50	1.52	25	14	0.46	109	72	3.17	3.2	36	145	
146	-	-	-	-	-	-	3	41	-	1.82	-	-	-	-	17	17	-	41	80	8.50	1.75	22	17	0.47	100	83	3.41	2.90	31	146	
147	-	-	-	-	-	-	4	51	-	2.59	-	-	-	-	18	17	-	41	79	8.66	1.86	25	17	0.47	118	45	2.89	2.84	25	147	
148	3 1/2	1.75	-	-	-	-	5	64	-	3.21	-	-	-	-	10	17	23	5	74	10.04	1.60	28	17	0.67	113	85	4.09	3.44	35	148	
149	-	-	-	-	-	-	5	64	-	3.02	-	-	-	-	20	20	24	3	38	8.80	1.10	34	25	0.63	64	88	2.94	2.22	77	149	
150	-	-	-	-	-	-	6	76	-	4.08	-	-	-	-	-	-	-	-	4.96	1.26	34	-	0.70	74	87	3.68	2.88	0.84	150		
151	3 1/2	2.0	-	-	-	-	8	107	-	5.03	-	-	-	-	21	21	-	21	81	8.11	1.81	33	21	0.73	89	49	7.55	6.59	0.86	151	
152	-	-	-	-	-	-	7	95	-	4.80	-	-	-	-	22	23	-	1	97	0	0	0	-	0	0	10	-	-	-	152	
153	-	-	-	-	-	-	10	128	-	5.84	-	-	-	-	22	23	-	1	96	34.65	3.34	38	23	1.16	174	65	19.75	17.00	2.75	153	
154	-	-	-	-	-	-	12	158	-	7.45	-	-	-	-	22	23	2	2	110	29.1	3.09	43	23	2.00	160	87	42.15	35.40	11.75	154	

SLIRE CONTRACT, MINING RESEARCH CORPORATION
 EXPLOSION TESTS IN FROZEN FRESHMAN SILT
 DATA SHEET
 September 30, 1954
 Experiment NO. 5
 Fig. A8

NUMBER	DIAMETER INCHES	DEPTH FEET	TYPE OF EXPLOSIVE	CARTRIDGE STRENGTH	WEIGHT STRENGTH	STOCK COUNT	INCHES OF EXPLOSIVE	CARTRIDGE FRACTION	EXPLOSIVE WEIGHT, LBS	WEIGHT OF CHARGE, LBS	VELOCITY CONFIRMED	VELOCITY UNCONFIRMED	HEIGHT OF CHARGE	HEIGHT OF STEMMING	DAMAGE TO CENTER OF GRAVITY INCHES	DEPTH OF FROZEN GROUND INCHES	CENTER OF GRAVITY TO INTERFERENCE INCHES	INTERFERENCE RATIO	CRATER AREA SQUARE FEET	CRATER RADIUS FEET	CRATER DEPTH INCHES	DEPTH OF BLASTING INCHES	DIAMETER RADIUS FEET	V/L RATIO	SIMILITUDE RATIO	CRATER VOLUME CUBIC FEET	SLAB VOLUME CUBIC FEET	CHARGE VOLUME CUBIC FEET	NUMBER	REMARKS	
179	5	2.25	1000	0.05	0.05	0.05	0.05	0.05	0.05	0.05	0.05	0.05	0.05	0.05	0.05	0.05	0.05	0.05	0.05	0.05	0.05	0.05	0.05	0.05	0.05	0.05	0.05	0.05	0.05	0.05	0.05
180	5	2.25	1000	0.05	0.05	0.05	0.05	0.05	0.05	0.05	0.05	0.05	0.05	0.05	0.05	0.05	0.05	0.05	0.05	0.05	0.05	0.05	0.05	0.05	0.05	0.05	0.05	0.05	0.05	0.05	0.05
181	5	2.25	1000	0.05	0.05	0.05	0.05	0.05	0.05	0.05	0.05	0.05	0.05	0.05	0.05	0.05	0.05	0.05	0.05	0.05	0.05	0.05	0.05	0.05	0.05	0.05	0.05	0.05	0.05	0.05	0.05
182	5	2.25	1000	0.05	0.05	0.05	0.05	0.05	0.05	0.05	0.05	0.05	0.05	0.05	0.05	0.05	0.05	0.05	0.05	0.05	0.05	0.05	0.05	0.05	0.05	0.05	0.05	0.05	0.05	0.05	0.05
183	5	2.25	1000	0.05	0.05	0.05	0.05	0.05	0.05	0.05	0.05	0.05	0.05	0.05	0.05	0.05	0.05	0.05	0.05	0.05	0.05	0.05	0.05	0.05	0.05	0.05	0.05	0.05	0.05	0.05	0.05
184	5	2.25	1000	0.05	0.05	0.05	0.05	0.05	0.05	0.05	0.05	0.05	0.05	0.05	0.05	0.05	0.05	0.05	0.05	0.05	0.05	0.05	0.05	0.05	0.05	0.05	0.05	0.05	0.05	0.05	0.05
185	5	2.25	1000	0.05	0.05	0.05	0.05	0.05	0.05	0.05	0.05	0.05	0.05	0.05	0.05	0.05	0.05	0.05	0.05	0.05	0.05	0.05	0.05	0.05	0.05	0.05	0.05	0.05	0.05	0.05	0.05

SIPLE CONTRACT, MINING RESEARCH CORPORATION
 EXPLOSION TESTS IN FROZEN GROUND BY
 DATA SHEET EXPERIMENT NO 7
 September 30, 1904 7x 10

BLAST HOLE			TYPE OF EXPLOSIVE	CARTRIDGE STRENGTH	WEIGHT STRENGTH	STICK COUNT 1-1/4 x 8"	INCHES OF EXPLOSIVE	CARTRIDGE FRACTION	EXPLOSIVE WEIGHT, LBS.	PER CARTRIDGE	WEIGHT OF CHARGE, LBS.	VELOCITY CONFINED	VELOCITY UNCONFINED	HEIGHT OF CHARGE	HEIGHT OF STEMMING	SURFACE TO CENTER OF GRAVITY INCHES	DEPTH OF FROZEN GROUND INCHES	CENTER OF GRAVITY TO INTERFACE INCHES	INTERFACE RATIO	CRATER AREA SQUARE FEET	CRATER RADIUS FEET	CRATER DEPTH INCHES	DEPTH OF SLABbing INCHES	CHAMBER RADIUS FEET	r/d RATIO	SIMILITUDE RATIO	CRATER VOLUME CUBIC FEET	SLAB VOLUME CUBIC FEET	CHAMBER VOLUME CUBIC FEET	NUMBER	REMARKS	
NUMBER	DIAMETER INCHES	DEPTH FEET																														
186	1 1/2	10	80% GELATIN	80	72.6	100	1 1/2	.09	.500	.045	20,000	20,000	1 1/2	10 1/2	11 1/2	20	8 1/2	.56													COLLAR CIRCLE 1" DEEP	
187														1 1/2	10 1/2	11 1/2		8 1/2	.57													
188								1/2		.050				1 1/2	10 1/2	11 1/2		8 1/2	.56													
189																																
190								.125		.055																						
191																																
192								.141		.065																						
193										.070																						
194								.156																								
195																																
196								.172		.075				1 1/2	10 1/2	11 1/2		8 1/2	.56													
197																																
198								.187		.085				3	9	10 1/2		9 1/2	.52	0.34	0.33	3	3	-	.38	.71	0.04	0.04	0.04	0.04	4" COLLAR PLUS	
199														3 1/2	8 1/2	10 1/2		9 1/2	.51	10.29	1.81	13 1/2	10 1/2	0.30	2.12	.34	2.99	2.96	0.04	0.04	CRITICAL	
200								.203		.090				3	9	10 1/2		9 1/2	.52	5.98	1.38	14 1/2	7	0.30	1.58	.38	1.82	1.78	0.04	0.04	2" CRATER	
201														3 1/2	8 1/2	10 1/2		9 1/2	.52	1.25	0.63	-	-	-	.73	1.0	-	-	-	-	201	
202								.209		.100				2 1/2	9 1/2	10 1/2		9 1/2	.55	3.14	1.00	-	-	-	1.13	1.0	-	-	-	-	202	
203														-	-	-		-	-	15.61	2.23	14 1/2	10 1/2	0.52	2.58	.40	4.72	4.56	0.14	0.14	203	
204								.180		.075				3	10	11 1/2		8 1/2	.57	-	-	-	-	-	-	1.0	-	-	-	-	204	
205																																
206																																
207																																
208								.196		.082				2 1/2	10 1/2	11 1/2		8 1/2	.58	8.91	1.68	15	11 1/2	0.40	1.73	.29	3.89	3.83	0.01	0.01	CRATER	
209														2 1/2	10 1/2	11 1/2		8 1/2	.59	3.26	1.01	4	4	0.0	1.02	.66	0.36	0.36	0.0	0.0	CRITICAL	
209														2	10	11		9	.55	6.22	1.41	13 1/2	11	0.30	1.54	.23	2.42	2.41	0.01	0.01	FULL CRATER	

S.I.R.R.E. CONTRACT, MINING RESEARCH CORPORATION
EXPLOSION TESTS IN FROZEN KENNELAW SILT
DATA SHEET EXPERIMENT NO. 8
September 30, 1964 Pg. A 11

C.I.P.R.E. CONTRACT, MINNESOTA RESEARCH CORPORATION
EXPLOSION TESTS ON FROZEN KEYSERMAN SILT
DATA SHEET EXPERIMENT NO. 9
September 30, 1964 F.N. A13

BLAST HOLE			TYPE OF EXPLOSIVE	CARTRIDGE STRENGTH	WEIGHT STRENGTH	STICK COUNT 1-1/4 x 8"	INCHES OF EXPLOSIVE	CARTRIDGE FRACTION	EXPLOSIVE WEIGHT, LBS. PER CARTRIDGE	WEIGHT OF CHARGE, LBS.	VELOCITY CONFINED	VELOCITY UNCONFINED	HEIGHT OF CHARGE	HEIGHT OF STEMMING	SURFACE TO CENTER OF GRAVITY INCHES	DEPTH OF FROZEN GROUND INCHES	CENTER OF GRAVITY TO INTERFACE INCHES	INTERFACE RATIO	CRATER AREA SQUARE FEET	CRATER RADIUS FEET	CRATER DEPTH INCHES	DEPTH OF SLABBING INCHES	CHAMBER RADIUS FEET	1/4 RATIO	SIMILITUDE RATIO	CRATER VOLUME CUBIC FEET	SLAB VOLUME CUBIC FEET	CHAMBER VOLUME CUBIC FEET	NUMBER	REMARKS	
NUMBER	DIAMETER INCHES	DEPTH FEET																													
232	2 1/4	1.5	80% GELATIN	80	72.6	100	4	.50	500	0.21	21,000	20,000	1 1/2	16 1/2	17 1/2	9 1/2	-7 1/2	1.81	2.01	0.80	20 1/2	5	0.40	.56	-.16	0.75	0.69	0.06	232	MODERATE CRITICAL	
233	"	"	"	"	"	"	"	"	"	"	"	"	1 1/2	16 1/2	17 1/2	10	-7 1/2	1.74	0.66	0.46	1 1/2	5	0.0	.32	.97	0.0	-	-	233	"	
234	"	"	"	"	"	"	"	"	"	"	"	"	"	"	"	"	"	"	"	8.54	1.65	5	5 1/2	0.0	1.14	.71	1.14	1.14	0.0	234	"
235	"	1.25	"	"	"	"	"	"	"	"	"	"	1 1/2	14 1/2	14 1/2	10 1/2	-4	"	1.40	9.37	1.73	24	7 1/2	0.48	1.41	-.63	4.11	3.83	0.28	235	"
236	"	"	"	"	"	"	"	"	"	"	"	"	"	"	"	"	"	1.40	7.52	1.55	17 1/2	14 1/2	0.33	1.26	-.17	3.78	3.75	0.03	236	"	
237	"	"	"	"	"	"	"	"	"	0.20	"	"	"	"	"	"	"	1.40	4.93	1.25	16	"	0.32	0.89	-.12	2.58	2.57	0.02	237	"	
238	"	1.0	"	"	"	"	"	"	"	"	"	"	"	11 1/2	11 1/2	"	"	1.12	4.44	1.19	15	11 1/2	0.42	1.22	-.26	2.15	2.09	0.06	238	"	
239	"	"	"	"	"	"	"	"	"	"	"	"	1 1/2	11 1/2	11 1/2	"	"	1.12	3.35	1.03	16 1/2	"	0.37	1.05	-.36	2.25	2.15	0.10	239	"	
240	"	"	"	"	"	"	"	"	"	"	"	"	1 1/2	8 1/2	8 1/2	"	"	1.10	5.32	1.30	15 1/2	11 1/2	0.42	1.34	-.33	2.63	2.53	0.10	240	"	
241	"	0.75	"	"	"	"	"	"	"	"	"	"	1 1/2	8 1/2	8 1/2	"	"	0.83	4.00	1.13	13 1/2	8 1/2	0.41	1.55	-.54	2.76	2.66	0.10	241	"	
242	"	"	"	"	"	"	"	"	"	"	"	"	"	"	"	"	"	0.83	3.14	1.00	12	"	0.27	1.37	-.37	1.17	1.02	0.02	242	"	
243	"	"	"	"	"	"	"	"	"	"	"	"	"	"	"	"	"	0.83	4.81	1.24	13 1/2	"	0.60	1.70	-.57	2.22	2.06	0.16	243	"	
244	"	0.50	"	"	"	"	"	"	"	"	"	"	"	5 1/2	5 1/2	"	"	0.55	4.54	1.20	10	5 1/2	0.74	2.50	-.74	1.72	1.52	0.20	244	"	
245	"	"	"	"	"	"	"	"	"	"	"	"	"	"	"	"	"	0.55	3.92	1.12	10 1/2	"	0.55	2.34	-.83	1.35	1.21	0.14	245	"	
246	"	"	"	"	"	"	"	"	"	"	"	"	"	"	"	"	"	0.55	3.34	1.03	9 1/2	"	0.45	2.15	-.65	0.90	0.84	0.06	246	"	

S. I. P. R. E. CONTRACT, MINING RESEARCH CORPORATION
EXPLOSION TESTS IN FROZEN KEWEEANAW SILT
DATA SHEET EXPERIMENT NO. II
September 30, 1954 Fig. A 13

BLAST HOLE			TYPE OF EXPLOSIVE	CARTRIDGE STRENGTH	WEIGHT STRENGTH	STICK COUNT 1-1/4 x 8"	INCHES OF EXPLOSIVE	CARTRIDGE FRACTION	EXPLOSIVE WEIGHT, LBS. PER CARTRIDGE	WEIGHT OF CHARGE, LBS.	VELOCITY CONFINED	VELOCITY UNCONFINED	HEIGHT OF CHARGE	HEIGHT OF STEMMING	SURFACE TO CENTER OF GRAVITY INCHES	DEPTH OF FROZEN GROUND INCHES	CENTER OF GRAVITY TO INTERFACE INCHES	INTERFACE RATIO	CRATER AREA SQUARE FEET	CRATER RADIUS FEET	CRATER DEPTH INCHES	DEPTH OF SLABBING INCHES	CHAMBER RADIUS FEET	1/4 RATIO	SIMILITUDE RATIO	CRATER VOLUME CUBIC FEET	SLAB VOLUME CUBIC FEET	CHAMBER VOLUME CUBIC FEET	NUMBER	REMARKS	
NUMBER	DIAMETER INCHES	DEPTH FEET																													
247	2 1/2	1.5	60% GELATIN	60.0	52.3	97	4 1/2	.52	.472	.22	20,000	16,000	2	16	17															247	LOW CRITICAL
248	-	-	-	-	-	-	4 1/2	.53	-	.24	-	-	-	-	-															248	MODERATE CRITICAL
249	-	-	-	-	-	-	4 1/2	.55	-	.27	-	-	-	-	-															249	HIGH CRITICAL
250	-	-	-	-	-	-	4 1/2	.52	-	.22	-	-	-	-	-															250	LOW CRITICAL
251	-	-	-	-	-	-	-	-	-	-	-	-	1 1/2	16 1/2	17 1/2	11														251	-
252	2 1/2	-	GELODYN I	55.0	64.6	110	6 1/2	.78	.446	.36	14,000	10,000	1 1/2	16 1/2	17 1/2															252	-
253	-	-	-	-	-	-	6 1/2	.81	-	.38	-	-	-	-	-															253	MEDIUM CRITICAL
254	-	-	-	-	-	-	6 1/2	.84	-	.39	-	-	2	16	17															254	-
255	-	-	-	-	-	-	6 1/2	.80	-	.37	-	-	1 1/2	16 1/2	17 1/2															255	LOW CRITICAL
256	-	-	-	-	-	-	-	-	-	-	-	-	-	1	17	17 1/2														256	-
257	-	-	-	-	-	-	-	-	-	-	-	-	1 1/2	16 1/2	17 1/2															257	VOID
258	3 1/2	-	COALITE 7-5	44.2	61.9	120	12	1.50	.407	.63	10,700	8,600	2	16	17															258	LOW CRITICAL
259	-	-	-	-	-	-	12 1/2	1.56	-	.66	-	-	-	-	-															259	NO CRATER
260	-	-	-	-	-	-	13	1.62	-	.68	-	-	1 1/2	16 1/2	17 1/2															260	-
261	-	-	-	-	-	-	-	-	-	-	-	-	1 1/2	16 1/2	17 1/2															261	LOW CRITICAL
262	-	-	-	-	-	-	-	-	-	-	-	-	-	-	-															262	-
263	-	-	-	-	-	-	-	-	-	-	-	-	-	-	-															263	-
264	-	-	-	-	-	-	-	-	-	-	-	-	1 1/2	16 1/2	17 1/2															264	NO CRATER

S.I.P.R.E. CONTRACT, MINING RESEARCH CORPORATION
 EXPLOSION TESTS IN FROZEN KEWEEHAW SALT
 DATA SHEET EXPERIMENT NO. 10
 September 30, 1964 Fig. A 14

NUMBER	BLAST HOLE		TYPE OF EXPLOSIVE	CARTRIDGE STRENGTH	WEIGHT STRENGTH	STUCK COUNT	INCHES OF EXPLOSIVE	CARTRIDGE FRACTION	EXPLOSIVE WEIGHT, LBS PER CARTRIDGE	WEIGHT OF CHARGE, LBS	VELOCITY UNCONFINED	HEIGHT OF CHARGE	HEIGHT OF STEMMING	SURFACE TO CENTERLINE INCHES	DEPTH OF PROGEN GROUND INCHES	CENTERLINE TO INTERSPACE INCHES	INTERSPACE RATIO	CRATER AREA SQUARE FEET	CRATER RADIUS FEET	CRATER DEPTH INCHES	DEPTH OF RADIUS INCHES	CHARGE RADIUS FEET	CHARGE RATIO	CHARGE FEET	SIMULTANEOUS RATIO	CRATER VOLUME CUBIC FEET	BLAST VOLUME CUBIC FEET	CHARGE VOLUME CUBIC FEET	NUMBER	REMARKS			
	DIAMETER INCHES	DEPTH FEET																															
265	2 1/2	1.5	60% UELATIN	50	52.5	97	4 1/2	32	472	32	472	1 1/2	10 1/2	17 1/2	11	3 1/2	1.50	2.85	0.32	18	14 1/2	11	11 1/2	11 1/2	11 1/2	11 1/2	11 1/2	11 1/2	11 1/2	265	NO CRATER		
266	-	-	-	-	-	-	-	-	-	-	-	-	-	-	-	-	-	2.10	0.32	-	-	-	-	-	-	-	-	-	-	-	266	-	
267	-	-	-	-	-	-	-	-	-	-	-	-	-	-	-	-	-	2.85	0.32	-	-	-	-	-	-	-	-	-	-	-	267	-	
268	-	1.25	-	-	-	-	-	-	-	-	-	-	-	-	-	-	-	2.85	0.32	-	-	-	-	-	-	-	-	-	-	-	268	-	
269	-	-	-	-	-	-	-	-	-	-	-	-	-	-	-	-	-	2.85	0.32	-	-	-	-	-	-	-	-	-	-	-	269	-	
270	-	-	-	-	-	-	-	-	-	-	-	-	-	-	-	-	-	2.85	0.32	-	-	-	-	-	-	-	-	-	-	-	270	-	
271	-	1.0	-	-	-	-	-	-	-	-	-	-	-	-	-	-	-	2.85	0.32	-	-	-	-	-	-	-	-	-	-	-	271	-	
272	-	-	-	-	-	-	-	-	-	-	-	-	-	-	-	-	-	2.85	0.32	-	-	-	-	-	-	-	-	-	-	-	272	-	
273	-	-	-	-	-	-	-	-	-	-	-	-	-	-	-	-	-	2.85	0.32	-	-	-	-	-	-	-	-	-	-	-	273	-	
274	-	0.75	-	-	-	-	-	-	-	-	-	-	-	-	-	-	-	2.85	0.32	-	-	-	-	-	-	-	-	-	-	-	274	-	
275	-	-	-	-	-	-	-	-	-	-	-	-	-	-	-	-	-	2.85	0.32	-	-	-	-	-	-	-	-	-	-	-	275	-	
276	-	-	-	-	-	-	-	-	-	-	-	-	-	-	-	-	-	2.85	0.32	-	-	-	-	-	-	-	-	-	-	-	276	-	
277	-	0.50	-	-	-	-	-	-	-	-	-	-	-	-	-	-	-	2.85	0.32	-	-	-	-	-	-	-	-	-	-	-	277	-	
278	-	-	-	-	-	-	-	-	-	-	-	-	-	-	-	-	-	2.85	0.32	-	-	-	-	-	-	-	-	-	-	-	278	-	
279	-	-	-	-	-	-	-	-	-	-	-	-	-	-	-	-	-	2.85	0.32	-	-	-	-	-	-	-	-	-	-	-	279	-	
280	2 1/2	1.5	HELLOVYN 1	50.0	54.5	110	6 1/2	36	444	36	444	1 1/2	10 1/2	17 1/2	12 1/2	-4 1/2	1.37	2.22	0.34	32	24	18	12 1/2	12 1/2	12 1/2	12 1/2	12 1/2	12 1/2	12 1/2	12 1/2	280	-	
281	-	-	-	-	-	-	-	-	-	-	-	-	-	-	-	-	-	1.14	0.34	23	23	23	23	23	23	23	23	23	23	23	23	281	-
282	-	-	-	-	-	-	-	-	-	-	-	-	-	-	-	-	-	1.06	0.34	24	24	24	24	24	24	24	24	24	24	24	24	282	-
283	-	1.25	-	-	-	-	-	-	-	-	-	-	-	-	-	-	-	0.87	0.34	25	25	25	25	25	25	25	25	25	25	25	25	283	-
284	-	-	-	-	-	-	-	-	-	-	-	-	-	-	-	-	-	0.87	0.34	25	25	25	25	25	25	25	25	25	25	25	25	284	-
285	-	-	-	-	-	-	-	-	-	-	-	-	-	-	-	-	-	0.87	0.34	25	25	25	25	25	25	25	25	25	25	25	25	285	-
286	-	1.0	-	-	-	-	-	-	-	-	-	-	-	-	-	-	-	0.87	0.34	25	25	25	25	25	25	25	25	25	25	25	25	286	-
287	-	-	-	-	-	-	-	-	-	-	-	-	-	-	-	-	-	0.87	0.34	25	25	25	25	25	25	25	25	25	25	25	25	287	-
288	-	-	-	-	-	-	-	-	-	-	-	-	-	-	-	-	-	0.87	0.34	25	25	25	25	25	25	25	25	25	25	25	25	288	-

ELVALE CONTRACT, MINE RESEARCH CORPORATION
 EXPLOSIVE TESTS IN PROGEN GROUND SILY
 DATA SHEET EXPERIMENT NO. 12
 September 30, 1954 FIG. A 12

BLAST HOLE		NUMBER	DIAMETER INCHES	DEPTH FEET	TYPE OF EXPLOSIVE	CARTRIDGE STRENGTH	WEIGHT STRENGTH	STICK COUNT 1-1/4" S"	INCHES OF EXPLOSIVE	CARTRIDGE FRACTION	EXPLOSIVE WEIGHT, LBS. PER CARTRIDGE	WEIGHT OF CHARGE, LBS.	VELOCITY FOUNDED	VELOCITY UNFOUNDED	HEIGHT OF CHARGE	HEIGHT OF STEMMING	SURFACE TO CENTER OF GRAVITY INCHES	DEPTH OF FROZEN GROUND INCHES	CENTER OF GRAVITY TO INTERFAC INCHES	INTERFAC RATIO	CRATER AREA SQUARE FEET	CRATER RADIUS FEET	CRATER DEPTH INCHES	DEPTH OF SLAMMING INCHES	CHARGE RADIUS FEET	1/2 RATIO	SIMILITUDE RATIO	CRATER VOLUME CUBIC FEET	SLAM VOLUME CUBIC FEET	CHARGE VOLUME CUBIC FEET	NUMBER	REMARKS
288	0	0.75	HELDON	5.5	64.6	110	1	18	448	28	14,000	10,000	1	1	1	0	1		6.3	1.30	15	8	0.51	1.52	50	1.88	12	288				
289	0	0.75																		5.8	1.38	11	11	0.53	1.04	48	2.27	15	289			
290	0	0.75																		4.32	1.17	10	10	0.43	1.75	57	1.64	17	290			
291	0	0.75																		4.28	1.16	8	8	0.65	2.72	56	1.31	12	291			
292	0	0.75																		5.08	0.99	5	5	0.40	2.32	78	1.01	18	292			
293	0	0.75	COMLITE 7-5	44.3	61.8	120	1	06	407	125	10,000	8,000	1	1	1	0	1													293		
294	0	0.75																												294	WATERLOGGED	
295	0	1.00																												295	LOW CRITICAL	
296	0	1.20																												296	HEAVY CRITICAL	
297	0	1.8																												297		
298	0	1.8																												298		
299	0	1.20																												299	NO CRATER	
300	0	1.20																												300	MID CRITICAL	
301	0	1.00																												301	FULL CRATER	
302	0	1.00																												302		
303	0	1.00																												303		
304	0	1.00																												304		
305	0	1.00																												305		
306	0	1.00																												306		
307	0	0.75																												307		
308	0	0.75																												308		
309	0	0.50																												309		
310	0	0.50																												310		
311	0	0.50																												311		
312	0	0.50																												312		
313	0	0.50																												313		

SLPR E. CONTRACT, MINING RESEARCH CORPORATION
EXPLOSION TESTS IN FROZEN GROUND ONLY
DATA SHEET EXPERIMENT NO. 12
September 30, 1954 Pg. A 16

BLAST HOLE			TYPE OF EXPLOSIVE	CARTRIDGE STRENGTH	WEIGHT STRENGTH	STICK COUNT 1-1/4" & 8"	INCHES OF EXPLOSIVE	CARTRIDGE FRACTION	EXPLOSIVE WEIGHT, LBS. PER CARTRIDGE	WEIGHT OF CHARGE, LBS.	VELOCITY CONFINED	VELOCITY UNCONFINED	HEIGHT OF CHARGE	HEIGHT OF STEMMING	SURFACE TO CENTER OF GRAVITY INCHES	DEPTH OF FROZEN GROUND INCHES	CENTER OF GRAVITY TO INTERFACE INCHES	INTERFACE RATIO	CRATER AREA SQUARE FEET	CRATER RADIUS FEET	CRATER DEPTH INCHES	DEPTH OF SLABING INCHES	CHAMBER RADIUS FEET	1/3 RATIO	SIMILITUDE RATIO	CRATER VOLUME CUBIC FEET	SLAB VOLUME CUBIC FEET	CHAMBER VOLUME CUBIC FEET	NUMBER	REMARKS		
NUMBER	DIAMETER INCHES	DEPTH FEET																														
295	1	0.50	COALITE 76	44.2	61.9	120	1	06	407	025	10,700	8,600	1	5 1/2	5 1/2				1	—	—					0			295			
296	1	0.75	"	"	"	"	1 1/2	19	"	085	"	"	1 1/2	7 1/2	8 1/2				—	—	—	10				1.15			296			
297	1	1.00	"	"	"	"	2 1/2	30	"	130	"	"	4	8	10				1.05	1.05	12	14 1/2				1.82			297	ESTIMATED		
298	1	1.21	"	"	"	"	3 1/2	41	"	180	"	"	4 1/2	10	12 1/2				1.45	1.20	14 1/2	12 1/2				1.82			298			
314	1	1.25	"	"	"	"	4 1/2	60	"	26	"	"	5 1/2	9 1/2	12 1/2				1.22	0.63	0	—		0.61	1.0		—			314	NO CRATER	
315	1	"	"	"	"	"	"	"	"	"	"	"	"	"	"				0.34	0.33	0	—		0.32	1.0		—			315	"	
316	1	"	"	"	"	"	"	"	"	"	"	"	6	9	12				0.38	0.35	0	—		0.35	1.0		—			316	"	
316A	1	"	"	"	"	"	"	"	"	"	"	"	7 1/2	7 1/2	11 1/2				3.38	1.04	19 1/2	11 1/2	0.28	1.10	—	—	1.70	1.62	0.8	316A		
317	1 1/4	1.10	"	"	"	"	"	"	"	"	"	"	4 1/2	9	11 1/2				5.48	1.32	16	11 1/2	0.26	1.42	—	—	2.46	2.42	0.4	317		
318	1	"	"	"	"	"	"	"	"	"	"	"	"	"	"				3.80	1.10	16 1/2	—	0.30	1.19	—	—	1.82	1.80	0.2	318		
319	1	"	"	"	"	"	"	"	"	"	"	"	"	"	"				0.97	0.56	—	0	—	0.60	1.0		—			319	NO CRATER	
320	2	1.03	"	"	"	"	"	"	"	"	"	"	2 1/2	9 1/2	10 1/2				3.73	1.09	15 1/2	11	0.51	1.20	—	—	2.11	1.98	0.13	320		
321	1	"	"	"	"	"	"	"	"	"	"	"	"	10	11 1/2				2.87	0.96	—	—	—	1.01	1.0		—			321	NO CRATER	
322	1	"	"	"	"	"	"	"	"	"	"	"	"	"	"				2.50	0.89	—	—	—	0.93	1.0		—			322	"	
323	2 1/2	1.00	"	"	"	"	"	"	"	"	"	"	1 1/2	10 1/2	11 1/2				2.98	0.97	14 1/2	11 1/2	0.33	1.03	—	—	1.18	1.13	0.5	323		
324	1	"	"	"	"	"	"	"	"	"	"	"	"	"	"				5.05	1.27	15 1/2	—	0.46	1.35	—	—	2.59	2.50	0.6	324		
325	1	"	"	"	"	"	"	"	"	"	"	"	"	"	"				5.51	1.32	—	—	0.50	1.41	—	—	2.73	2.62	0.11	325		
326	4	.98	"	"	"	"	"	"	"	"	"	"	1 1/2	11 1/2	11 1/2				1.50	0.69	—	—	—	0.72	1.0		—			326	NO CRATER	
327	1	"	"	"	"	"	"	"	"	"	"	"	"	"	"				1.07	0.58	—	—	—	0.61	1.0		—			327	"	
328	1	"	"	"	"	"	"	"	"	"	"	"	"	"	"				1.40	0.67	—	—	—	0.70	1.0		—			328	"	
329	1	.90	"	"	"	"	"	2 1/2	29	.11	"	"	—	—	—						—	—	—	—	—	—	—				329	
330	1	"	"	"	"	"	"	"	"	"	"	"	—	—	—						—	—	—	—	—	—	—				330	
331	1	"	"	"	"	"	"	"	"	"	"	"	—	—	—						—	—	—	—	—	—	—				331	

S.L.P.R.E. CONTRACT, MINING RESEARCH CORPORATION
EXPLOSION TESTS IN FROZEN KEWEEAW SILT
DATA SHEET EXPERIMENT NO. 13
September 30, 1964 Fig. A17

UNCLASSIFIED

AD 15156

Armed Services Technical Information Agency

Reproduced by

DOCUMENT SERVICE CENTER

KNOTT BUILDING, DAYTON, 2, OHIO

This document is the property of the United States Government. It is furnished for the duration of the contract and shall be returned when no longer required, or upon recall by ASTIA to the following address: Armed Services Technical Information Agency, Document Service Center, Knott Building, Dayton 2, Ohio.

NOTICE: WHEN GOVERNMENT OR OTHER DRAWINGS, SPECIFICATIONS OR OTHER DATA ARE USED FOR ANY PURPOSE OTHER THAN IN CONNECTION WITH A DEFINITELY RELATED GOVERNMENT PROCUREMENT OPERATION, THE U. S. GOVERNMENT THEREBY INCURS NO RESPONSIBILITY, NOR ANY OBLIGATION WHATSOEVER; AND THE FACT THAT THE GOVERNMENT MAY HAVE FORMULATED, FURNISHED, OR IN ANY WAY SUPPLIED THE SAID DRAWINGS, SPECIFICATIONS, OR OTHER DATA IS NOT TO BE REGARDED BY IMPLICATION OR OTHERWISE AS IN ANY MANNER LICENSING THE HOLDER OR ANY OTHER PERSON OR CORPORATION, OR CONVEYING ANY RIGHTS OR PERMISSION TO MANUFACTURE, USE OR SELL ANY PATENTED INVENTION THAT MAY IN ANY WAY BE RELATED THERETO.

UNCLASSIFIED